Persulfate Persistence and Treatability of Gasoline Compounds

by

Kanwartej Singh Sra

A thesis
presented to the University of Waterloo
in fulfilment of the
thesis requirement for the degree of
Doctor of Philosophy
in
Civil Engineering

Waterloo, Ontario, Canada, 2010

Author's Declaration

I hereby declare that I am the sole author of this thesis. This is a true copy of the thesis, including any required final revisions, as accepted by my examiners.

I understand that my thesis may be made electronically available to the public.

Abstract

Petroleum hydrocarbons (PHCs) such as gasoline are ubiquitous organic compounds present at contaminated sites throughout the world. Accidental spills and leakage from underground storage tanks results in the formation of PHC source zones that release hundreds of organic compounds, including the high impact, acutely toxic and highly persistent aromatics (e.g., benzene, toluene, ethylbenzene, xylenes, trimethylbenzenes and naphthalene) into groundwater. Contamination by these compounds continues to persist until the PHC source zone is treated in place or removed. *In situ* chemical oxidation (ISCO) employing persulfate was identified as a potentially viable technology for the treatment of PHC source zones. The effectiveness and efficiency and, therefore, the overall economic feasibility of a persulfate-based ISCO treatment system depend upon the reactivity of the target organic compounds and the interaction of persulfate with aquifer media. The objective of this research was to investigate the persistence of unactivated and activated persulfate in the presence of aquifer materials, and to examine persulfate oxidation of PHC compounds at both the bench- and pilot-scales.

A series of bench-scale studies were performed to estimate persulfate degradation kinetic parameters in the presence of seven well-characterized, uncontaminated aquifer materials and to quantify the changes in specific properties of these materials. Batch experiments were conducted in an experimental system containing 100 g of solids and 100 mL of persulfate solution at 1 or 20 g/L. Column experiments were designed to mimic *in situ* conditions with respect to oxidant to solids mass ratio and were performed in a *stop-flow* mode using a 1 g/L persulfate solution. The degradation of persulfate followed a first-order rate law for all aquifer materials investigated. An order of magnitude decrease in reaction rate coefficients was observed for systems that used a persulfate concentration of 20 g/L as compared to those that used 1 g/L due to ionic strength effects. As expected, the column experiments yielded higher reaction rate coefficients than batch experiments for the same persulfate concentration due to the lower oxidant to solids mass ratio. Bench-scale data was used to develop a kinetic model to estimate the kinetic response of persulfate degradation during these tests. The push-pull tests involved the injection of persulfate (1 or 20 g/L) and a conservative tracer into a hydraulically isolated portion of the sandy aquifer at CFB Borden, Canada. The kinetic model developed from the bench-scale data was able to reproduce the observed persulfate

temporal profiles from these push-pull tests. This implies that persulfate degradation kinetics is scalable from bench-scale to *in situ* scale, and bench tests can be employed to anticipate *in situ* degradation. The estimated reaction rate coefficients indicate that persulfate is a persistent oxidant for the range of aquifer materials explored with half lives ranging from 2 to 600 days, and therefore *in situ* longevity of persulfate will permit advective and diffusive transport in the subsurface. This is critical for successful delivery of oxidant to dispersed residuals in the subsurface.

Activation of persulfate is generally recommended to enhance its oxidation potential and reactivity towards organic compounds. This approach may influence the stability of persulfate-activator system in the presence of aquifer materials. A series of batch tests were performed to investigate persistence of persulfate at two concentrations (1 or 20 g/L) using three contemporary activation strategies (citric acid chelated-ferrous, peroxide and high pH) in the presence of 4 well-characterized, uncontaminated aquifer materials. Chelation by citric acid was ineffective in controlling the interaction between persulfate and Fe(II) and a rapid loss in persulfate concentration was observed. Higher Fe(II) concentration (600 mg/L) led to greater destabilization of persulfate than lower Fe(II) concentration (150 mg/L) and the persulfate loss was stoichiometrically equivalent to the Fe(II) concentration employed. Subsequent to this rapid loss of persulfate, first-order degradation rate coefficients (k_{obs}) were estimated which were up to 4 times higher than the unactivated case due to the interaction with Fe(III) and CA. Total oxidation strength (TOS) was measured for peroxide activation experiments and was observed to decrease rapidly at early time due peroxide degradation. This was followed by slow degradation kinetics similar to that of unactivated persulfate implying that the initial TOS degradation was peroxide dominated and the long-term kinetics were dominated by persulfate degradation. The k_{obs} used to capture TOS degradation for later time were shown to depend upon unactivated persulfate and peroxide degradation rate coefficients, and peroxide concentration. Either a slow peroxide degradation rate and/or higher peroxide concentration allow a longer time for peroxide and persulfate to interact which led to k_{obs} ~1 to 100 times higher than k_{obs} for unactivated persulfate. For alkaline activation, k_{obs} were only 1 to 4 times higher than unactivated persulfate and therefore alkaline conditions demonstrated the least impact on persulfate degradation among the various activation strategies used. For all activation trials, lower stability of persulfate was

observed at 1 g/L as compared to 20 g/L due to insufficient persulfate and/or ionic strength effects.

A series of batch reactor trials were designed to observe the behavior of the nine high impact gasoline compounds and the bulk PHC fraction measures subjected to various persulfate activation strategies over a 28-day period. This bench-scale treatability used unactivated persulfate (1 or 20 g/L) and activated persulfate (20 g/L). Activation employed chelated-Fe(II), peroxide, high pH or two aquifer materials as activators. No significant oxidation of the monitored compounds was observed for unactivated persulfate at 1 g/L, but 20 g/L persulfate concentration resulted in their near-complete oxidation. Oxidation rates were enhanced by 2 to 18 times by activation with peroxide or chelated-Fe(II). For alkaline activation, pH 11 trials demonstrated ~2 times higher oxidation rates than the unactivated results. For pH 13 activation the oxidation rates of benzene, toluene and ethylbenzene were reduced by 50% while for the remaining monitored compounds they were enhanced by 5 to 100%. Natural activation by both aquifer materials produced oxidation rates similar to the unactivated results, implying that either activation by minerals associated with aquifer material was not significant or that any potential activation was offset by radical scavenging from aquifer material constituents. Acid-catalyzation at pH <3 may enhance oxidation rates in weakly buffered systems. Oxidation of the monitored compounds followed first-order reaction kinetics and rate coefficients were estimated for all the trials. Overall, activated and unactivated persulfate appear to be suitable for *in situ* treatment of gasoline.

Persulfate under unactivated or naturally activated conditions demonstrated significant destruction of gasoline compounds and showed higher persulfate persistence when in contact with aquifer solids as compared to chelated-Fe(II) or peroxide-activated persulfate systems. This observation was used as the basis for selecting unactivated sodium persulfate for a pilot-scale treatment of gasoline-contaminated source zone at CFB Borden, Canada where a ~2000 L solution of persulfate (20 g/L) was injected into a PHC source zone. Concentration of organics and inorganics were frequently monitored over a 4 month period across a 90 point monitoring fence line installed down-gradient. Treatment performance was measured by estimating organic and inorganic mass loading across the monitoring fence. Increased mass loading for Na^+ was observed over time as the treatment volume moved across the fence-line indicating transport of the inorganic slug created upon oxidant injection. The mass loading

also increased for SO_4^{2-} which is a by-product generated either due to persulfate degradation during oxidation of organic compounds or during its interaction with aquifer materials. Oxidation of organic compounds was evident from the enhanced mass loading of dissolved $CO_{2(aq)}$. More importantly, a significant (45 to 86%) decrease in mass loading of monitored compounds was observed due to oxidation by injected persulfate. The cumulative mass crossing the monitoring fence-line was 20 to 50% lower than that expected without persulfate treatment. As the inorganic slug was flushed through the source zone and beyond the monitoring fence, the mass loading rate of Na^+, SO_4^{2-} and $CO_{2(aq)}$ decreased and approached background condition. Mass loading of the monitored compounds increased to within 40 to 80% of the pre-treatment conditions, suggesting partial rebound.

These investigations assessed the impact of activation on persulfate persistence and treatability of gasoline and served to establish guidelines for anticipating field-scale persulfate behavior under similar conditions. In summary, unactivated persulfate is a stable oxidant in the presence of aquifer materials and its persistence depends upon TOC and Fe_{Am} content of the materials, ionic strength, and aquifer to solids mass ratio. Persulfate exhibits significant destruction of gasoline compounds and can be employed for the remediation of gasoline-contaminated sites. Peroxide and chelated-Fe(II) enhance oxidation rates of these compounds, but reduce stability of the persulfate-activator system. Persulfate activation using high pH conditions does not significantly impact persulfate persistence but reduces the overall destruction of gasoline compounds. Therefore, activation imposes a trade-off between enhanced oxidation rates and reduced persulfate persistence. Kinetic model is representative of persulfate degradation at bench- and pilot-scales and can be used for estimation of *in situ* degradation. The quantification of oxidation rates for gasoline compounds under activated and unactivated persulfate conditions will assist decision-making for identification of appropriate remediation options when targeting contamination by gasoline or by specific high impact gasoline compounds. While persulfate oxidation resulted in partial treatment of a small gasoline source zone, aggressive persulfate load will be required during injection for a complete clean-up. Overall, persulfate-based *in situ* chemical oxidation was demonstrated to be an effective and a viable technology for the remediation of contaminated soil and groundwater.

Acknowledgements

God, as some cynic has said, is on the side with the best football coach. Who would have needed a god when one had two world-class coaches? I have the utmost respect and express sincere gratitude for Neil Thomson and Jim Barker, firstly, for giving me the opportunity to join their team, and then coaching me through the near-5 year game of my doctoral studies. Just like football (or, less famously, soccer), I usually played up front, scoring and missing goals as the game went on. Never did I feel arrogant about the hits and depressed about the misses. The presence of my coaches had a very humbling effect. Equally, it encouraged me to try new moves and methods, and their support was pivotal in the shaping and making of this thesis. They ensured that I was provided with appropriate resources and pitch conditions for a smooth game. Their attitude was truly inspirational and hopefully some of that has rubbed on to me as well. I thank them for all their help and giving me a chance to learn some of their skills.

Thesis writing seemed to be like a set piece, a dead-ball situation. There were so many angles that you have a chance to score from. However, achieving a particular goal required a particular shot. Making the ball (manuscript) follow (flow in) a specific trajectory needed a lot of guidance, patience, effort and practice. This also would not have been possible without the help and encouragement of my coaches.

Like in football, several support staff professionals spend numerous hours with players, assisting them hone their skills, working with them on particular issues, and at times jump into coach's shoes and take the players through the intricacies and set-ups. I gratefully acknowledge these efforts of my support staff. Marianne vanderGriendt worked tirelessly through the lab and field samples, advised on performance issues and areas to improve, and assisted me with the set-up of the bench-scale experiments. Bob Ingelton was like a physical trainer, working with me on the field, and assisting with set-up and operation of pilot-scale experiments. He taught me the use and names of a number of field tools. Mark Sobon and Bruce Stickney were very resourceful in acquiring equipment, assisting with the how-to of using the equipments and devices. I am also thankful to Shirley Chatten for her assistance with the sample analysis.

At times I required advice and remarks from experts in a particular skill area. My advisory committee consisting of Eric Reardon, Wayne Parker, Steve Forsey and Susan

Andrews played the role of this panel of experts. They not only highlighted critical issues for improving the overall research, they also assisted in development of specific skills. I am thankful to them for their valuable contributions and assessment of the game.

Unlike football, a PhD candidate does not have the luxury of substitutes. However to ease pressure and to attempt to extract more than 24 hours of work in a given day, there was a provision for short-term rolling substitutions where my work-load was shared by colleagues and coop- students. At times we all played together at the same time, and at other times I could afford to send a replacement to play in my stead. I was able to relax, knowing that my job was in safe hands. I am extremely thankful to the people for agreeing to play by my side. These include Maureen O'Connell, Gillian Roos, Juliana Freitas, Chao Huo, Barb Fletcher, Tyler Gale, Ashley Mathai, Dan Princz, Katrina McLean, David Thompson, Victoria Chennette, Charmaine Baxter, and Jessica Whitney. I particularly remember and acknowledge the time when Maureen, Chao and Dan worked through the semi-northern winter in 2008 while I went away to get married.

During this research, several strategy meetings were held and led to stimulating discussions and knowledge sharing with the team players mentioned above and with Vahid Sohrabi, Neelmoy Biswas, Bobby Katanchi, Erika Williams, Tapesh Ajmera and Jennifer Lambert. These inputs only improved my perspective of the field. Xiuyuan Xu was a former player and passed on some important tricks on to me. Massimo Marchesi and I were trying to score the same goal and realized it would be more effective if we achieve it together, and therefore, we collaborated for the study on advancement of isotopes as performance metrics.

I have special memories from the time off the field. I spent great time with my friends Avisek Chatterjee, Barry Brouwers, Shanee Raizada, Aniket Kate, Samad Bazargan, Deeparnab Chakraborty, Rajesh Tripathi, Tapesh Ajmera and Fred Bosche. They also, thankfully, found time outside their own academic games to play actual sports and board games rather than trying to find amusement through research games.

Surprisingly, the last role that I played in this doctoral study was that of a defender. Like football, I have gotten used to the idea of being useful in different roles, being adaptable and being able to respond as the situation requires. Fortunately, the final moments did not go down to a penalty shoot-out. There were some tough and some predictable shots that I was able to defend. There were some that stretched the limits of my skill. There were others that I

simply conceded to, acknowledging that this study was not the end of learning but a part of learning.

Lastly, I am thankful to my family for encouraging me to keep playing. Puneet has given me immense love and cheered me vociferously from the sidelines. She remains, a seemingly quiet but, in reality, my loudest cheerer.

Table of Contents

List of Figures

List of Tables

Chapter 1

Introduction

1.1. GENERAL BACKGROUND

Groundwater is an immensely important and conditionally renewable natural resource that is used as a supply for domestic and agricultural consumption and sustains a physical and chemical balance with the surface water system (Pankow and Cherry, 1996; Langmuir, 1997). However, accidental spills and ignorant, short-sighted and non-complying human practices (e.g., waste disposal, transport and storage of industrial chemicals, agricultural abuse, etc.) have led to widespread contamination of this resource (ITRC, 2005a). Contamination caused by a wide spectrum of hazardous organic compounds such as petroleum hydrocarbons (PHCs), saturated and unsaturated chlorinated solvents, polycyclic aromatic hydrocarbons (PAHs) and polychlorinated biphenyls (PCBs) pose an imminent health risk to ecosystems and humans due, in part, to their toxicity and persistence in the subsurface systems. While the use and production of numerous harmful organic compounds is banned or limited, PHCs such as gasoline are one of the most extensively used class of organic compounds and hence are also the most widespread contaminants found in soil and groundwater (Tiburtius et al., 2005; Ferrarese et al., 2008; ITRC, 2005b; USEPA, 2006). The latest National Priority List (NPL) released by the USEPA identified more than 1000 active superfund sites that suffer from groundwater and subsurface soil contamination which require immediate restoration or clean-up (USEPA, 2010). In addition, numerous other contaminated sites are known to exist and continue to act as long-term sources of toxic

compounds. In the absence of site remediation or restoration efforts, the number of these sites is likely to increase since contaminants continue to enter the natural systems. For instance, one-third of all underground storage tanks (USTs) are potentially leaking PHCs to the subsurface soil and groundwater (Shih et al., 2004).

An increased awareness of the health risk of contaminants and a better scientific understanding of the underlying processes in the past three decades has fostered the growth and introduction of a number of site restoration and containment technologies. These technologies range from passive methods (e.g., monitored natural attenuation, containment walls, and permeable reactive barriers) to more active methods (e.g., soil excavation, pump-and-treat and other *in situ* techniques). Technology choice depends on site characteristics (e.g., type and extent of contamination and geologic considerations) and is influenced by robustness and economic viability (Watts and Teel, 2006; Huling and Pivetz, 2006). A thorough understanding of the impact of the interrelationships between these factors helps to evaluate and establish the usefulness of a technology. *In situ* chemical oxidation (ISCO), an *in situ* technology, involves the addition of chemical oxidants to the subsurface. ISCO is potentially operatable over a wide range of conditions and provides economical advantages over other conventional technologies (ITRC, 2005a).

1.2. *IN SITU* CHEMICAL OXIDATION (ISCO)

The concept of *in situ* chemical oxidation is based on an extension of the already well-established water and wastewater treatment processes (Houston, 1913; Cleasby et al., 1964; Taki and Hashimoto, 1977) wherein chemical oxidants are added to water to destroy target contaminants and thereby improve water quality (USEPA, 1999). Similarly, the ISCO technology involves the injection of an oxidant or combination of oxidants into contaminated

subsurface zones to minimize the organic contaminant mass through chemical oxidation (Siegrist et. al, 2001). The design of an ISCO remedial system involves a comprehensive understanding of the underlying physical and chemical processes and hence in general, requires an oxidant have (1) a high rate and extent of reactivity towards target contaminants, and (2) a high stability and persistence in the subsurface (Crimi and Taylor, 2007). These criteria serve to establish the usefulness, effectiveness and efficiency of an oxidant.

Permanganate (MnO_4^-) and peroxide (H_2O_2) are the two aqueous oxidants which have been extensively researched in bench and field-scale applications since the inception of ISCO (Watts et al., 1990; Hood et. al, 1997; Schnarr et al., 1998; Siegrist et. al, 2001; ITRC, 2001). Apart from the hydrodynamic properties that play a role in controlling oxidant transport in the subsurface, it has been acknowledged that the interaction of oxidants with reductive species (organic carbon, transition metals etc.) is also an important process (Appelo and Postma, 1996; Christensen et. al, 2000). Permanganate poses a natural oxidant demand or NOD (defined as the mass of $KMnO_4$ required to completely oxidize reductants naturally occurring in the solid and aqueous phase) implying that its consumption by non-target species associated with the aquifer materials is not insignificant as compared to the oxidant loading required by the target contaminant mass (Siegrist et. al, 2001; Mumford et. al, 2004; ITRC, 2005a; Huling and Pivetz, 2006; Xu and Thomson, 2008 and 2009). In fact, some aquifer materials with a high NOD systems exert a significant permanganate demand which may be 10 to 100 times greater than the theoretical requirement of the target contaminant (Mumford et al., 2004; NFESC, 2004), thus driving the remediation costs (Haselow et al., 2003). Moreover, permanganate selectively oxidizes mostly unsaturated aliphatic hydrocarbons (e.g., chlorinated solvents) but is ineffective in treatment of PHCs, substituted

alkanes, fuel-related contaminants and oxygenates (ITRC, 2005a, b; Watts and Teel, 2006; Huling and Pivetz, 2006). Peroxide exhibits a widespread reactivity towards majority of the environmentally relevant compounds but its performance is adversely influenced by its very low stability and enhanced decomposition in the presence of aquifer materials (Xu and Thomson, 2010). This lack of persistence restricts the peroxide zone of influence around an injection well (Block et. al, 2004; Smith et. al, 2005; Watts and Teel, 2006) and thus requires a larger number of injection points and higher oxidant loading rate to achieve a given remediation goal.

1.3. PERSULFATE

Persulfate ($S_2O_8^{2-}$) is the newest oxidant used in ISCO applications and presents several advantages over MnO_4^- and H_2O_2. It has a high oxidation potential on activation to sulfate free radicals (E^o = 2.6 V), a high solubility in water, potentially a wide range of reactivity towards environmental organic contaminants and appears to be relatively stable in the subsurface (Huang et. al, 2002; Liang et. al, 2003; Huang et. al, 2005; Watts and Teel, 2006; Huling and Pivetz, 2006). Recent studies have reported the effectiveness of persulfate to treat contaminants ranging from chlorinated solvents to petroleum hydrocarbons and PAHs (Kronholm and Reikkola, 1999; Liang et. al, 2004; Huang et. al, 2005, Crimi and Taylor, 2007). However, the literature on its interaction with aquifer materials is scarce and since these interactions have adversely affected the field-scale utility of permanganate (high NOD) and peroxide (enhanced degradation rates), it becomes important that this issue be examined in detail. Studies conducted to date to establish the affects of aquifer materials on persulfate degradation or mass consumption have been narrow and contradictory (Brown and Robinson,

2004; Dahmani et. al, 2006). Brown and Robinson (2004) concluded that oxidant demand of permanganate was much greater than that of persulfate for the same soil, and the nature of interactions were fundamentally different. This finding was contrary to another study (Dahmani et. al, 2006) which reported that natural organic matter (NOM) was equally oxidizable by permanganate and persulfate and suggested the use of persulfate to reduce NOD prior to permanganate injection. The structural and functional similarity between peroxide and persulfate suggests that the interaction between persulfate and aquifer materials ought to be more similar to the enhanced decomposition behavior of peroxide than mass consumption characteristics of permanganate (Watts and Teel, 2006).

Persulfate can be activated to powerful free radicals (e.g., $SO_4^{-\bullet}$, $OH^{\bullet}$) to potentially enhance the range of applicability and rate of oxidation of organic compounds. The use of peroxide, chelated-ferrous and high pH has been proposed to be effective in persulfate activation (Block et al., 2004; Huling and Pivetz, 2006). While activation may enhance oxidant effectiveness and performance, it is anticipated that the persistence of the persulfate-activator system will be compromised in the presence of aquifer materials. Similar to peroxide, the presence of natural catalysts in the subsurface (e.g., transition metals like iron and manganese) has the potential to catalyze production of the sulfate free radical (Gates-Anderson et al., 2001; Watts and Teel; 2006; Dahmani et. al, 2006; Huling and Pivetz; 2006). Therefore, knowledge of persulfate behavior in the presence of aquifer materials is required to establish persulfate as an oxidant for ISCO.

1.4. PERSULFATE TREATMENT OF PETROLEUM HYDROCARBONS

PHCs such as gasoline are a mixture of hundreds of organic compounds which once introduced to the subsurface through leakage of USTs or accidental spills can act as long-

term contamination sources and release acutely toxic and highly persistent compounds (e.g., benzene, toluene, naphthalene). Serious health and ecological concerns have been raised over the adverse effects of the release of these compounds into groundwater. Regulatory bodies (Health Canada and USEPA) have established specific guidelines on the maximum concentration of these contaminants that can exist in natural systems. Frequent and serious impacts on the subsurface and strict cleanup regulations have resulted in the inclusion of PHC contaminated sites on the NPL list and have encouraged and promoted remedial action. The relatively high solubility as compared to maximum concentration limits (MCLs) of the PHC compounds, low retardation and relatively low biodegradation leads to increased plume lengths and higher impact in receptors. PHC contamination continues to persist until the source zone is removed, quarantined, attenuated or treated in place (Lundegaard and Johnson, 2007). Bench-scale studies have demonstrated the ability of using activated persulfate to destroy BTEX compounds (Crimi and Taylor, 2007, Liang et al., 2009). Unfortunately, these studies either investigated the treatment of an individual compound or by simulating a mixture of a few constituent compounds. Lab-scale treatability studies, while illustrative, are not representative and therefore not sufficient for evaluation of persulfate performance at pilot- or field-scale. The current empirical assessment of these interactions in a field-scale groundwater system containing persulfate, petroleum hydrocarbons, and aquifer materials is very limited and necessitates a comprehensive analysis.

1.5. RESEARCH OBJECTIVES

To improve our understanding of the macro-level chemical interactions between persulfate and aquifer material constituents and to enhance the knowledge of ISCO remediation specific

to activated persulfate utilization and performance in PHC contaminated subsurface systems, the following research objectives were proposed:

1. Investigate the persistence of unactivated and activated persulfate in the presence of aquifer materials.
2. Investigate persulfate treatability of PHCs in dissolved phase.
3. Evaluate persulfate treatment of a pilot-scale PHC source zone.

1.6. THESIS SCOPE

The thesis is organized into 6 chapters of which 4 are core chapters (Chapters 2 to 5) addressing the research objectives. These chapters focus on particular issues with respect to persulfate stability in aquifer media (Chapters 2 and 3) and the treatability of PHCs (Chapters 4 and 5). When persulfate is introduced into the subsurface for treatment of a contaminated source zone, it distributes around the injection well creating a zone of influence. Within this zone, persulfate interacts not only with the target organics but can also react with aquifer material constituents. A fast reaction may limit the persistence of persulfate within the zone of influence and this diminished persulfate strength and coverage will adversely impact the overall treatment efficiency. Increased persistence is more beneficial since this will allow greater residence time for the oxidation of targets compounds, and also permit advective and diffusive transport of persulfate. This issue of unactivated persulfate persistence in the presence of aquifer materials and identification of controlling factors is the focus of Chapter 2.

Persulfate activation potentially enhances the oxidation rates of organic compounds and hence may be injected into the subsurface along with activating agents such as peroxide, chelated-ferrous or NaOH. The presence of these co-amendments may impact the way

persulfate interacts with the aquifer materials. Additionally, for sustaining activation of persulfate over the long-term the stability of the activating agent is also necessary. This is examined through bench-scale experiments and discussion of the persistence of activated persulfate and the stability of activating agents is presented in Chapter 3.

Persulfate effectiveness for the treatment of organic compounds is the fundamental requirement for remediation to be successful within the unactivated or activated persulfate zone of influence. Before a field-scale application is designed and implemented, bench-scale treatability studies are necessary in order to make a well-informed decision on the choice of activating conditions and to evaluate persulfate treatment effectiveness. The treatability of gasoline compounds under different persulfate activating conditions is examined and discussed in Chapter 4.

As persulfate oxidizes the target organics, in this case gasoline compounds, and destroys organic mass within the source zone, the strength of the source zone will decrease. As a consequence, the length of the contaminant plume will be shortened or the organic mass load from the source zone to the plume will be reduced. Following treatment the mass loading of oxidation by-products such as $CO_{2(aq)}$ and SO_4^{2-} will increase. Therefore, to explore some key issues surrounding the use of persulfate to treat a gasoline source zone a pilot-scale experiment was conducted. Chapter 5 presents and discusses the comprehensive data set that was collected during this pilot-scale experiment.

Chapters 2-5 are intended for publication in suitable high quality journals and hence are written as stand-alone chapters and some repetition is unavoidable. Chapter 2 dealing with the persistence of unactivated persulfate in the presence of aquifer materials has been published in *Environmental Science and Technology* in February 2010 (Sra et al., 2010) and

is presented here without change. Chapters 3, 4 and 5 have been prepared with the intent to submit them to *Journal of Hazardous Materials*, *Chemosphere,* and *Journal of Contaminant Hydrology* respectively.

Chapter 6 concludes the thesis with summary of important conclusions and implications emerging from this research. It also provides an overview for recommendations for future research to support remediation of contaminated sites, particularly using persulfate-based ISCO.

Chapter 2

[1]Persistence of Persulfate in Uncontaminated Aquifer Materials

Overview

Batch and stop-flow column experiments were performed to estimate persulfate decomposition kinetic parameters in the presence of seven well-characterized aquifer materials. Push-pull tests were conducted in a sandy aquifer to represent persulfate decomposition under *in situ* conditions. The decomposition of persulfate followed a first-order rate law for all aquifer materials investigated. Reaction rate coefficients (k_{obs}) increased by an order of magnitude when persulfate concentration was reduced from 20 g/L to 1 g/L, due to ionic strength effects. The column experiments yielded higher k_{obs} than batch experiments due to the lower oxidant to solids mass ratio. The kinetic model developed from the batch test data was able to reproduce the observed persulfate temporal profiles from the push-pull tests. The estimated k_{obs} indicate that unactivated persulfate is a persistent oxidant for the range of aquifer materials explored with half-lives ranging from 2 to 600 days.

[1]Reproduced in part with permission from Sra, K.S., Thomson, N.R., Barker, J.F., 2010. Persistence of persulfate in uncontaminated aquifer materials. Environmental Science and Technology, 44 (8), 3098-3104.

2.1. INTRODUCTION

The treatment of contaminated soil and groundwater by *in situ* chemical oxidation (ISCO) relies on the oxidation potential of chemical reagents to destroy harmful organic compounds. The interaction of these oxidants with target and non-target compounds in the subsurface plays an important role in oxidant choice and overall loading requirements. These interactions in conjunction with the site specific oxidant delivery technique to maximize contact with target compounds determine the effectiveness and efficiency of an ISCO treatment system. Over the last two decades studies conducted at the bench- and pilot-scale employing permanganate or peroxide have highlighted critical issues related to the ability of these oxidants to destroy environmentally relevant organic contaminants and how they interact with aquifer media (Brown and Robinson, 2004; Crimi and Siegrist, 2005). Permanganate has a limited ability to oxidize aromatic hydrocarbons and other fuel related contaminants relative to catalyzed hydrogen peroxide, and the interaction of peroxide and permanganate with aquifer solids is very different (Gate-Anderson et al., 2001). The latest oxidant to gain widespread use is persulfate which has a high oxidation potential on activation to the sulfate radical ($E^o = 2.6\,V$), exhibits widespread reactivity towards organic compounds, is relatively stable in near-neutral aqueous solutions, and has a minimal impact on soil microorganisms (Eberson, 1987; Watts and Teel, 2006; Tsitonaki et al., 2008). Persulfate alone can be an effective oxidant or it can be activated by aquifer material constituents. The study of unactivated persulfate stability also forms the basis for further evaluation of activated persulfate persistence. The peer-reviewed literature that focuses on persulfate interaction with potentially reductive and catalytic constituents in aquifer materials, and its stability in groundwater systems is limited (Watts and Teel, 2006).

In the presence of aquifer materials peroxide undergoes enhanced decomposition without significantly changing the total reductive capacity (TRC) of the aquifer solids such that repeated addition of peroxide leads to continual peroxide decomposition (Xu and Thomson, 2010). This enhanced decomposition or degradation is so rapid that it limits the treatment radius of influence in the subsurface to a few meters around injection locations (Watts and Teel, 2006). In contrast to peroxide, permanganate is consumed by the natural organic matter (NOM) and inorganic reductants associated with aquifer materials (Mumford et al., 2005). Thus aquifer materials exposed to permanganate exhibit a finite or an ultimate natural oxidant demand (NOD) (Haselow et al., 2003; Mumford et al., 2005; Xu and Thomson, 2008). Once the ultimate NOD of the solids has been satisfied, permanganate is relatively stable in the subsurface for extended periods of time (Gates-Anderson et al., 2001; Xu and Thomson, 2009).

The TRC of an aquifer material can be theoretically determined by estimating the sum of specific reductive species (e.g., natural organic matter (NOM), Fe(II), and Mn(II)) or experimentally quantified by the chemical oxidant demand (COD) test (Barcelona and Holm, 1991; Xu and Thomson, 2008). For some aquifer materials the reductive minerals may be the largest oxidant sink while for others it may be the NOM (Xu and Thomson, 2008). Recent efforts by Xu and Thomson (2008, 2009, 2010) using a variety of aquifer solids have shown that permanganate mass consumption and peroxide enhanced decomposition are highly correlated with the total organic carbon (TOC) content and/or the amorphous iron (Fe_{Am}) content.

The limited data on persulfate interaction with aquifer materials is conflicting. The data presented by Dahmani et al. (2006) support the view that persulfate is stable once the

persulfate demand of the aquifer solids has been satisfied, similar to the behavior of permanganate. In contrast, Brown and Robinson (2004) indicate that persulfate interaction with aquifer materials was fundamentally different than permanganate with persulfate mass loss increasing with time similar to the decomposition behavior of peroxide. In some shallow soils, persulfate only mildly oxidized the amorphous and relatively young NOM (Cuypers et al., 2002; Eusterhues et al., 2003) while others (Kiem and Kögel-Knabner, 2002) observed a 93% decrease in the TOC content of loamy and sandy surface soils. Most of these studies were performed on single aquifer material or soil samples from surficial horizons and hence the findings, while illustrative, have limited applicability to different aquifer materials.

This paper identifies relevant aquifer material properties that control the stability of persulfate in the presence of multiple aquifer solids, and defines kinetic parameters that can be used in predictive tools for the design of a persulfate-based ISCO system. The observations reported here are of practical interest and provide the most comprehensive picture of persulfate decomposition in the presence of typical aquifer materials.

2.2. MATERIALS AND METHODS

A series of batch and column experiments were conducted using seven well-characterized, uncontaminated, sandy to silty-sand calcite-rich aquifer materials collected from across North America. These aquifer materials exhibit a range of physico-chemical properties and variations in composition (Xu and Thomson, 2008) that are widely applicable to subsurface conditions where persulfate ISCO treatment may be used (Table 2.1). The initial COD or reductive capacity of these materials is largely due to the presence of TOC and a minor amount of mineral-based Fe and Mn. To avoid handling difficulties, only

materials <2 mm grain size were air-dried to a constant weight at 80 ^{o}C and used in these bench-scale investigations. To support the bench-scale findings a sequence of pilot-scale experiments using the well established push-pull methodology (Haggerty et al., 1998) were performed at Canadian Forces Base (CFB) Borden located near Aliston, Ontario, Canada to quantify persulfate stability under *in situ* conditions.

2.2.1. Chemicals

Sodium persulfate ($Na_2S_2O_8$, purity ≥ 98%, Aldrich Chem. Co., Milwaukee), ACS grade ferrous ammonium sulfate ($Fe(NH_4)_2(SO_4)_2 \cdot 6H_2O$) (EMD Chemicals, Gibbstown), ammonium thiocyanate (NH_4SCN) (Baker, Phillipsbourg) and sulfuric acid (H_2SO_4) (EMD Chemicals, Gibbstown) solutions were prepared to required concentrations using Milli-Q water. Sodium persulfate ($Na_2S_2O_8$) (Klozur, FMC) and lithium chloride (LiCl, purity 99+%, ACS grade, Aldrich Chem. Co., Milwaukee) injection solutions for the pilot-scale tests were prepared using uncontaminated ambient groundwater collected on-site.

2.2.2. Batch Tests

To observe persulfate degradation rates and to evaluate the impact of persulfate exposure on the reductive capacity of the aquifer materials used in this study, well-mixed batch reactor tests were conducted at a low (1.0 g/L) and high (20 g/L) persulfate concentration. Each reactor (300 mL) was filled with 100 g of aquifer solids and 100 mL of Milli-Q water and mixed manually for 5 min. Following a 24 hr equilibration period, each reactor was spiked with the requisite persulfate mass (0.1 or 2.0 g) to establish an initial persulfate concentration of ~1.0 or 20 g/L (~4 or 80 mM), or an oxidant to solids mass ratio of 1.0 or 20 g/kg. Temporal sampling for persulfate concentration and pH was performed frequently (~5 days

at early time to >15 days at later time). The reactors were shaken by hand ~2 hr prior to sampling and frequently between sampling events. All reactors where stored at ~20 ^{o}C in the dark. Quantification of persulfate was performed in duplicate on 0.1 mL aqueous aliquot using the procedure described in Huang et al. (2002) with a slight variation to correct for aquifer solids color interference. An Orion pH meter (Model 290A) was used to measure pH. Controls consisted of persulfate at the two concentrations in Milli-Q water only. All experiments were conducted in triplicate. For all aquifer materials, except LC34-LSU, the mass of persulfate in the high concentration reactors exceeded the stoichiometric requirement for persulfate to oxidize the TRC (captured as COD) based on the following two electron half reaction

$$S_2O_8^{2-} + 2e^- \rightarrow 2SO_4^{2-} \qquad (2.1)$$

For post-oxidation COD estimate from the batch tests, solids were removed from each reactor, washed with sufficient amount of Milli-Q water (>1000 mL) to remove residual persulfate, air-dried at 80 ^{o}C and sub-samples were analyzed in triplicate following the method described in Xu and Thomson (2008).

2.2.3. Column Tests

Column tests were conducted to closely mimic *in situ* conditions with respect to the oxidant to solids mass ratio of ~0.25 g/kg for a persulfate concentration of 1 g/L. Based on the slow persulfate depletion observed in the batch experiments a stop-flow column operation scheme as opposed to continuous flow was adopted. The inherent assumption in these stop-

flow column experiments is that there is insignificant depletion of the aquifer material reduction capacity on exposure to persulfate. This allows repeated sampling from the same location in the column to represent prolonged persulfate/aquifer material contact.

Plexiglass columns (length of 40 cm, internal diameter of 5 cm) were packed with air-dried solids. CO_2 was flushed through the columns for ~5 min followed by Milli-Q water for 24 hr in the up-flow mode. Following this initial water saturation process, ~2 pore volumes (PVs) of the low persulfate concentration solution were injected into the column in up-flow mode at a flow rate of ~8 mL/min for ~1 hr to establish a uniform initial persulfate concentration throughout the column. Once complete breakthrough was achieved (effluent concentration ~1 g/L), the injection was stopped and the tubing at both ends of the column was clamped. A sampling port located at the bottom of the column (0 cm) was used to repeatedly obtain ~5 mL samples of the column pore-water as required. Sampling was performed frequently during the first 10 days and then less frequent in response to observed concentration changes.

For the COD estimation from column tests, at the termination of each experiment, the column was flushed with Milli-Q water for ~10 PVs to remove residual persulfate and then ~10 g of aquifer solids were collected at three locations along the length of the column (0, 20 and 40 cm from the bottom) to quantify changes in COD using the method as above.

2.2.4. Push-Pull Tests

Push-pull tests were conducted in a presumably no-drift, hydraulically isolated section of a sheet-pile walled gate, similar to that described by Devlin et al. (2002). A steel drive point (3 cm diameter, 20 cm long screened section) was driven to 2.75 m below ground surface such that the screen was approximately in the middle of the saturated aquifer thickness of

~3 m. The water table remained stable during the course of these experiments. The push-pull tests were designed to capture persulfate degradation with respect to the depletion of a conservative tracer (Li^+) and were conducted at both the low (1 g/L) and high (20 g/L) persulfate concentration in duplicate. Similar to the column experiments, an assumption relating to an insignificant depletion in the aquifer material reduction capacity was made to facilitate multiple tests at the same location and depth. Bromide was deliberately not used as a conservative tracer since it showed signs of depletion within ~5 days of exposure to persulfate (data not shown).

A 100 L solution of the desired persulfate concentration and ~220 mg/L of Li^+ (as LiCl) was injected into the aquifer over a period of ~4 hr under a gravity controlled flow rate of ~0.5 L/min. Periodic groundwater samples over ~25 days were collected from the drive point at an extraction rate of ~0.4 L/min after purging the drive point and tubing by >3 times their volume. Once the sample was collected the extraction system was turned off and not activated again until the next sampling episode. The samples were analyzed for persulfate using the procedure outlined above, and Li^+ using Ion Chromatography (DIONEX, DX300) with a MDL of 0.1 mg/L.

2.3. RESULTS AND DISCUSSION

2.3.1. Batch Tests

Normalized persulfate and pH temporal profiles from the batch reactor experiments conducted at the low and high persulfate concentration are shown in Figure 2.1. Each data point represents the average from triplicate reactors (SD < 7 %).

Data from the control reactors indicated that persulfate at the low concentration was stable for the entire ~80 days experimental period, while persulfate at the high concentration was stable for the first 80 days and then decreased significantly (2 data points) until the experiment was terminated at ~300 days. Uncatalyzed degradation of persulfate can be initiated through homolytic cleavage of persulfate to produce hydrogen sulfate and oxygen (Kolthoff and Miller, 1951; House, 1962; Berlin, 1986) as given by

$$S_2O_8^{2-} + H_2O \rightarrow 2HSO_4^- + \frac{1}{2}O_2 \qquad (2.2)$$

At the experimental temperature conditions used here (~20 ºC) this is a very slow reaction with an estimated first-order rate coefficient of 3.7×10^{-4} day^{-1} (House, 1962), and therefore leads to little (<5%) persulfate degradation in the controls over the first 80 days. The ratio of the observed pH in the persulfate controls to the theoretical pH (calculated from Eq. 2.2) was 1.04 indicating that the persulfate degradation as described by the hydrolysis reaction accounts for the observed H^+ production. In the high persulfate concentration controls the solution pH reduced to ~3 by Day 40 as a result of the acidity generated (Eq. 2.2). When the pH decreases to <3 persulfate degradation also occurs through the acid-catalyzed reaction (Kolthoff and Miller, 1951; House, 1962; Goulden and Anthony, 1978; Peyton, 1993) to yield Caro's acid represented by

$$S_2O_8^{2-} + H_2O \xrightarrow{H^+} H_2SO_5 + SO_4^{2-} \qquad (2.3)$$

This acid-catalyzed reaction was assumed to be responsible for much of the enhanced persulfate degradation observed after Day 80 in the high persulfate concentration controls. Loss of persulfate to acid-catalyzed degradation has been observed to be detrimental to persulfate treatment efficiency of some organic contaminants (Liang et al., 2007).

Consistent with the notation used in (House, 1962), the overall rate law for the decomposition of persulfate in acid to neutral conditions in an aqueous solution (no solids present) is given as

$$\frac{d[S_2O_8^{2-}]}{dt} = -k_1[S_2O_8^{2-}] - k_2[H^+][S_2O_8^{2-}] = -(k_1 + k_2[H^+])[S_2O_8^{2-}] \quad (2.4)$$

where k_1 is the first-order reaction rate coefficient for uncatalyzed degradation of persulfate (Eq. 2.2), and k_2 is the second-order reaction rate coefficient for acid catalyzed degradation of persulfate (Eq. 2.3) estimated as 1.1×10^{-1} L mol^{-1} day^{-1} at 20 ^{o}C (House, 1962).

In general, the solution pH in all the aquifer material systems decreased from the initial pH value due to the generation of H^+ during persulfate degradation (Eq. 2.2) although the pH profiles were different for the two concentrations employed (Figure 2.1). As expected the decrease in pH was more pronounced in the high persulfate concentration systems since the degradation of a higher persulfate concentration generates a larger H^+ concentration. The significant pH decrease observed in the controls due to persulfate degradation was not, in general, observed in the presence of aquifer materials due to the buffering capacity of the solids. The total organic carbon (TOC) content is only a small fraction of the total carbon (TC) content for 5 of the 7 aquifer materials used in this study (Table 2.1), and this high TC content is primarily due to the presence of calcite (carbonate) (Xu and Thomson, 2010).

Since the buffering capacity of carbonate minerals is well known (Langmuir, 1997) it is expected that as persulfate is degraded, the high buffering capacity solids (i.e., Borden, LC34-LSU, LC34-USU, NIROP) would maintain the solution pH at near initial levels while the solution pH associated with the lower buffering capacity solids (i.e., DNTS, LAAP, MAAP) would decrease continuously. In fact, the aquifer material with the lowest TC content (i.e., MAAP) shows the largest reduction in solution pH for both persulfate concentrations. As the rate of H^+ production decreases at later times the solution pH associated with the strongly buffered systems show a slight rebound. By Day 40, a solution pH ~3 was observed in the MAAP aquifer material systems at the high persulfate concentration and further decreased to ~1 by Day 290. It was assumed that acid-catalyzed degradation was responsible for the enhanced persulfate degradation observed beyond Day 80 for the high persulfate concentration MAAP aquifer material systems.

For all aquifer materials the decrease in persulfate concentration followed a first-order kinetic mass action law which is consistent with the decomposition of persulfate in the presence of catalysts and other reductants in aqueous systems, and in the presence of soil (Kolthoff and Miller, 1951; Kolthoff et al., 1951; House, 1962; Berlin, 1986; Johnson et al., 2008). To avoid complexities arising from acid-catalyzed persulfate decomposition for the MAAP aquifer material the degradation kinetics for this system at the high persulfate concentration were determined using data collected during the first 80 days. Best-fit reaction rate coefficients (k_{obs}) for the low persulfate concentration systems varied from 10^{-3} to 10^{-2} day^{-1} for the 7 aquifer materials used (Table 2.1). The k_{obs} for the high concentration experiments was estimated to be between 6 to 39% of the k_{obs} for the low concentration experiments indicating higher persulfate stability at higher concentrations given the same

mass of aquifer solids. In general, the estimated k_{obs} show that persulfate half-life varies from ~15 to 600 days in the presence of aquifer materials over a range of persulfate concentrations and hence appears to be stable at this scale of investigation. From the observed persulfate degradation trends it is clear that the stability of persulfate over a long-term (weeks to months) cannot be evaluated based on batch tests conducted over a 10-day period (Dahmani et al., 2006).

Since k_{obs} for the aquifer materials are up to an order of magnitude higher than those which can be estimated from Eq. 2.4 for pH > 3 at 20°C, the enhanced degradation of persulfate in the presence of aquifer solids is due to reactions with transition metal catalysts and other reductants (e.g., NOM and reduced inorganics) associated with these solids (Kislenko et al., 1996; Johnson et al., 2008). Persulfate reactions with mineral catalysts are not well-characterized (Johnson et al., 2008) but based on homogenous aqueous solution studies the persulfate degradation rate law in the presence of transition metal catalysts can be represented as first-order with respect to persulfate concentration and 3/2 order with respect to the catalyst concentration (House, 1962; Kislenko et al., 1995; Kislenko et al., 1996; Balazs et al., 2000). The reaction between persulfate and NOM is complicated (Berlin, 1986; Peyton, 1993; Cuypers et al., 2002; Eusterhues et al., 2003) and various reaction orders have been proposed provided there is no mass transport limitation (Goulden and Anthony, 1978; Berlin, 1986; Peyton, 1993, Balazs et al., 2000).

In this investigation we are interested in capturing the behavior of persulfate decomposition in subsurface systems so an appropriate rate expression can be given by

$$\frac{d[S_2O_8^{2-}]}{dt} = -(k_1 + k_2[H^+])[S_2O_8^{2-}] - k_{cat}[S_2O_8^{2-}][C_{cat}]^{n_{cat}} - k_{NOM}[S_2O_8^{2-}][C_{NOM}]^{n_{NOM}} \qquad (2.5)$$

with

$$[C_{cat}] = C_{cat}^{solids}\, m_{solids} / V_W \;, \quad \text{and} \quad [C_{NOM}] = C_{NOM}^{solids}\, m_{solids} / V_W \tag{2.6}$$

where k_{cat} is the mineral catalyzed reaction rate coefficient, k_{NOM} is NOM reaction rate coefficient, n_{cat} and n_{NOM} is the reaction order with respect to the catalysts and the NOM respectively, C_{cat}^{solids} is the solids catalyst concentration (mg/g), and C_{NOM}^{solids} is the solids NOM concentration (mg/g), m_{solids} is the mass of solids (g) and V_W is the aqueous volume (mL). For simplicity we have assumed that the reaction order with respect to persulfate is unity for all reactions. If the concentration of H^+, C_{cat} and C_{NOM} are assumed constant then a bulk pseudo first-order reaction rate coefficient (k_{bulk}) can be defined as

$$k_{bulk} = k_1 + k_2 [H^+] + k_{cat} [C_{cat}]^{n_{cat}} + k_{NOM} [C_{NOM}]^{n_{NOM}} \tag{2.7}$$

The k_{obs} estimated using all the data from low concentration experiments and the data from the early portion (≤ 40 days) of the high concentration experiments are strongly correlated ($r^2 \geq 0.95$) with the initial TOC and Fe_{Am} as given by

$$k_{obs,40}^{high} = (0.856 \pm 0.115) \times 10^{-3} [C_{NOM}]^{1.5} + (2.27 \pm 0.48) \times 10^{-3} [C_{cat}]^{1.5} \tag{2.8a}$$

$$k_{obs}^{low} = (13.9 \pm 1.7) \times 10^{-3} [C_{NOM}]^{1.5} + (32.3 \pm 7.1) \times 10^{-3} [C_{cat}]^{1.5} \tag{2.8b}$$

where C_{cat}^{solids} and C_{NOM}^{solids} in Eq. 2.6 are represented by the concentration of Fe_{Am} and TOC respectively with a m_{solids}/V_w of 1 g/mL. In general, a n_{NOM} of 1.5 provided a higher

correlation as compared with n_{NOM} of zero to 1. These relationships are also synonymous with observations made using permanganate or peroxide (Xu and Thomson, 2008, 2010) and support the functional form of Eq. 2.7 when $k_1 + k_2[H^+] << k_{obs}$.

Ionic Strength. It has been shown that an increase in ionic strength has a detrimental effect on k_{cat} and k_2 (Kolthoff and Miller, 1951; Henderson and Winkler, 1959; House, 1962), and on the degradation of target organics (House, 1962; Sharp, 1973; Huang et al., 2002; Kim et al., 2009). The ionic strength is primarily controlled by the initial persulfate concentration, and as persulfate decomposes to sulfate (SO_4^{2-}) and acid (H^+), the ionic strength will be enhanced. Dissolution of calcite ($CaCO_3$) and other minerals in response to buffer H^+ production will release other ionic species. No attempt was undertaken to monitor the ionic strength during these experiments, but it is expected that the following ions would contribute: Na^+, $S_2O_8^{2-}$ H^+, SO_4^{2-} Ca^{2+}, HCO_3^-/CO_3^{2-} and some dissolved metals (e.g., Fe^{2+}, Fe^{3+}, Mn^{2+}). Over time the ionic strength will increase as persulfate degrades and this will result in the continual suppression of k_2, k_{cat} and k_{NOM}. During early time (≤ 40 days) when the changes in ionic strength can be ignored (Figure 2.2), the difference in the ionic strength for the two concentrations we used is mainly a result of the initial persulfate concentration. During this time period (0 to 40 days) the estimated k_{obs} for the two concentrations are highly correlated (r >0.96). Beyond Day 40, the k_{obs} for the high concentration experiments are likely to decrease as degradation proceeds because of an increase in ionic strength over time whereas the change in ionic strength in the low concentration experiments is relatively negligible. This trend was observed for 4 of the 7 aquifer materials (Borden, LC34-LSU, LC34-USU and NIROP) while an increase in the k_{obs} was determined for the remaining 3 materials (DNTS, LAAP, MAAP). The increase in k_{obs} corresponds with the onset of acid-

catalyzed reaction in the systems for these 3 low buffering capacity materials. Accounting for the effects of ionic strength, Eq. 2.7 can be written as

$$k_{bulk} = k_1 + \gamma_{S_2O_8^{2-}} \left(\gamma_{H^+} k_2[H^+] + \gamma_{cat}^{ncat} k_{cat}[C_{cat}]^{ncat} + \gamma_{NOM}^{nNOM} k_{NOM}[C_{NOM}]^{nNOM} \right) \quad (2.9)$$

Assuming $n_{cat} = n_{NOM} = 1.5$ from Eq. 2.8, the rate of homolytic cleavage is insignificant and pH>3, then k_{bulk} becomes

$$k_{bulk} = \gamma_{S_2O_8^{2-}} \left(\gamma_{cat}^{1.5} k_{cat}[C_{cat}]^{1.5} + \gamma_{NOM}^{1.5} k_{NOM}[C_{NOM}]^{1.5} \right) \quad (2.10)$$

Activity coefficients, $\gamma_{S_2O_8^{2-}}$ and γ_{cat} were estimated to be 0.662 and 0.255 at the low and the high persulfate concentrations respectively using the extended DeBye-Hückel approximation and initial ionic strengths. We assumed that Fe_{Am} is represented by Fe^{2+} as the active species. Due to lack of information on NOM, the estimate for γ_{cat} was arbitrarily applied to γ_{NOM} at the two ionic strengths such that $\gamma_{cat} = \gamma_{NOM} = \gamma_{reactants}$, and Eq. 2.10 can be rewritten as

$$k_{bulk} = \gamma_{S_2O_8^{2-}} \gamma_{reactants}^{1.5} (k_{cat}[C_{cat}]^{1.5} + k_{NOM}[C_{NOM}]^{1.5}) \quad (2.11)$$

The k_{obs} at high and low concentration were normalized by $\gamma_{cat} \gamma_{reactants}^{1.5}$ and the 14 normalized k_{obs} values were used to develop ($r^2 = 0.84$)

$$k_{obs}^0 = (32.4 \pm 5.1) \times 10^{-3}[C_{NOM}]^{1.5} + (79.6 \pm 21.0) \times 10^{-3}[C_{cat}]^{1.5} \quad (2.12)$$

Eq. 2.12 can be combined with Eq. 2.9 to yield

$$k_{bulk} = k_1 + \gamma_{S_2O_8^{2-}} \left\{ \gamma_{H^+} k_2 \left[H^+ \right] + \gamma_{\text{reactants}}^{1.5} \left(32.4 \times 10^{-3} \left[C_{NOM} \right]^{1.5} + 79.6 \times 10^{-3} \left[C_{cat} \right]^{1.5} \right) \right\} \quad (2.13)$$

that can be used to estimate persulfate degradation in the presence of aquifer materials where Fe_{Am} represents the mineral catalyst and TOC represents the NOM.

Depletion of Reactants. The use of k_{bulk} as defined in Eq. 2.13 represents a "pseudo" first-order rate coefficient since TOC and Fe_{Am} may be depleted while the H^+ concentration generally increases over time. One potential avenue to assess loss of the overall reduction capacity of the aquifer solids is to examine changes in the COD test results.

Fe_{Am} may exist as Fe^{2+} or Fe^{3+} and activation of persulfate by Fe^{2+} will result in the formation of Fe^{3+}. It has been shown that Fe^{3+} can also activate persulfate, or can form organo-complexes resulting in the regeneration of Fe^{2+} (Henderson and Winkler, 1959; Kislenko et al., 1995; Block et al., 2004). Hence, the total concentration of Fe ions capable of persulfate activation may not deplete over time supporting the notion of a constant k_{obs} with respect to Fe_{Am} in a batch system.

The NOM content is very likely to decrease but the exact rate and extent of NOM loss may not be entirely predictable. Persulfate oxidation of NOM is complicated and depends upon a number of factors including the NOM form, desorption, protection by mineral surfaces, pH and clay content (Clifton and Huie, 1989; Menegatti et al., 1999; Cuypers et al., 2002; Eusterhues et al., 2003; Mikutta et al., 2005).

COD test results illustrated loss of the overall reduction capacity of the aquifer solids (Figure 2.3). In general, there was a reduction in the COD values following persulfate exposure with a maximum of ~42±10% reduction for the NIROP aquifer material at the low concentration and ~65±12% reduction for Borden aquifer material at the high concentration. For the high concentration experiments, the reduction in COD after ~300 days of persulfate exposure was greater than that for low concentration experiments for the same aquifer material implying that a higher persulfate concentration and a longer exposure time can lead to a greater depletion of the reductive capacity. The observed COD reduction was statistically significant (*t*-test, $\alpha = 0.05$) for all aquifer materials except for the LAAP and LC34-USU aquifer materials at both persulfate concentrations, and the LC34-LSU and MAAP aquifer materials at the low persulfate concentration. Since the NOM associated with the aquifer materials used in this study is mainly responsible for the TRC as captured by the COD test (Xu and Thomson, 2008), a significant reduction in COD implies a significant oxidation of NOM occurred as a result of persulfate exposure. This reduction in NOM was statistically significant for 5 of 7 aquifer materials at the high persulfate concentration, and only 3 of 7 aquifer materials at the low persulfate concentration.

Although, the persulfate mass employed in the high concentration experiments exceeded the stoichiometric requirement to satisfy the initial COD for all aquifer materials except LC34-LSU, the maximum observed depletion of 65±12% over ~300 days exposure period indicates that not all of the aquifer material reductive capacity as captured by the COD test can be satisfied by persulfate (Dahmani et al., 2006). Aquifer materials with high clay content (e.g., LAAP) can be expected to be more resistant to NOM oxidation by persulfate (Eusterhues et al., 2003) as was observed at both concentrations. Although no experimental

investigation was undertaken to evaluate the organo-chemical composition of NOM, it is speculated that LC34-USU has a relatively condensed form of OM and hence exposure to persulfate resulted in an insignificant change in COD.

Based on COD results, the estimated k_{obs} for the LAAP and LC34-USU aquifer materials (low and high concentration) and for the LC34-LSU and MAAP aquifer materials (low concentration) can be assumed to represent first-order persulfate degradation rates. For the remaining five materials at the high concentration and three materials at low concentration the k_{obs} represents an underestimated first-order rate coefficient since the concentration of reactant (NOM represented as TOC) likely decreased. Correlation of the observed COD reduction with k_{obs} or persulfate mass loss was low ($r < 0.45$) suggesting that a significant portion of the observed persulfate mass loss was due to catalytic processes rather than only due to the persulfate reaction with NOM.

2.3.2. Column Tests

During the persulfate flush the column effluent concentration quickly reached the injection concentration indicating that little persulfate decomposition occurred over this period. The normalized persulfate concentration profiles from the stop-flow experiments for each aquifer material (Figure 2.4) indicate that persulfate degradation rates can be represented by a first-order rate law consistent with the batch experiment results (k_{obs} of 10^{-3} to 10^{-1} day^{-1}). The k_{obs} from the stop-flow column tests which are more representative of an *in situ* oxidant to solids mass ratio of 0.25 g/kg were ~8 times ($r^2 > 0.99$) higher than the corresponding batch test k_{obs} (Figure 2.5).

For these column experiments the k_{bulk} as given by Eq. 2.13 is appropriate and the only difference between the batch and column experiments is the larger solids to solution ratio (1

g/mL vs. 3.9±0.4 g/mL). This will manifest as an increase in the concentration of the catalyst and NOM (Eq. 2.6), and the average k_{bulk} ratio for the column and batch tests is given by

$$\frac{k_{bulk}^{column}}{k_{bulk}^{batch}} = \left(\frac{m_{solids}^{column} / V_w^{column}}{m_{solids}^{batch} / V_w^{batch}} \right)^{1.5} = \left(\frac{3.9}{1} \right)^{1.5} = 7.7 \qquad (2.14)$$

which is very similar to the observed ratio. This indicates that persulfate degradation kinetics is scalable from the batch to the *in situ* scale. The ratio m_{solids}/V_w will likely govern the availability or dissolution of aquifer material-bound active species (i.e., TOC and Fe_{Am}) in the aqueous phase (Langmuir, 1997).

Oxidant to Solids Mass Ratio. The eightfold increase in k_{obs} from the batch to the column experiments, and multifold decrease for the batch experiments from the low to the high concentration experiments represents a strong dependence of persulfate decomposition on the oxidant to solids mass ratio which correspondingly decreased from 1.0 to ~0.25 g/kg at the low concentration between batch and column experiments. Given that the column results are more representative of potential *in situ* oxidant to solids mass ratio, persulfate half-lives of 2 to 90 days may be more appropriate than those reported from the batch tests. This dependence was further examined through additional batch and column tests.

Based on the batch and column test results, k_{obs} was found to depend upon oxidant to solids mass ratio. For further examination of this dependence, an additional batch reactor system with 150 g of aquifer solids at the low persulfate concentration, and a stop-flow column experiment with a 2 g/L persulfate concentration were conducted using the LC34-LSU aquifer material. The data from these additional experiments (Figure 2.6) indicate a higher k_{obs} from the batch experiment and lower k_{obs} from the column experiment. These

changes in k_{obs} are consistent with changes in the oxidant to solids mass ratio in these additional experiments and demonstrate that an increase in the oxidant to solids mass ratio decreases the persulfate degradation rate.

In general, the data including these additional results indicate that approximately an order of magnitude increase in the oxidant to solids mass ratio leads to an order of magnitude decrease in k_{obs} across all aquifer materials used in this study (Figure 2.7).

Depletion of Reactants. Results from the COD tests conducted on sub-samples collected from three locations (0, 20 and 40 cm from the bottom) of each column capture the impact of persulfate exposure on depletion of TRC of the aquifer materials (Figure 2.3). Since repeated pore water sampling was performed at the bottom of the column and subsequent de-saturation was observed at the top, samples collected from the three locations are representative of persulfate exposure time. The solids samples collected at 0 cm were the most exposed while the samples collected at 40 cm were the least exposed to persulfate. Similar to the findings from the batch experiments, the LAAP, LC34-LSU, and LC34-USU aquifer materials showed no significant difference in the COD results at the three sampling locations following persulfate exposure relative to the initial COD value indicating that minimal depletion of TRC occurred. The remaining four aquifer materials showed a moderate (Borden – 20 to 30%; NIROP – 10 to 20%) to a high (DNTS – 60 to 80%; MAAP – 4 to 90%) decrease in the COD results at the three sampling locations relative to the initial COD. For the materials that showed a significant decrease in COD the depletion was directly proportional to the exposure time with the greatest decrease in COD at the bottom of the column. Since this observation violates the fundamental assumption under which the stop-

flow mode of column operation was used, the k_{obs} estimated from these column experiments is underestimated.

2.3.3. Push-Pull Tests

The injected persulfate and tracer solution will distribute within the aquifer leading to variable initial concentration of the ions involved ($S_2O_8^{2-}$, Na^+, Li^+, Cl^-). Since Li^+ is conservative, the initial distribution of the injection solution can be estimated from the Li^+ concentration. During an extraction episode the Li^+ data should provide information on the initial condition of the injected solution in the sampled zone. Therefore, Li^+ data from each sampling event was assumed to represent the initial concentrations of the ions in the sampled zone and was used to estimate the initial ionic strength for each zone. A non-monotonic Li^+ concentration profile as sampling proceeded implies that the injection solution was not ideally distributed around the injection point. However, persulfate within these zones should then undergo degradation at the rate controlled by the initial ionic strength (Eq. 2.13).

Dispersion of the persulfate solution during injection will lead to radially decreasing persulfate concentration as we move away from the injection point. The farthest zones will have a lower ionic strength and persulfate will undergo degradation at higher k_{bulk} as compared with zones closer to the drive point. Therefore, sampling of more distal zones (as indicated by lower Li^+ concentrations) during successive sampling events will lead to a persulfate concentration profile similar to the experimental curves with apparently lower degradation at early time and higher degradation at later time.

Assuming homolytic cleavage is insignificant, the buffering capacity of the Borden aquifer will maintain a pH>3, and using C_{NOM} and C_{cat} from Table 2.1 and a m_{solids}/V_w (≡(1-

porosity)$\rho_{particle}$/porosity) of 5.5, the theoretical persulfate degradation is then given by (from Eqs. 2.5 and 2.13)

$$\frac{d[S_2O_8^{2-}]}{dt} = -0.218\,\gamma_{S_2O_8^{2-}}\,\gamma_{reactants}^{1.5}[S_2O_8^{2-}] \qquad (2.15)$$

Both activity coefficients in Eq. 2.15 can be estimated from the initial ionic strength appropriate for the aquifer zone captured by each sampling episode. Comparison of the observed and theoretical persulfate concentration push-pull profiles at both the low and high concentrations is excellent ($r > 0.94$) (Figure 2.8). This implies that the expression derived from bench-scale data (Eq. 2.13) can be used to predict *in situ* behavior as represented in a push-pull test.

Under an ideal distribution of injected solution such that a constant concentration exists around the injection point, persulfate degradation would be expected to proceed at a constant rate throughout the zone of influence. The expected first-order reaction rate coefficients governed by the initial ionic strength under these ideal conditions are estimated to be 2.82×10^{-2} day^{-1} for the low concentration, and 2.87×10^{-3} day^{-1} for the high concentration.

2.4. IMPLICATIONS

The findings reported here have implications on the use and persistence of persulfate at the field-scale. For all the aquifer materials investigated persulfate mass was lost continually and an ultimate persulfate NOD was not determined. The decomposition of persulfate followed the behavior of peroxide. However, the kinetic data indicate that unactivated persulfate is relatively stable over a wide range of concentrations.

Pilot-scale data are representative of *in situ* conditions while bench-scale kinetic data underestimate the half-life by more than an order of magnitude. Either an increase in ionic strength or concentration of persulfate per unit mass of aquifer solids will increase the stability of persulfate. Hence, an increase in the injected persulfate concentration will enhance the persistence of persulfate which will allow for advective, dispersive and diffusive mechanisms to transport persulfate away from the injection/release locations ensuring greater coverage of the treatment zone. The observed reaction rate coefficients are highly dependent on the initial TOC and Fe_{Am} content of the aquifer solids and knowledge of these properties can provide insight into persulfate stability. Poorly buffering aquifer solids will quickly establish acid-catalyzing conditions and lead to enhanced persulfate degradation. While enhanced persulfate degradation is detrimental to oxidant persistence and transport, the degradation pathway may involve activation of persulfate which may be beneficial for treatment of target organics.

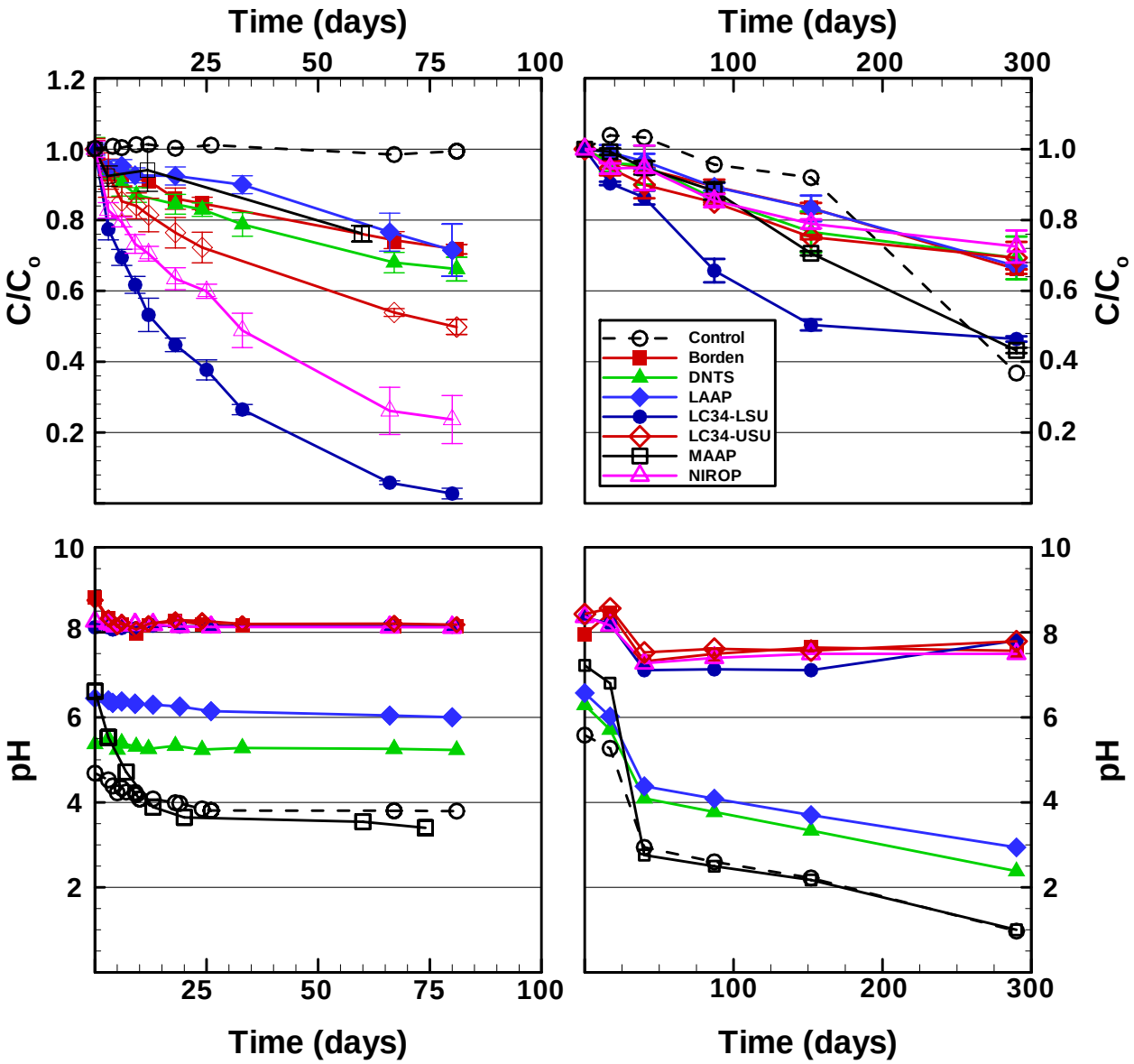

Figure 2.1. Persulfate and pH profiles from the batch test experiments for an initial persulfate concentration of (a) and (c) 1 g/L, and (b) and (d) 20 g/L.

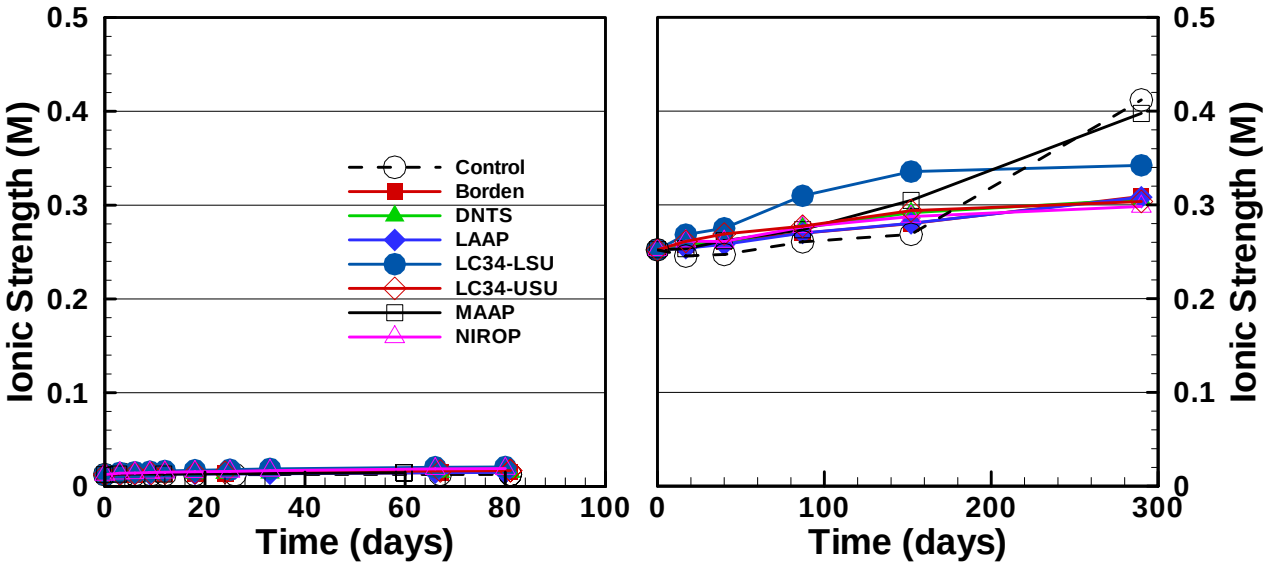

Figure 2.2. Ionic strength profiles for batch tests conducted at a persulfate concentration of (a) 1 g/L and (b) 20 g/L.

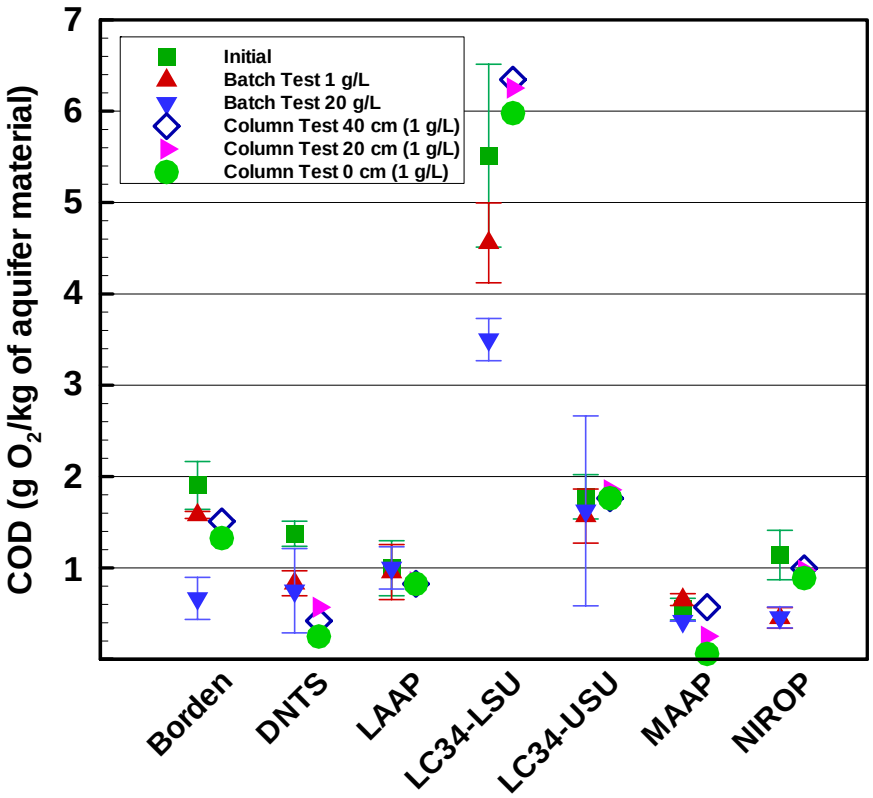

Figure 2.3. Change in chemical oxidant demand (COD) of the seven aquifer materials following exposure to persulfate during batch tests at 1 and 20 g/L, and column tests at 1 g/L.

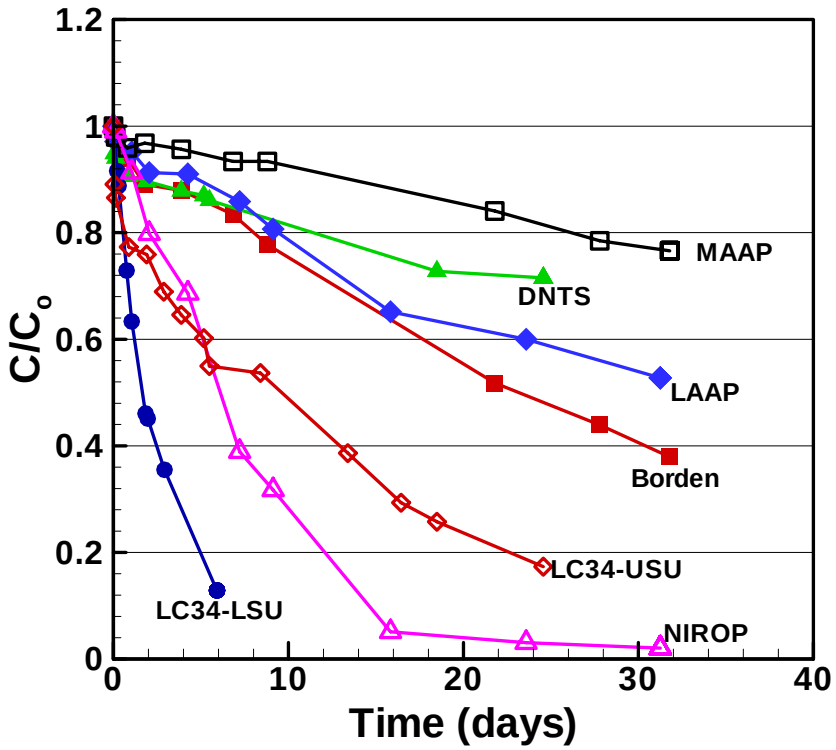

Figure 2.4. Persulfate profiles from stop-flow column experiments for an initial persulfate concentration of 1 g/L.

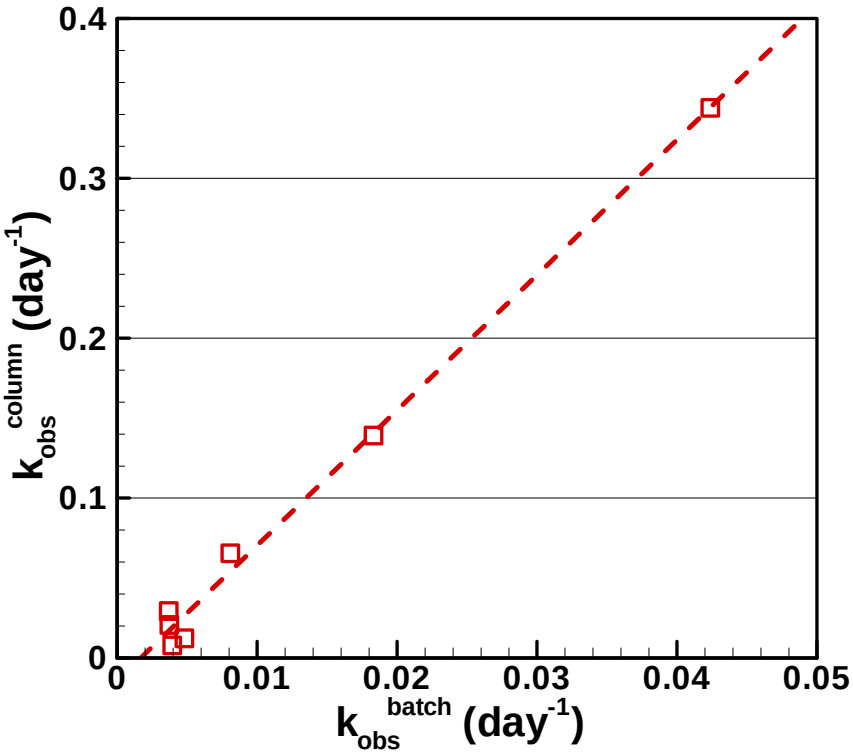

Figure 2.5. Stop-low column rate coefficients versus batch rate coefficients for experiments using a persulfate concentration of 1 g/L.

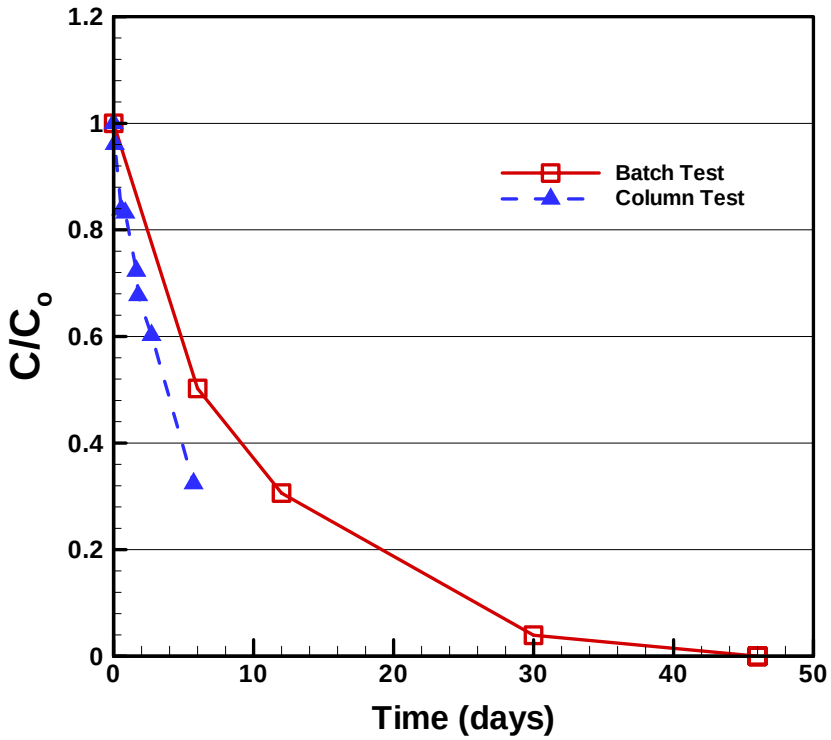

Figure 2.6. Persulfate profiles for batch test with 150 g LC34-LSU material at 1 g/L persulfate and column test with LC34-LSU material at 2 g/L persulfate.

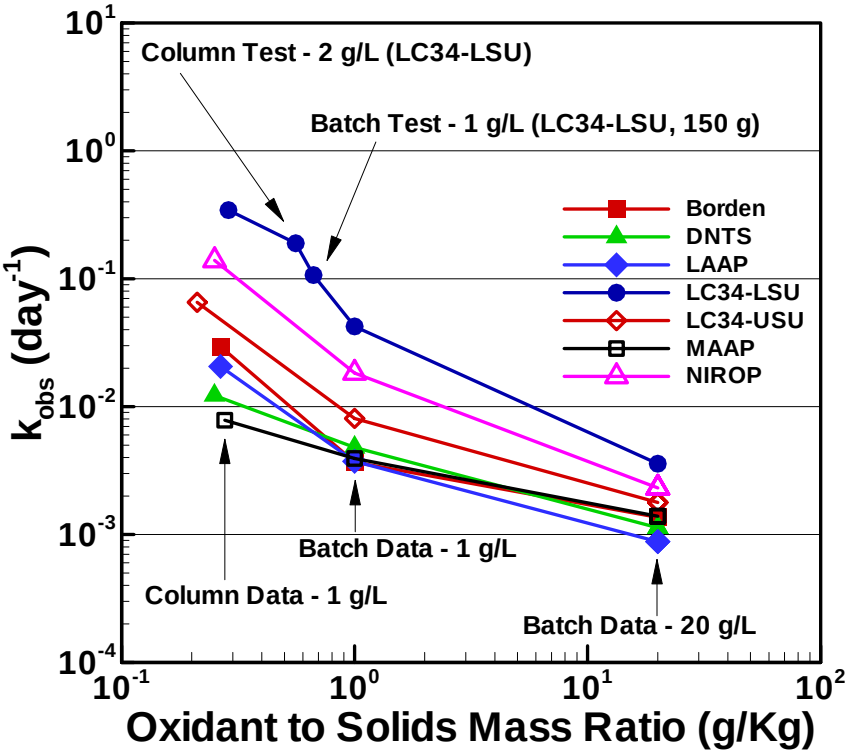

Figure 2.7. Bench-scale reaction rate coefficients as a function of oxidant to solids mass ratio.

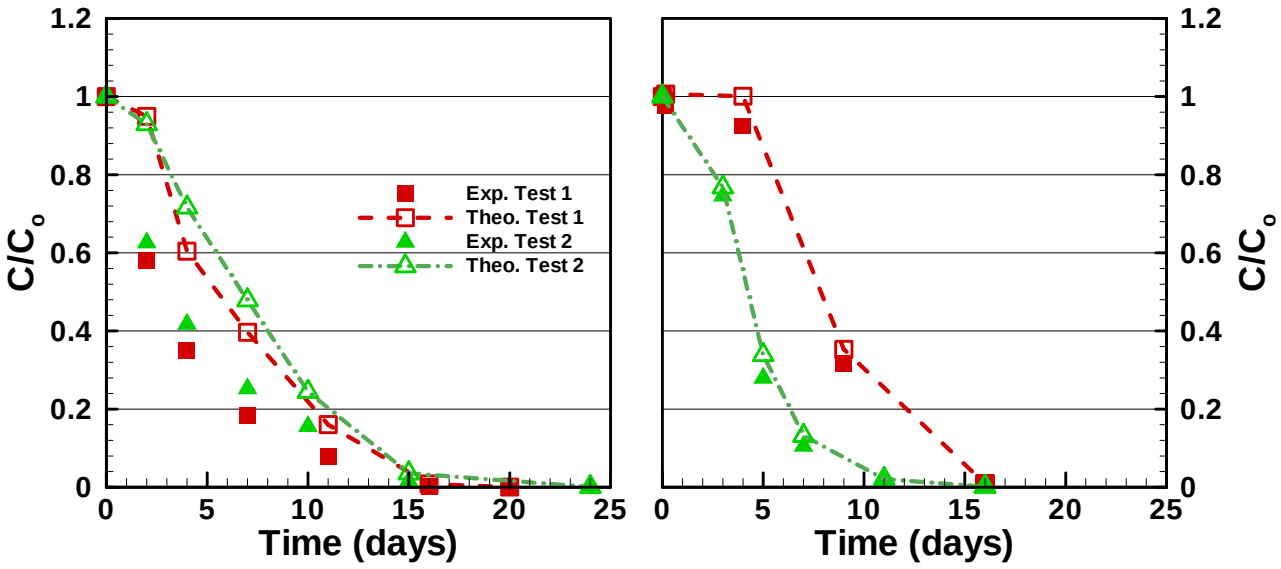

Figure 2.8. Experimental (bold symbols) and theoretical (open symbols and lines) persulfate profiles from multiple push-pull tests conducted at CFB Borden at an initial persulfate concentration of (a) 1 g/L and (b) 20 g/L.

Table 2.1. Selective chemical properties of aquifer materials and persulfate degradation first-order reaction rate coefficients estimated from the batch and column data

Site ID	TC[a] [mg/g]	TOC[a] [mg/g]	Total Fe[a] [mg/g]	Fe_{Am}[a] [mg/g]	Total Mn[a] [mg/g]	Mn_{Am}[a] [mg/g]	Pre-oxidation COD[b] [g O_2/ kg solids]	k_{obs}[c], [10^{-4} day^{-1}] (Half-life, [day]) Batch 1 g/L	Batch 20 g/L	Column 1 g/L
Borden	15.8	0.24	17.5	0.30	0.421	0.004	1.903	36.8 ± 2.1 (188.2)	13.6[d], 13.3 ± 0.5 (521.0)	293.6 ± 7.1 (23.6)
DNTS	1.4	0.28	63.8	0.36	0.154	0.002	1.374	48.1 ± 2.1 (144.2)	11.3[d], 13.3 ±1.3 (521.0)	122.5 ±12.2 (56.6)
LAAP	0.6	0.46	22.7	0.26	0.112	0.007	0.997	37.3 ± 2.7 (186.7)	8.8[d], 13.7 ± 0.7 (505.5)	206.1 ± 10.2 (33.6)
LC34-LSU	41.5	1.84	6.1	0.50	0.068	0.002	5.513	423.8 ± 5.7 (16.4)	35.8[d], 28.4 ± 2.9 (243.9)	3440.7 ± 107.3 (2.0)
LC34-USU	31.5	0.88	3.7	0.41	0.098	0.002	1.778	80.9 ± 3.6 (85.7)	17.8[d], 12.7± 1.2 (546.9)	654.4 ± 22.2 (10.6)
MAAP	0.1	0.77	0.9	0.04	0.025	0.008	0.549	39.3 ± 3.2 (176.3)	13.9[d], 15.2 ± 1.5[e] (457.3)	78.3 ± 3.3 (88.5)
NIROP	35.5	0.32	12.9	0.75	0.297	0.033	1.140	183.2 ± 6.6 (37.8)	23.1[d], 10.9 ± 1.2 (637.2)	1391.1 ± 104.3 (5.0)

[a]Aquifer material properties from Xu and Thomson (2008). TC=Total carbon, TOC=Total organic carbon, Fe=Iron, Mn=Manganese, Fe_{Am} and Mn_{Am} refer to amorphous iron and manganese respectively, COD=Chemical oxygen demand

[b]COD was estimated following method developed by Xu and Thomson (2008)

[c]Error based on ± 95% confidence interval

[d]Rate constant based on data collected for ≤ 40 days

[e]Rate constant based on data collected for ≤ 87 days

Chapter 3

Stability of Activated Persulfate in the Presence of Aquifer Solids

Overview

Bench-scale experiments were performed to investigate the persistence of activated persulfate at two concentrations (1 or 20 g/L) using citric acid (CA) chelated ferrous (Fe(II)), peroxide (H_2O_2) or hydroxide (OH^-) activation in the presence of well-characterized aquifer materials. Chelated-Fe(II) trials were conducted at 150 or 600 mg/L Fe(II) and CA:Fe(II) molar ratio of 0.2 or 1. H_2O_2 was employed at four concentrations (0.01, 0.1, 1 or 10 mol H_2O_2/mol $S_2O_8^{2-}$) and OH^- was used at three concentrations to achieve initial pH conditions of 10, 11 or 12. Chelation by citric acid was ineffective in controlling the interaction between persulfate and Fe(II) and rapid oxidation of Fe(II) was observed which caused a rapid initial decrease in persulfate concentration. Subsequent to this rapid loss of persulfate, first-order degradation rate coefficients (k_{obs}) were estimated which were up to 4 times higher than the unactivated case due to the interaction with Fe(III) and CA. Total oxidation strength (TOS) was measured for peroxide activation experiments and was observed to decrease rapidly at early time due to peroxide degradation. This was followed by slow degradation kinetics similar to that of unactivated persulfate implying that the initial TOS degradation was peroxide-dominated and the long-term kinetics were dominated by persulfate degradation. The k_{obs} used to capture TOS degradation for later time were shown to depend upon unactivated persulfate and peroxide degradation rate coefficients, and peroxide concentration. Either a slow peroxide degradation rate and/or higher peroxide concentration allow a longer time for peroxide and persulfate to interact which led to k_{obs} ~1 to 100 times higher than k_{obs} for unactivated persulfate. For alkaline activation, k_{obs} were only 1 to 4 times higher than unactivated persulfate and therefore alkaline conditions demonstrated the least impact on persulfate degradation among the various activation strategies used. For all

activation trials, lower stability of persulfate was observed at 1 g/L as compared to 20 g/L due to insufficient persulfate and/or ionic strength effects.

3.1. INTRODUCTION

Sodium persulfate ($Na_2S_2O_8$) is the latest oxidant to be proposed for *in situ* chemical oxidation (ISCO) applications and has been demonstrated to have immense potential for the remediation of contaminated soil and groundwater (Watts and Teel, 2006; Liang et al. 2008; Sra et al., 2010a). Unactivated persulfate is relatively stable in the presence of aquifer solids and can be used to treat a wide range of target contaminants (Kolthoff et al., 1951; Huang et al., 2002; Sra et al. 2010a,b). However, direct persulfate oxidation has limited reactivity towards some organic contaminants (e.g., saturated chlorinated solvents, normal chain alkanes) (Block et al., 2004). The oxidation potential and reactivity of persulfate towards a wider range of organic compounds can be enhanced by its activation to free radicals and other highly oxidative species (e.g., $SO_4^{-\bullet}$, $OH^{\bullet}$, $O_2^{-\bullet}$ H_2O_2, $HO_2^{\bullet}$, H_2SO_5) (Anipsitakis and Dionysiou, 2004; Tsai et al., 2008; Block et al., 2004; Miraglio, 2009; Sra et al., 2010a). The choice of an activation system will depend upon its impact on the oxidation of target organic compounds, its ease of applicability in the subsurface, and its effect on the persistence of the persulfate-activator system in the presence of aquifer materials (Block et al., 2004).

A number of activation strategies have been proposed and are being investigated for potential use in the subsurface (e.g., chelated-iron, hydrogen peroxide, hydroxide and heat) (Kolthoff et al., 1951; Liang et al. 2004; Crimi and Taylor 2007; Huang et al., 2005; Liang et al. 2003; Sra et al. 2010a). While higher costs preclude the widespread use of heat as an activator, research over the past 5 years has mainly focused on the use of chelated-iron, peroxide or hydroxide as activating agents, and oxidation by activated persulfate has been shown to be very effective and efficient in the treatment of the target organics (e.g., petroleum hydrocarbons (PHCs), polycyclic aromatic hydrocarbons (PAHs) and chlorinated

solvents) (Anipsitakis and Dionysiou, 2004; Huang et al., 2005; Crimi and Taylor, 2007; Liang et al., 2008; Sra et al., 2010a).

Although the use of activating agents in conjunction with persulfate increases the reactivity of the oxidant system by producing a suite of active species, the overall persistence of persulfate in this system will be influenced by the interaction of persulfate, activators and reactive species with each other and with the aquifer materials (Liang et al. 2004, Crimi and Taylor 2007). For a viable and cost-effective ISCO technology, a persistent persulfate-activator system is required to achieve effective spatial coverage across the treatment area allowing time for dispersive and diffusive transport, and reactions with target organic compounds to occur. In order to make an informed decision on which, if any, persulfate-activator system to use, the physico-chemical conditions of the site represented by the aquifer materials and their interaction with a persulfate-activator system must be explored (Watts and Teel, 2005; Crimi and Taylor, 2007). However, there has been no peer-reviewed literature reporting on the stability of the various persulfate-activator systems in the presence of aquifer materials. The persistence of unactivated persulfate was investigated by Sra et al. (2010b), and first-order persulfate degradation rate coefficients were shown to depend upon total organic carbon (TOC) and amorphous iron (Fe_{Am}) content of the aquifer materials, and the persulfate to solids mass ratio. Enhanced ionic strength resulting from an increase in persulfate concentration suppressed the rate coefficients. This effort is used here as the basis to evaluate persulfate persistence in the presence of aquifer materials under activated conditions.

During the current investigation, bench-scale experiments were conducted to evaluate the persistence of persulfate or total oxidant strength (TOS) for three activation strategies in the

presence of aquifer materials. While peroxide strength is inherently captured within TOS, the semi-quantitative analysis of the evolution of the activating conditions (total Fe and pH) was also undertaken over the experimental period. The results from this study will assist in establishing guidelines for *in situ* applications of activated persulfate.

3.2. BACKGROUND

3.2.1 Chelated-Iron Activation

Activation by transition metals such as Fe(II) is known to accelerate persulfate reactivity through a one electron transfer process resulting in the formation of sulfate radicals ($SO_4^{-\bullet}$) at ambient temperature conditions (Kolthoff et al., 1951; House, 1962; Block et al., 2004; Dahmani et al., 2006) as given by

$$S_2O_8^{2-} + Fe^{2+} \rightarrow SO_4^{-\bullet} + SO_4^{2-} + Fe^{3+} \quad (k_1 \sim 83.3\ M^{-1}s^{-1}, \text{Kolthoff et al., 1951}) \qquad (3.1)$$

The resulting free radical can react with target organic compounds or oxidize Fe(II) to Fe(III) as

$$SO_4^{-\bullet} + Fe^{2+} \rightarrow SO_4^{2-} + Fe^{3+} \qquad (k_2 \sim 1 \times 10^9\ M^{-1}s^{-1}, \text{Neta et al., 1988}) \qquad (3.2)$$

The loss of persulfate and Fe(II) is governed by the reaction rate coefficients (i.e., k_1 and/or k_2). While a high k_1 implies low persulfate stability, a high k_2 implies loss of Fe(II) or activator strength. It is speculated that Fe(III) may also activate persulfate (Block et al., 2004) but may be less reactive (Crimi and Taylor, 2007), or under certain conditions may be converted to Fe(II) (House, 1962; De Laat and Gallard, 1999; Anipsitakis and Dionysiou, 2004). Fe(II) and Fe(III) can precipitate under neutral to alkaline conditions leading to

catalyst drainage from the aqueous phase. Therefore, in order to control the interaction between Fe(II) and persulfate, Fe(II) is chelated using chemical reagents such as citric acid (CA), ethylene diamine tetraacetic acid (EDTA), and ethylene diamine disuccinic acid (EDDS). Acid based chelating agents may maintain a higher Fe(II) or Fe(III) for a longer period of time and prevent drainage of the activators from the aqueous system (Rastogi et al., 2009). CA is capable of producing more stable complexes as compared to other chelating agents (Liang et al., 2004, 2008; Killian et al., 2007) and is biodegradable and environmentally friendly (Muller et al. 1996; Li et al., 2005). The effectiveness of a chelating agent depends upon the relative concentrations, and the CA:Fe(II) molar ratios ranging from 0.2 to 2 have been employed in bench-scale treatability of organic compounds (Liang et al., 2004, 2008; Crimi and Taylor, 2007). The concentration of Fe(II) is identified as a potential controlling factor in this activation scheme, and therefore an optimum concentration range of Fe(II) (150 to 600 mg/L) is usually recommended (Block, 2008). The presence of chelating agents may enhance the availability of transition metals (e.g., Fe, Mn) associated with aquifer materials and CA may be oxidized by persulfate (Rastogi et al., 2009). Aquifer materials can also interfere with the catalyzation of persulfate by chelated-iron (Dahmani et al., 2006).

3.2.2. Peroxide Activation

Hydrogen peroxide is also used to activate persulfate to potential radicals and other reactive species (e.g., $SO_4^{-\bullet}$ $OH^{\bullet}$) (Kwan and Voelkar, 2003). This hypothesized suite of multi-radicals may be capable of enhancing the oxidation rates of a number of organic compounds and hence improve the applicability of persulfate ISCO technology (Block et al., 2004; Watts and Teel, 2005; Crimi and Taylor 2007). This persulfate-peroxide system involves complex

reactions and oxidation mechanisms which are not clearly understood. Peroxide reactivity with minerals associated with aquifer materials may initiate and promote the formation of free radicals which can then activate persulfate (Kwan and Voelkar, 2003; Block et al., 2004). The elevation in temperature due to exothermicity of peroxide degradation in the aqueous phase may also contribute to persulfate activation (Watts and Teel, 2005; Cronk and Cartwright, 2006). Direct reaction between peroxide and persulfate may produce oxygen involving sulfate radicals ($SO_4^{-\bullet}$), hydroperoxide (HO_2^-) and hydroxyl radical ($OH^\bullet$) as intermediates (House, 1962). Peroxide is a strong oxidant (E^o = 1.8 V) and can react with target organics, aquifer material constituents and other reactive species. However, its use is limited by its rapid decomposition in aquifer media, particularly in solids with a high Fe_{Am} content, which restricts oxidant transport, spatial coverage and effectiveness (Watts and Teel, 2006; Xu and Thomson, 2010). Since persulfate is more stable than peroxide (Sra et al., 2010), the strength and persistence of this cooxidant system will depend upon their relative concentrations or the H_2O_2: $S_2O_8^{2-}$ molar ratios.

3.2.3. Hydroxide/Alkaline Activation

Use of hydroxide (OH^-) to create highly alkaline conditions (pH ≥10) has been suggested to be the most aggressive form of persulfate activation (Block et al., 2004). It has been reported that persulfate in an excess of OH^- may promote the formation of HO_2^- which can react with persulfate to yield $SO_4^{-\bullet}$ and superoxide radicals ($O_2^{-\bullet}$). Once formed, $SO_4^{-\bullet}$ can then react with OH^- resulting in the formation of $OH^\bullet$ given by the following sequence (Hayon et al., 1972; Miraglio, 2009):

$$S_2O_8^{2-} + 3OH^- \rightarrow HO_2^- + 2SO_4^{2-} + H_2O \qquad (3.3)$$

$$S_2O_8^{2-} + HO_2^- + OH^- \rightarrow 2SO_4^{2-} + SO_4^{-\bullet} + O_2^{-\bullet} + H_2O \quad (3.4)$$

$$SO_4^{-\bullet} + OH^- \rightarrow SO_4^{2-} + OH^{\bullet} \quad (3.5)$$

Alternately, hydroxide activation can result in persulfate fission to peroxymonosulfate (SO_5^{2-}) which decomposes to form sulfate and oxygen (Chandra and Venkatrao, 1976) according to

$$S_2O_8^{2-} + OH^- \rightarrow HSO_4^- + SO_5^{2-} \quad (3.6)$$

$$SO_5^{2-} \rightarrow SO_4^{2-} + 1/2\,O_2 \quad (3.7)$$

Similar to the other activation schemes, the excessive use of OH^- may be beneficial for destruction of target organics, but may compromise the overall effectiveness of the system by limiting the stability of persulfate and other oxidizing species. In order to maintain a suitablly high pH, acid production upon persulfate decomposition and buffering capacity of materials also need to be considered (Sra et al., 2010b).

3.3. MATERIALS AND METHODS

Sodium persulfate solutions ($Na_2S_2O_8$) (Aldrich Chem. Co., Milwaukee), activation solutions for ferrous sulfate heptahydrate ($FeSO_4 \cdot 7H_2O$) (J.T.Baker, Phillipsbourg, NJ) and citric acid ($C_6H_8O_7$, Fischer, Fair Lawns, NJ), (EMD Chemicals, Gibbstown), 30% hydrogen peroxide (H_2O_2, EMD, Gibbstown, NJ) or sodium hydroxide (NaOH, Fischer, Fair Lawns, NJ), analytical reagent solutions for ferrous ammonium sulfate (FAS) ($Fe(NH_4)_2(SO_4)_2 \cdot 6H_2O$), ammonium thiocyanate (NH_4SCN) (Baker, Phillipsbourg) and sulfuric acid (H_2SO_4) (EMD Chemicals, Gibbstown) were prepared to required concentrations using Milli-Q water. Four

aquifer materials identified as Borden, LC34-LSU, LC34-USU and NIROP (Xu and Thomson, 2009, 2010; Sra et al., 2010b) were used.

3.3.1. Methods

The objective of this investigation was to quantify the persistence of activated persulfate, and to examine the stability of the various activators. Concentration ranges for persulfate and activators were selected based on Sra et al. (2010b) and/or existing general guidelines (Block, 2008). The four selected aquifer materials exhibit a wide range of physical and chemical properties which may be representative of numerous sites suitable for ISCO applications. These materials were also used by Sra et al. (2010b) to illustrate unactivated persulfate stability.

All activated persulfate bench-scale experiments were conducted in nominal 40 mL reactors at two persulfate concentrations (1 or 20 g/L). Three activation strategies were employed – citric acid chelated-ferrous (CA-Fe(II)), hydrogen peroxide (H_2O_2) and hydroxide (OH^-). These experiments were performed in the presence of four well-characterized aquifer materials using solids that passed through the 2 mm sieve (Xu and Thomson, 2009, 2010; Sra et al., 2010b).

In general, a known mass of solids was loaded into the reactors followed by addition of Milli-Q water and persulfate stock solution. Following this, a specified volume of the activator stock solution was added to the reactors (see Table 3.1 for details). No-solids reactors for each experimental trial were also set up for the purpose of comparing persulfate response without the addition of aquifer materials. All trials were performed in duplicate. Following the addition of all reagents, each reactor was tightly capped with a Teflon septa

lined plastic cap and manually shaken for ~10 s. The reactors were then placed in the dark at ambient temperature (~20 ^{o}C) and were manually shaken multiple times between sampling episodes. Sampling was conducted more frequently at early times (<10 days) than at later times in response to persulfate and/or H_2O_2 degradation profiles. Experiments were terminated after 3 to 5 weeks. Data for unactivated trials are available in Sra et al. (2010b).

CA-Fe(II) activation experiments were conducted at a Fe(II) concentration of 150 mg/L (Fe_{low}) or 600 mg/L (Fe_{high}) at CA:Fe(II) molar ratios of 0.2 (CA_{low}) or 1.0 (CA_{high}). Hydrogen peroxide activation experiments encompassed four H_2O_2:$S_2O_8^{2-}$ molar ratios of 0.01, 0.1, 1.0 or 10 mol H_2O_2/mol $S_2O_8^{2-}$. Three different concentrations of sodium hydroxide (NaOH) were prepared at molar concentrations at 0.1, 1.0 and 10 mM such that the initial pH in the reactors was 10, 11 or 12.

3.3.2 Analytical Procedures

Persulfate or total oxidant analysis was performed following Huang et al. (2002) with a slight variation to account for soil coloration. For peroxide activation trials, the analytical method was assumed to capture the combined or total oxidant strength (TOS) and was defined as the strength of persulfate that was capable of forming an equivalent amount of ferric from excess ferrous (FAS) in a sample aliquot. Similar to persulfate (House, 1962; Killian et al., 2007), one mole of peroxide oxidizes two moles of Fe(II) when Fe(II) is used in excess (Mummery, 1913; Stirling, 1934) according to

$$S_2O_8^{2-} + 2Fe^{2+} \rightarrow 2SO_4^{2-} + 2Fe^{3+} \quad (3.8)$$

$$H_2O_2 + 2Fe^{2+} + 2H^{+} \rightarrow 2H_2O + 2Fe^{3+} \quad (3.9)$$

Therefore, the molar concentrations of persulfate and peroxide are assumed to be additive. TOS degradation was studied for this activation system to provide a comprehensive evaluation of the evolution of the oxidant strength. The TOS profiles were constructed using TOS normalized by the initial persulfate concentration (C_{TOS}/C_o). As expected, the initial C_{TOS}/C_o was measured to be between 1 and 11 as the H_2O_2:$S_2O_8^{2-}$ molar ratio was increased from 0 to 10.

Persulfate analysis relies upon the equivalent production of Fe(III) from oxidation of Fe(II) (source FAS) which is then measured on spectrophotometer following complexation with thiocyanate. During CA-Fe(II) activation trials, the presence of Fe(III) was expected in the samples. Therefore during persulfate analysis for these experiments, two spectrophotometer measurements were obtained from two sample aliquots withdrawn during each sampling event. The first measurement was obtained by immediate addition of thiocyanate to one sample and represented Fe(III) concentration in the reactor. For the second measurement, persulfate was allowed to oxidize the equivalent Fe(II) in FAS to Fe(III) after excess FAS was added. Therefore the second measurement represents the total Fe(III) in solution. Additional analytical experiments were conducted to confirm that persulfate and ferric concentrations were additive when employing this persulfate analysis method (data not reported here). Hence, the equivalent persulfate concentration was assumed to be the difference between the second and the first measurement. Since a direct measurement of Fe(III) or Fe(II) was not employed but deduced from the spectrophotometric data, the results were considered qualitative. For hydroxide activation trials, the activator (OH^-) strength was measured as pH (Orion pH meter, Model 290A).

3.4. RESULTS AND DISCUSSION

3.4.1. Chelated-Fe(II) Activation

Persulfate degradation for the low persulfate concentration (1 g/L) in the no-solids trials and in the trials involving aquifer materials (Figure 3.1.) was rapid at Fe_{high} (600 mg/L) irrespective of the CA:Fe molar ratio (i.e., for both CA_{low} and CA_{high}). This was due to fast oxidation of Fe(II) to Fe(III) and consequently a fast degradation of persulfate (Eq. 3.1). Complete oxidation of 600 mg/L Fe(II) requires 1.28 g/L of persulfate (Eq. 3.8). Since the available persulfate concentration was lower than the required, the complete and rapid degradation of persulfate was observed. In the trials employing Fe_{low} (150 mg/L), persulfate mass was ~3 times higher than that required for complete oxidation of Fe(II) to Fe(III) and hence significant concentration of persulfate was observed to persist. However, a 20 to 25% decrease in persulfate concentration was observed within <1 day for the trials involving all the aquifer solids. This initial decrease is consistent with the persulfate requirement (~30%) for complete oxidation of Fe(II). Significant persulfate concentration was observed to persist over the experimental period for all the 20 g/L persulfate trials involving solids since the initial persulfate concentration was much higher (>15 times) than the stoichiometric requirement for the complete oxidation of Fe(II) at both Fe(II) concentrations. An initial decrease in the persulfate concentration was observed within the first day for these trials and this decrease was more distinguishable for Fe_{high} (10 to 25%) than for Fe_{low} (<10%) at both CA:Fe molar ratios. Therefore, CA chelation at the molar ratios studied was not very effective in controlling the interaction between persulfate and Fe(II).

After the initial loss, the remaining persulfate (>1 day) followed first-order degradation kinetics for both initial persulfate concentrations. The estimated k_{obs} for 20 g/L persulfate concentration were generally 2 to 8 times lower than that observed for 1 g/L persulfate concentration for all aquifer solids which is consistent with the ionic strength effects observed during unactivated persulfate trials (Sra et al., 2010b). For both the initial persulfate concentrations, the k_{obs} were up to 1 to 4 times higher than the unactivated case (Sra et al., 2010b) for all the aquifer materials except for NIROP where k_{obs} was 0.5 to 0.8 times the k_{obs} for the unactivated case. For a given Fe(II) concentration, k_{obs} was faster for a higher CA ratio implying that CA contributed to enhancing the persulfate degradation. Overall, the k_{obs} generally followed similar trends as the unactivated case between various aquifer materials with LC34-LSU solids exhibiting the highest k_{obs} and Borden solids exhibiting the lowest k_{obs} (Table 3.2).

The higher persulfate degradation during these chelated-Fe(II) activation trials as compared to the unactivated case was due to the presence of Fe(III), CA (Rastogi et al., 2009) or H^+ produced upon degradation of persulfate or sulfate radical (House, 1962) and during dissociation of CA (Hastings and van Slyke, 1922). It is also speculated that Fe(II) was regenerated from Fe(III) and the reaction between Fe(II) and persulfate resulted in increased degradation of persulfate.

The no-solids trials behaved very differently as compared to the no-solids trials for the unactivated case, and persulfate persistence was lower than the trials involving aquifer solids. Continual degradation of persulfate was observed even when the persulfate mass was in excess of the stoichiometric requirement for complete oxidation of Fe(II). Rapid initial persulfate degradation was observed for all combinations of Fe(II) and CA due to the

reaction with Fe(II) (Figure 3.1). Complete degradation of persulfate was observed for 1 g/L trials at Fe_{high} concentration. For the remaining 1 g/L no-solids trials, >30% initial decrease in persulfate was observed. The 20 g/L persulfate no-solids trials exhibited ~20% initial decrease for Fe_{high} and ~10% for Fe_{low} at both CA:Fe(II) molar ratios. Following this initial decrease, persulfate continued to degrade depending upon the initial Fe(II) and CA concentrations. For example, in the 1 g/L persulfate case, complete degradation of persulfate was observed in the $Fe_{low}CA_{high}$ no-solids trial in <3 days, whereas persulfate degradation was relatively slower for the $Fe_{low}CA_{low}$ trial. The presence of higher Fe or CA clearly led to higher k_{obs}. Overall, the continual loss of persulfate despite an initial sink due to Fe(II) oxidation was likely a result of Fe(II) or Fe(III)-catalyzed degradation, oxidation of CA and/or acid catalyzed degradation of persulfate until the oxidant was consumed (Block et al., 2004; Rastogi et al., 2009). Fe(III) will remain in solution due to a low pH from persulfate degradation and from CA in the absence of aquifer solids, and hence will be available for interaction with persulfate. In contrast, the availability of Fe(III) in the trials involving aquifer solids will be limited since the solids buffer pH to mildly alkaline conditions (Sra et al., 2010) which will cause Fe(III) to precipitate. Therefore, higher persulfate persistence was observed during trials involving solids as compared to trials without solids. In the trials with Fe_{low} concentration at 1 g/L persulfate, a higher concentration of Fe(III) (>80% of 150 mg/L) was observed (data not shown) in the no-solids trial than in any of the trials involving aquifer materials. This observation suggests that the catalyzing potential of Fe(III) or its regeneration to Fe(II) led to significant degradation of persulfate in the no-solids trial.

Overall, these trials demonstrate that once chelated-Fe(II) is oxidized and Fe(III) precipitated, the degradation of persulfate is dominated by reactions with aquifer material

constituents (e.g., Fe_{Am}, TOC), but can be enhanced by the presence of Fe(III) and CA in the aqueous phase.

3.4.2. Peroxide Activation

In the trials employing aquifer solids, TOS degradation was generally rapid at all H_2O_2: $S_2O_8^{2-}$ molar ratios for both persulfate concentrations. This rapid degradation was more pronounced at higher $H_2O_2:S_2O_8^{2-}$ molar ratios of 1 and 10 as compared to molar ratios <1 (Figure 3.2). All trials with aquifer solids demonstrated an initially high TOS degradation followed by relatively slower degradation kinetics. The initial TOS degradation within ~10 days was due to the rapid loss of peroxide as a result of interactions with Fe_{Am} (Xu and Thomson, 2010). For instance, the NIROP and Borden aquifer materials exhibit the highest and lowest Fe_{Am} content, respectively (Xu and Thomson, 2010), and hence resulted in the fastest and the slowest loss in TOS for all molar ratios at both persulfate concentrations.

Since the kinetics associated with the interaction between peroxide and persulfate is not well understood, first-order kinetics was assumed to represent TOS degradation once TOS was <1 in order to compare and capture the difference in persistence from the unactivated case (Table 3.2). It is acknowledged that the first-order kinetics is not truly representative of the TOS degradation behavior but was used to illustrate controlling factors. For $H_2O_2:S_2O_8^{2-}$ molar ratios ≤1 with an initial 1 g/L persulfate concentration, the first-order TOS degradation rate coefficient (k_{obs}^{TOS}) were 0.5 to 1.5 times of those for unactivated persulfate suggesting that the overall impact of lower $H_2O_2:S_2O_8^{2-}$ molar ratios on persulfate persistence was insignificant for a persulfate concentration of 1 g/L.

At a molar ratio of 10 for the 1 g/L trials, and at all molar ratios for the 20 g/L trials, a decrease in TOS stability as compared to unactivated persulfate was observed. The impact of a higher $H_2O_2:S_2O_8^{2-}$ molar ratio or peroxide concentration depends upon the interaction between peroxide and persulfate. When peroxide is more persistent, (e.g., Borden solids) and/or $H_2O_2:S_2O_8^{2-}$ molar ratio is high, peroxide concentration was elevated for a longer period of time. This provides time for the interaction between peroxide and persulfate to occur, which results in higher persulfate degradation as compared to the unactivated persulfate. An increase in molar ratio from 0.01 to 10 increased the k_{obs}^{TOS} during later time from 1.8 to >100 times of k_{obs} for unactivated persulfate in trials involving Borden solids. In contrast, peroxide degradation in NIROP was rapid and demonstrated a low impact on late--term k_{obs}^{TOS} which were <3 times of the unactivated case for all molar ratios. Based on these observations, a regression analysis was performed to examine the dependence of k_{obs}^{TOS} on unactivated persulfate and peroxide degradation rate coefficients for different solids. Trials involving Borden materials at $H_2O_2:S_2O_8^{2-}$ molar ratio of 10 demonstrated very high degradation rates and were removed from this analysis. The remaining k_{obs}^{TOS} generally demonstrated a good correlation (r >0.91) with unactivated persulfate degradation rate coefficients (Sra et al., 2010b), peroxide concentration, and peroxide first-order degradation rate coefficients (Xu and Thomson, 2010) and yielded the following relationship

$$k_{obs}^{TOS} = k_0^{S_2O_8^{2-}}\left(1+\frac{[H_2O_2]^{0.5}}{k_0^{H_2O_2}}\right) \tag{3.10}$$

where, k_{obs}^{TOS} is the estimated first-order TOS degradation rate coefficient for TOS<1, [day^{-1}], $k_0^{S_2O_8^{2-}}$ is the first-order unactivated persulfate degradation rate coefficient, [day^{-1}], and $k_0^{H_2O_2}$ is the first-order peroxide degradation rate coefficient, [day^{-1}].

The TOS in the no-solids trials for all $H_2O_2:S_2O_8^{2-}$ molar ratios at both persulfate concentrations was more stable than trials involving aquifer solids. This was due to the absence of aquifer material-bound chemical species (e.g., Fe_{Am}, TOC) in the no-solids trial reactor that can degrade peroxide and/or persulfate (Kwan and Voelkar, 2003; House, 1962; Sra et al., 2010b).

3.4.3. Alkaline Activation

Under alkaline conditions, persulfate degradation in the presence of aquifer solids was also captured by first-order kinetic rate law and the k_{obs} were 1 to 4 times higher than the unactivated case for both persulfate concentrations (Figure 3.3.). Unlike chelated-Fe(II) or peroxide activation, no initial rapid loss of oxidant strength was observed. The k_{obs} for 1 g/L persulfate trials were 3 to 8 times higher than those for 20 g/L persulfate trials in accordance with the ionic strength effects (Sra et al., 2010b). No clear relationship was observed between k_{obs} and the initial pH. Similar to the unactivated persulfate degradation trends, the k_{obs} from the 1 g/L persulfate trials were the highest for LC34-LSU solids followed by NIROP, LC34-USU and Borden for all pH conditions. However, for the 20 g/L persulfate trials, NIROP solids exhibited a lower k_{obs} than LC34-USU solids. Significant (~50%) persulfate degradation was also observed in no-solids trials at the 1 g/L persulfate concentration whereas for the 20 g/L persulfate no-solids trials the persulfate degradation was <10%. Although the impact of pH was not distinguishable from these data, it was seen

that persulfate degradation was influenced by persulfate interactions with aquifer material constituents (i.e., TOC and Fe_{Am}) and ionic strength similar to the unactivated case. Further, it is speculated that persulfate reactivity with hydroxide and the impact of hydroxide concentration on the availability of TOC and Fe_{Am} may also play a role in determining the persistence of persulfate.

Stability of the activating agent (hydroxide) was captured by monitoring pH which dropped in all trials due to acid production upon persulfate degradation and/or due to buffering by solids (Figure 3.4.). Similar to the unactivated case, drop in pH was faster in experiments with 20 g/L persulfate concentration compared to 1 g/L. As expected, suitable alkaline conditions were maintained for longer periods of time by using a higher initial pH. In the presence of aquifer materials, change in pH depends upon total carbonate (TC) content of the solids which act to buffer the solution pH (Sra et al., 2010b). For example, a slow decrease in pH was observed for the Borden solids which contain the lowest TC, while a fast pH decrease was observed for the LC34-LSU material which has the highest TC content. In the absence of buffering in the no-solids trials, persulfate degradation resulted in a significant decrease in pH.

3.5. CONCLUSIONS

The impact of activation on degradation of persulfate and/or TOS in the presence of aquifer materials was low to very high over the range of the three activation agents (Table 3.3). Chelated-Fe(II) and peroxide activation trials demonstrated rapid loss of activator strength that consequently led to overall reduction in persistence of the activated persulfate system. Chelation of Fe(II) by citric acid was ineffective in controlling the contact with persulfate

and rapid oxidation of Fe(II) occurred resulting in a rapid initial loss of persulfate. Oxidation of citric acid may be a potential sink for persulfate. Fe(III) produced upon Fe(II) oxidation was also capable of catalyzing persulfate degradation but was susceptible to precipitation under alkaline conditions. Peroxide availability over the long-term was limited by its fast degradation in Fe_{Am}-rich aquifer materials and in such cases minimal influence on persulfate stability was observed. When peroxide degradation was slow, impact on persulfate persistence was high and signified interaction between the peroxide and persulfate. In general, higher concentration of the Fe(II) or peroxide led to higher depletion of persulfate and/or TOS. While use of these activating agents may initially provide suitable conditions for enhancement of oxidation rates of target organics, oxidation performance will be limited by lack of long-term availability of activating agents and by enhanced depletion of persulfate. Under such scenarios, advective and diffusive transport processes will be relatively slow to assist in adequate spatial coverage of the contaminated zone by activated persulfate. Once activating agents are consumed or depleted, persulfate degradation behavior will generally follow unactivated persulfate degradation kinetics. Activation by highly alkaline conditions had a comparatively lower impact than the other activation strategies investigated here. Required pH conditions (>10) were maintained for a limited duration due to buffering capacity and acid production upon persulfate degradation.

These observations are important for use in activated persulfate application for ISCO remediation systems. Depletion of persulfate and activating agents due to their mutual interactions and interaction with aquifer materials can greatly limit persistence of the activated system. Long-term availability of persulfate and activators is critical to the success of persulfate-based ISCO. These persistence results should be combined with activated

persulfate treatability studies to improve and optimize the overall design of persulfate-based ISCO treatment systems.

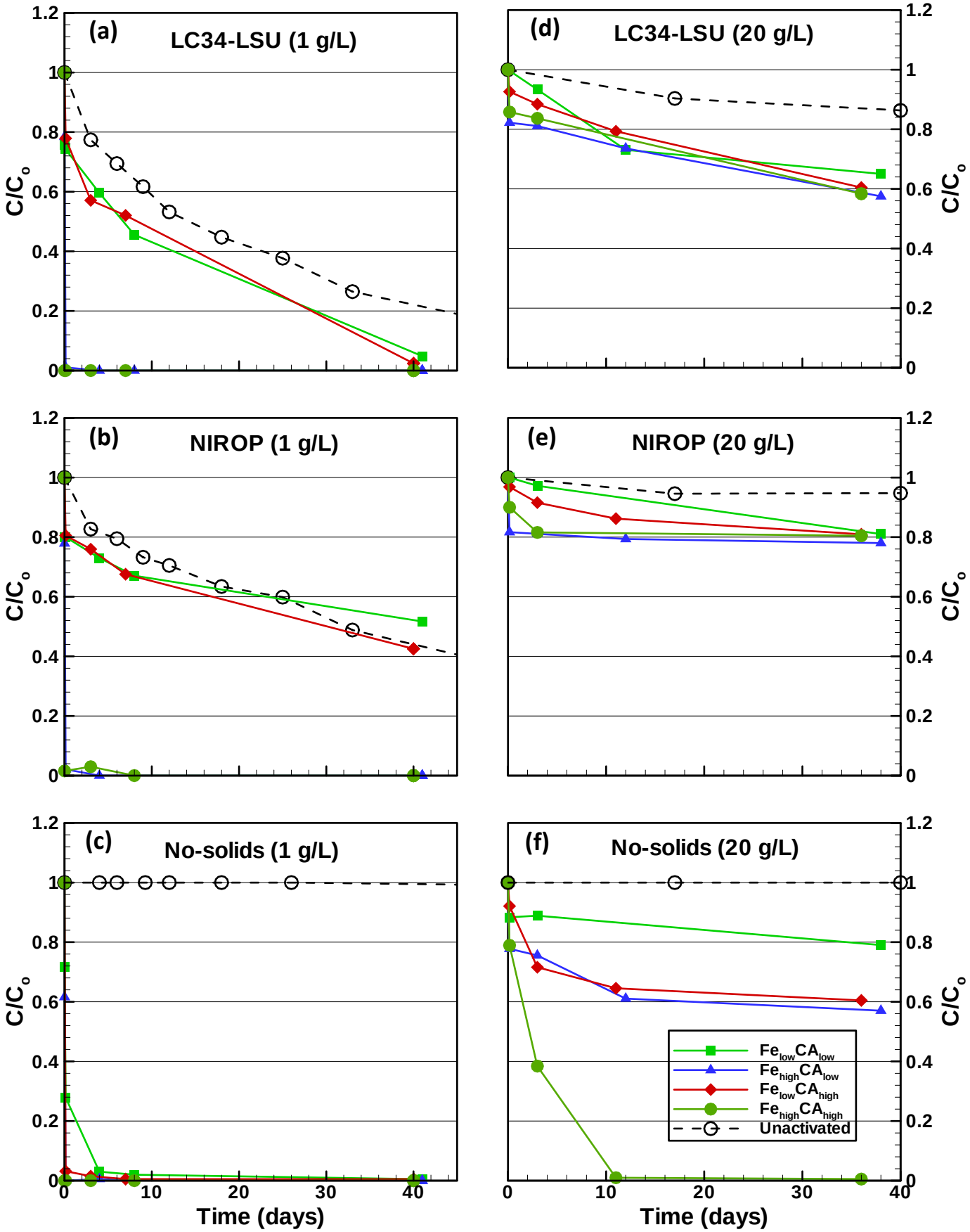

Figure 3.1. Persulfate profiles from chelated-Fe(II) activation trials for an initial persulfate concentration of (a-c) 1 g/L, and (d-f) 20 g/L.

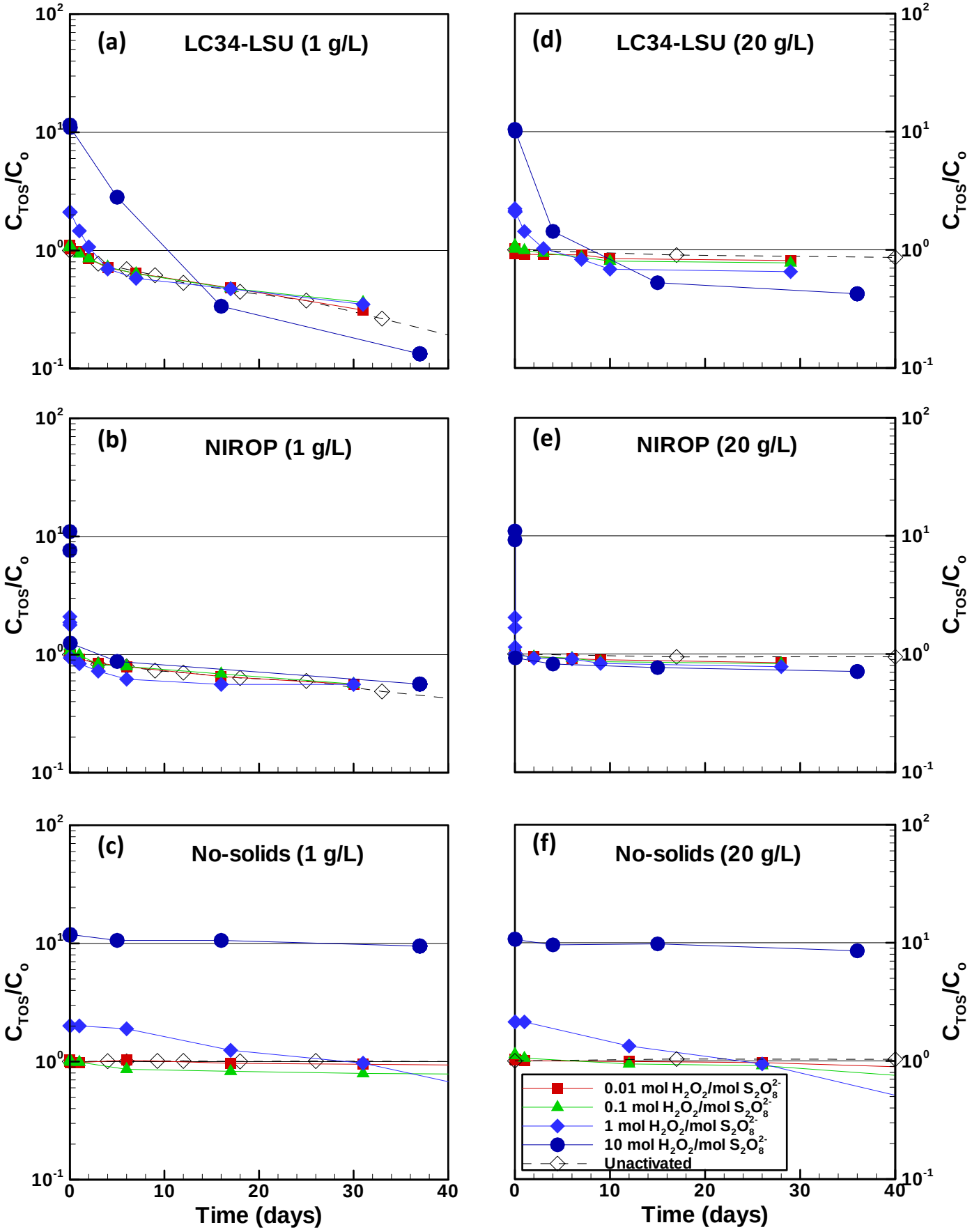

Figure 3.2. Total oxidation strength (TOS) profiles for peroxide activation trials for an initial persulfate concentration of (a-c) 1 g/L, and (d-f) 20 g/L.

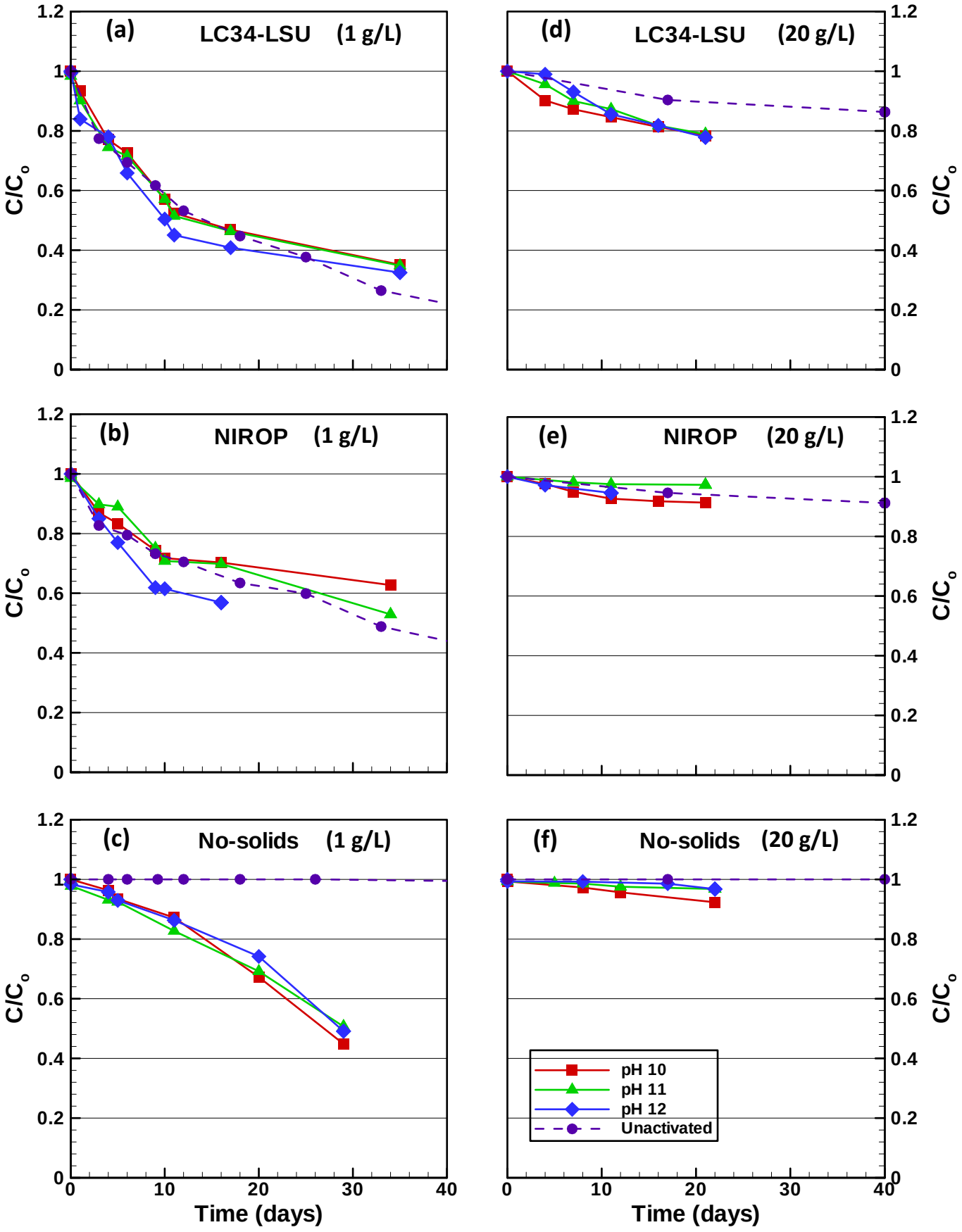

Figure 3.3. Persulfate profiles from high pH activation trials for an initial persulfate concentration of (a-c) 1 g/L, and (d-f) 20 g/L.

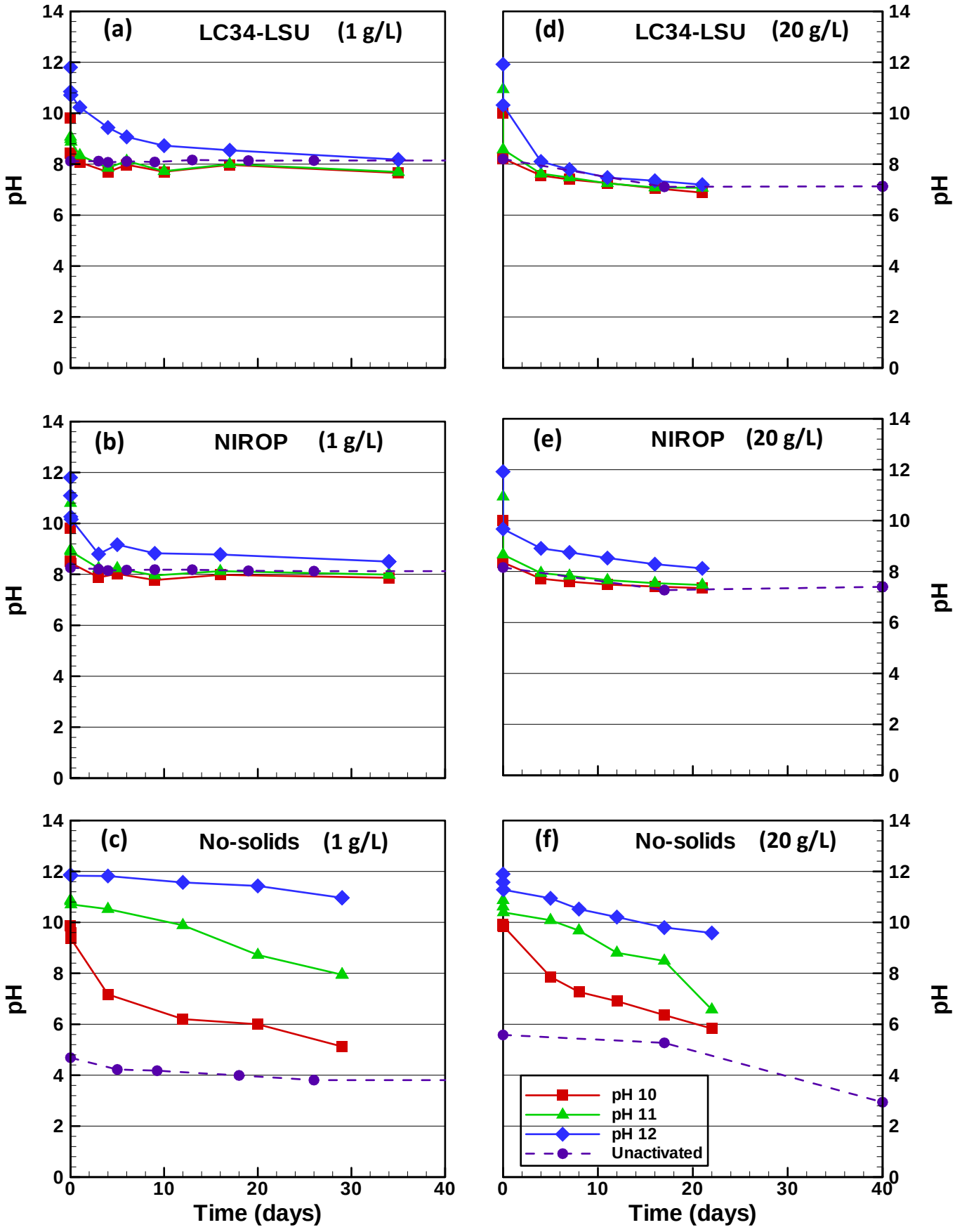

Figure 3.4. Profiles for pH from high pH activation trials for an initial persulfate concentration of (a-c) 1 g/L, and (d-f) 20 g/L.

Table 3.1. Summary of experimental conditions

Activator	Activator Trial Label	Initial Reactor Conditions			
		Activator Concentration	Persulfate Concentration (g/L)	Total Aqueous Volume (mL)	Solids Mass (g)
CA-Fe(II)	$Fe_{low}CA_{low}$	150 mg/L Fe(II) + 0.2 mol CA/mol Fe(II)	1	20	20
CA-Fe(II)	$Fe_{high}CA_{low}$	600 mg/L Fe(II) + 0.2 mol CA/mol Fe(II)	1	20	20
CA-Fe(II)	$Fe_{low}CA_{high}$	150 mg/L Fe(II) + 1.0 mol CA/mol Fe(II)	1	20	20
CA-Fe(II)	$Fe_{high}CA_{high}$	600 mg/L Fe(II) + 1.0 mol CA/mol Fe(II)	1	20	20
CA-Fe(II)	$Fe_{low}CA_{low}$	150 mg/L Fe(II) + 0.2 mol CA/mol Fe(II)	20	20	20
CA-Fe(II)	$Fe_{high}CA_{low}$	600 mg/L Fe(II) + 0.2 mol CA/mol Fe(II)	20	20	20
CA-Fe(II)	$Fe_{low}CA_{high}$	150 mg/L Fe(II) + 1.0 mol CA/mol Fe(II)	20	20	20
CA-Fe(II)	$Fe_{high}CA_{high}$	600 mg/L Fe(II) + 1.0 mol CA/mol Fe(II)	20	20	20
H_2O_2	0.01	0.01 mol H_2O_2/mol $S_2O_8^{2-}$	1	20	20
H_2O_2	0.1	0.1 mol H_2O_2/mol $S_2O_8^{2-}$	1	20	20
H_2O_2	1	1.0 mol H_2O_2/mol $S_2O_8^{2-}$	1	20	20
H_2O_2	10	10 mol H_2O_2/mol $S_2O_8^{2-}$	1	20	20
H_2O_2	0.01	0.01 mol H_2O_2/mol $S_2O_8^{2-}$	20	20	20
H_2O_2	0.1	0.1 mol H_2O_2/mol $S_2O_8^{2-}$	20	20	20
H_2O_2	1	1.0 mol H_2O_2/mol $S_2O_8^{2-}$	20	20	20
H_2O_2	10	10 mol H_2O_2/mol $S_2O_8^{2-}$	20	20	20
OH^-	pH 10	pH 10	1	25	25
OH^-	pH 11	pH 11	1	25	25
OH^-	pH 12	pH 12	1	25	25
OH^-	pH 10	pH 10	20	25	25
OH^-	pH 11	pH 11	20	25	25
OH^-	pH 12	pH 12	20	25	25

Table 3.2. Summary of activated persulfate or TOS degradation rate coefficients in the presence of aquifer solids

Persulfate Concentration (g/L)	Activation Trial	k_{obs} [10^{-4} day^{-1}]			
		Borden	LC34-LSU	LC34-USU	NIROP
1	Unactivated	[a]36.8 ± 2.1	[a]423.8 ± 5.7	[a]80.9 ± 3.6	[a]183.2 ± 6.6
20	Unactivated	[a]13.6	[a]35.8	[a]17.8	[a]23.1
1	$Fe_{low}CA_{low}$	37.4 ± 18.8	672.4 ± 6.0	147.6 ± 17.5	97.8 ± 15.6
1	$Fe_{high}CA_{low}$	[b]Too fast	[b]Too fast	[b]Too fast	[b]Too fast
1	$Fe_{low}CA_{high}$	75.2 ± 14.4	876.0 ± 42.4	149.9 ± 17.7	155.5 ± 11.4
1	$Fe_{high}CA_{high}$	[b]Too fast	[b]Too fast	[b]Too fast	[b]Too fast
20	$Fe_{low}CA_{low}$	53.6 ± 1.5	106.8 ± 34.3	56.4 ± 5.4	54.6 ± 2.2
20	$Fe_{high}CA_{low}$	36.0 ± 0.6	96.0 ± 2.4	30.4 ± 4.8	11.4 ± 2.8
20	$Fe_{low}CA_{high}$	[c]-na-	117.1 ± 5.2	62.6 ± 3.3	50.9 ± 14.1
20	$Fe_{high}CA_{high}$	[c]-na-	108.0 ± 1.4	[c]-na-	[c]-na-
1	0.01 mol H_2O_2/mol $S_2O_8^{2-}$	28.6 ± 11.8	349.0 ± 34.7	98.5 ± 25.2	165.0 ± 17.9
1	0.1 mol H_2O_2/mol $S_2O_8^{2-}$	[c]-na-	300.1 ± 37.5	100.0 ± 32.5	169.4 ± 28.7
1	1 mol H_2O_2/mol $S_2O_8^{2-}$	55.2 ± 20.2	317.7 ± 85.4	107.2 ± 38.4	117.7 ± 50.3
1	10 mol H_2O_2/mol $S_2O_8^{2-}$	1008.8 ± 437.4	885.9 ± 375.9	415.0 ± 212.3	183.0 ± 72.4
20	0.01 mol H_2O_2/mol $S_2O_8^{2-}$	18.1 ± 5.7	44.5 ± 12.2	26.8 ± 6.0	41.7 ± 9.2
20	0.1 mol H_2O_2/mol $S_2O_8^{2-}$	80.6 ± 18.5	61.4 ± 29.1	[c]-na-	54.1 ± 14.7
20	1 mol H_2O_2/mol $S_2O_8^{2-}$	118.0 ± 93.2	139.2 ± 79.5	[c]-na-	61.9 ± 18.8
20	10 mol H_2O_2/mol $S_2O_8^{2-}$	1858.7 ± 287.7	343.7 ± 203.4	232.1 ± 145.2	63.8 ± 20.2
1	pH 10	45.6 ± 2.2	553.4 ± 34.4	209.0 ± 27.2	256.3 ± 44.4
1	pH 11	34.4 ± 2.5	457.0 ± 38.1	298.7 ± 25.3	189.0 ± 19.3
1	pH 12	38.5 ± 5.9	677.9 ± 42.4	231.5 ± 55.1	402.1 ± 47.5
20	pH 10	[c]-na-	105.7 ± 15.8	66.3 ± 9.2	44.3 ± 7.7
20	pH 11	[c]-na-	97.2 ± 15.4	[c]-na-	23.6 ± 3.1
20	pH 12	[c]-na-	112.5 ± 17.7	67.6 ± 12.5	46.3 ± 12.2

[a]Data from Sra et al. (2010b).

[b]Degradation occurred within <1 day and could not be captured during analysis.

[c]Insufficient data quality (r^2 <0.6).

Table 3.3. Summary of the impact of activation on the persistence of persulfate

Activator	Persulfate Concentration (g/L)	
	1	**20**
Fe_{low}	High	Moderate
Fe_{high}	Very High	High
CA_{low}	Low	Low
CA_{high}	Moderate	Moderate
0.01 mol H_2O_2/mol $S_2O_8^{2-}$	Low	Low
0.1 mol H_2O_2/mol $S_2O_8^{2-}$	Low	Low
1.0 mol H_2O_2/mol $S_2O_8^{2-}$	Low	Moderate
10 mol H_2O_2/mol $S_2O_8^{2-}$	Moderate	High
pH 10	Low	Low
pH 11	Low	Low
pH 12	Low	Low

Chapter 4

Persulfate Oxidation of Gasoline

Overview

Groundwater contamination from gasoline range organics (C_6 to C_{16}) is persistent and may result in a significant dissolved phase plume. *In situ* chemical oxidation treatment using persulfate has been identified as a potential treatment strategy. Bench-scale treatability of dissolved gasoline compounds was investigated using unactivated persulfate and activated persulfate employing chelated-ferrous, peroxide, alkaline conditions or aquifer materials as activation strategy. A series of batch reactor trials were designed with an initial total petroleum hydrocarbon (TPH) concentration of ~25 mg/L and 9 gasoline compounds were monitored over a 28-day reaction period. Unactivated persulfate at a concentration of 20 g/L resulted in complete oxidation. Oxidation rates were enhanced by ~2 to 15 times using the peroxide or chelated-Fe(II) activation strategy. Alkaline activation at pH of 11 yielded oxidation rates that were ~2 times higher than the unactivated case. For activation at pH of 13 the oxidation rates for benzene, toluene and ethylbenzene were reduced by 50% while for the remaining monitored compounds the rates were enhanced by 5 to 100%. Natural activation by two aquifer materials resulted in oxidation rates similar to the unactivated case implying that activation by minerals associated with either aquifer material was not significant or that the potential activation was offset by radical scavenging. First-order oxidation rate coefficients were estimated for all experimental trials. Acid-catalyzation when pH <3 may enhance oxidation rates in weakly buffered systems. Significant oxidant strength (60-85%) was observed in all 20 g/L persulfate reactors implying significant persulfate persistence under gasoline-contaminated conditions. The overall bulk gasoline stoichiometry for these experimental trials varied from 120 to 340 g-persulfate/g-TPH. Unactivated persulfate at 20 g/L demonstrated the best treatment efficiency which was estimated as the inverse of the measure for overall bulk stoichiometry.

4.1. INTRODUCTION

Gasoline is one of the most extensively used petroleum hydrocarbons (PHCs) in the world and hence, is among the most widespread and abundant of all organic contaminants occurring in soil and groundwater (McCarthy et al., 2004; Ferguson et al., 2004; Tiburtius et al., 2005; Ferrarese et al., 2008). Accidental spills during production, transportation and consumption of gasoline, and leakage from approximately one-third of all underground storage tanks (USTs) (Nadim et al., 2000; Shih et al., 2004; Kunucku, 2007; Liang et al. 2008) are the common sources of subsurface contamination. Gasoline constituents such as benzene, toluene, ethylbenzene, xylenes (BTEX), trimethylbenzenes (TMBs) and naphthalene are acutely toxic (Nadim et al., 2000; ATSDR, 2004; Zhou et al., 2005). BTEX compounds, in particular, are very mobile in groundwater and hence have a high potential to impact groundwater users and the aquatic environment (Tiburtius et al., 2005). Gasoline related PHC contamination will prevail until the source and resulting dissolved phase plume are remediated (Lundegaard and Johnson, 2007).

A number of *in situ* remediation technologies have been investigated to treat gasoline-contaminated soil and groundwater (e.g., pump-and-treat, enhanced bioremediation, soil vapor extraction, air-sparging), but most of these technologies exhibit limitations at the field-scale (Nadim et al., 2000; Zhou et al., 2005; Dadkhah and Akgerman, 2007; Kunucku 2007). *In situ* chemical oxidation (ISCO), which involves the injection or release of a strong oxidant (e.g,. permanganate, peroxide, or persulfate) into the subsurface, offers a rapid and aggressive alternative that has the potential for complete mineralization of the target organic compounds (Ferguson et al., 2004; Tiburtius et al., 2005). ISCO can lead to reduction in overall treatment time without the cost associated with soil excavation and treatment, can

minimize disturbance to above ground structures and is generally not sensitive to contaminant concentrations (Killian et al. 2007; Dadkhah and Akgerman, 2007). Permanganate is incapable of treating PHCs (Huling and Pivetz, 2006; Crimi and Taylor, 2007) and may be consumed in the subsurface by competing reactions with other reductants (e.g., natural organic matter, and Fe or Mn species) which affect treatment efficiency (Xu and Thomson, 2009). The persistence of peroxide (Fenton's reagent) is generally very low in the presence of aquifer materials therefore limiting its radius of influence to a few meters around an injection location and increasing delivery costs (Watts and Teel, 2006; Huling and Pivetz, 2006; Xu and Thomson, 2010). Persulfate is more stable than peroxide in the presence of aquifer materials (Sra et al., 2010) and is capable of treating a wider range of organic compound than permanganate (Watts and Teel, 2006; Huling and Pivetz, 2006; Crimi and Taylor, 2007).

Oxidation by persulfate at ambient conditions may occur either by direct oxidation or through the activation of persulfate to sulfate radicals ($SO_4^{-\bullet}$) using heat, ferrous iron, hydroxide or peroxide (Kolthoff and Miller 1951; Latimer, 1952; House, 1962; Eberson, 1987; Huang et al., 2002; Liang et al., 2004a; Crimi and Taylor, 2007; Miraglio 2009; Liang and Su, 2009)

$$2\,S_2O_8^{2-} + 2e^- \rightarrow 2SO_4^{2-} \qquad (E^o = 2.01\ V) \qquad (4.1)$$

$$S_2O_8^{2-} \xrightarrow{\Delta,\, Fe^{2+},\, OH^-,\, H_2O_2} 2SO_4^{-\bullet} \quad (\text{or } OH^\bullet, O_2^{-\bullet}, \text{ etc.}) \qquad (4.2)$$

The reduction half reaction for the sulfate radical and hydroxyl radical ($OH^\bullet$) which is an important species during peroxide or alkaline activation of persulfate is given by

$$SO_4^{-\bullet} + e^- \rightarrow SO_4^{2-} \qquad (E^o = 2.6\ V) \qquad (4.3)$$

$$OH^{\bullet} + e^- \rightarrow OH^- \qquad (E^o = 2.8\ V) \qquad (4.4)$$

Since UV is impractical and heat is costly as an activation method for subsurface applications (ITRC, 2001), the utility of chelated-ferrous, peroxide and high pH as persulfate activation strategies has been the primary focus of research over the last 5 years (Block et al., 2004; Crimi and Taylor, 2007; Liang et al. 2008). These strategies have been shown to destroy a wide range of organic compounds including chlorinated solvents, volatile organic compounds and BTEX (Huang et al., 2002; Liang et al., 2004a,b; Forsey, 2004; Crimi and Taylor, 2007; Liang et al. 2008). However, there is no peer-reviewed literature that addresses the treatability of dissolved gasoline as an ensemble of organic compounds using either unactivated or activated persulfate. Gasoline consists of the high impact, low molecular weight compounds (BTEX, TMBs and naphthalene) in addition to hundreds of other organic compounds (Prince et al., 2007). Our understanding of gasoline treatability by persulfate has been limited to the oxidation of a simulated mixture of BTEX compounds (Forsey, 2004; Crimi and Taylor, 2007; Liang et al. 2008) or oxidation of a mixture of volatile organic compound in which gasoline compounds were not well represented (Huang et al., 2005). Bulk measures in PHC concentrations are normally captured as total petroleum hydrocarbons (TPHs) along with PHC fractions based on the carbon chain length (e.g., F1 (C_6 to C_{10}) or F2 (C_{10} to C_{16})) and have been useful to indicate the presence and magnitude of gasoline contamination (Shih et al., 2004).

The focus of this investigation was to examine the treatability of gasoline compounds by persulfate oxidation and establish the utility of persulfate as a viable oxidant for *in situ*

remediation of gasoline contaminated sites. A series of batch reactor experiments were conducted to understand the aqueous phase treatability of gasoline compounds (BTEX, TMBs and naphthalene), TPH, and PHC fractions F1 and F2 using unactivated and activated persulfate (peroxide, chelated-ferrous and alkaline pH). The ability of unactivated persulfate was used here since it is a strong oxidant (Eq. 4.1), is more stable when not activated (Sra et al., 2010) and provides a basis for comparison to the experimental trials performed with the activation strategies. Additionally, we also sought to understand the impact of activation by naturally occurring species (e.g., Fe or Mn) associated with aquifer materials. Performance of the different activation strategies was quantified and compared by estimating oxidation rate coefficients of the monitored compounds.

4.2. MATERIALS AND METHODS

4.2.1. Chemicals and Aquifer Materials

Aqueous solutions of sodium persulfate ($Na_2S_2O_8$, ACS, Aldrich, Milwaukee), American Petroleum Institute (API) gasoline 91-01 (Prince et al., 2007), 30% hydrogen peroxide (H_2O_2, EMD, Gibbstown, NJ), ferrous sulfate heptahydrate ($FeSO_4 \cdot 7H_2O$, ACS, J.T.Baker, Phillipsbourg, NJ), citric acid ($C_6H_8O_7$, Fischer, Fair Lawns, NJ) and sodium hydroxide (NaOH, Fischer, Fair Lawns, NJ) were prepared in distilled (DI) water. ACS grade analytical reagents ferrous ammonium sulfate (FAS) ($Fe(NH_4)_2(SO_4)_2 \cdot 6H_2O$) (EMD, Gibbstown, NJ), ammonium thiocyanate (NH_4SCN) (J.T. Baker, Phillipsbourg, NJ) and sulfuric acid (H_2SO_4) (EMD, Gibbstown, NJ) solutions were prepared to required concentrations using Milli-Q water. Two aquifer materials identified as Borden and LC34-LSU (Xu and Thomson, 2009; Sra et al., 2010) were employed for the natural activation experiments.

4.2.2. Experimental Setup

Batch experiments were conducted to observe the destruction of dissolved gasoline compounds in the presence of unactivated or activated persulfate. All batch experiments were performed in 25 mL glass vials except for the natural activation experiments where 40 mL glass vials were use to accommodate the addition of aquifer solids. Details of the experimental conditions are presented in Table 4.1. An initial TPH concentration of ~25 mg/L in each reactor was selected which is within the typical aqueous phase TPH range of 6 to 30 mg/L encountered in groundwater emanating from gasoline-contaminated source zones (Shih et al., 2004; Lundegaard and Johnson, 2007).

A gasoline-saturated water stock solution was prepared by mixing the API 91-01 gasoline (180 mL) and DI water (1800 mL) at a ratio of 1:10 v/v in a 2.2 L separatory funnel and manually shaking for ~20 min. This solution was left undisturbed for >48 hours following mixing for equilibration. The TPH concentration of this gasoline-saturated solution was ~110 mg/L. The required volume of this gasoline-saturated solution was withdrawn and diluted to obtain the dissolved gasoline stock to be used in the experimental trials. During the dilution process, 10% sodium azide (0.1 mL/10 mL) was added to inhibit biodegradation (Freitas and Barker, 2008).

In general, pre-calculated volumes of the persulfate stock and activating agent solutions were added to the reactors followed immediately by the gasoline stock solution to achieve a final aqueous volume of ~19 mL in the 25 mL reactors. Headspace was deliberately left in the reactors to accommodate any pressure buildup due to the production of gases (likely CO_2). For the experimental trials designed to investigate persulfate activation by aquifer

materials, ~29 g of the selected solids were loaded into a 40 mL reactor and wetted with 13 mL of Milli-Q water followed by the addition of persulfate and gasoline solutions.

Treatment of gasoline compounds by unactivated persulfate was performed at a concentration of 1 or 20 g-$Na_2S_2O_8$/L (Unactivated–1, Unactivated–20). The high persulfate concentration (i.e., 20 g/L) was deemed to be representative of a location in the core of the treatment zone, while the low concentration represents a situation that may exist near the fringe of the treatment zone or in the case where the injected persulfate solution has had an opportunity to spread due to dispersion and/or diffusion processes. All activated persulfate trials were conducted at 20 g/L persulfate concentration. Peroxide activation trials employed a molar ratio 0.1 or 1.0 mol H_2O_2/mol $S_2O_8^{2-}$ (Peroxide–0.1, Peroxide–1.0). Since peroxide itself is a strong oxidant and may potentially oxidize gasoline compounds, we sought to examine this effect by establishing peroxide controls at the two concentrations equivalent to those used for activating persulfate (Peroxide Control–0.1, Peroxide Control–1.0). Chelated-ferrous trials were performed at 150 or 600 mg/L Fe (II) concentration (Fe–150, Fe–600) which correspond with the lower and upper bounds of Fe(II) typically used (Block, 2008). Ferrous sulfate heptahydrate ($FeSO_4 \cdot 7H_2O$) was chelated with citric acid (CA) at a molar ratio of 1:1. Alkaline activation trials were conducted at two hydroxide strengths providing initial pH conditions of 11 or 13 (pH–11, pH–13). Organic compounds may be susceptible to alkaline hydrolysis at high pH (Jeffers et al., 1989), and hence pH controls (without persulfate) were established at the two conditions (pH Control–11, pH Control–13).

To evaluate the potential for natural activation or activation by mineral species (e.g. Fe^{2+}, Mn^{2+}) associated with aquifer materials (Watts et al., 1990), two aquifer materials were used in these trials (Natural–Borden, Natural–LC34-LSU). The LC34-LSU aquifer material

exhibits a higher persulfate degradation rate than the Borden aquifer material due to a higher total organic carbon (TOC) and amorphous iron (Fe_{Am}) content (Sra et al., 2010). Since both aquifer materials contain a significant TOC concentration (>0.24 mg/g; Xu and Thomson, 2009), controls were established to estimate the mass of organic compounds removed from the aqueous phase due to sorption (Natural Control–Borden, Natural Control–LC34-LSU).

A sufficient number of treatment replicates for all experimental trials were prepared to accommodate triplicate sacrificed reactors for organics analysis, and one sacrificed replicate for analysis of persulfate (or total oxidant strength) and pH (as needed). Seven to eight sampling episodes were spread over 21 to 28 days for each trial. All reactors were kept in the dark at a temperature of ~20 ^{o}C.

4.2.3. Analytical Methods

Organic analyses were performed using gas chromatography and focused on 9 gasoline components: benzene, toluene, ethylbenzene, o-xylene, m,p-xylene (meta- and para-xylene are reported together), 1,2,3-trimethylbenzene, 1,2,4-trimethylbenzene, 1,3,5-trimethylbenzene and naphthalene. Methylene chloride (1 mL) was injected in the aqueous phase reactors followed by extraction and analyses as outlined by Freitas and Barker (2008). For natural activation trials, 9 mL of supernatant was withdrawn and diluted to 19 mL in a 25 mL glass vial to avoid analytical complexities arising from the presence of solids prior to solvent injection and extraction. Bulk PHC fractions F1 (C_6 to C_{10}), F2 (C_{10} to C_{16}) and TPH (F1 + F2) were obtained from chromatographs generated during PHC analysis. The PHC F1 fraction included integration of all area counts beginning just after the hexane (nC_6) peak to the apex of the decane (nC_{10}) peak, while PHC F2 included integration from the apex of the decane peak to the apex of the hexadecane (nC_{16}) peak.

Residual oxidant analysis was performed following Huang et al. (2002). For the peroxide activation trials this analytical method was assumed to capture the combined or total oxidant strength (TOS) of the sample and was defined as the strength of persulfate that was capable of forming an equivalent amount of ferric from excess ferrous (FAS) as the sample aliquot. Similar to persulfate (House 1962; Killian et al., 2007), 1 mole of peroxide oxidizes 2 moles of excess Fe(II) (Mummery, 1913; Stirling, 1934) and therefore molar concentrations of peroxide and persulfate were found to be additive and used to estimate TOS. An Orion pH meter (Model 290A) was used to measure pH.

4.3. RESULTS AND DISCUSSION

As detailed above, the behavior of nine selected gasoline compounds and bulk PHC fractions were used to investigate persulfate treatment in this study. However for discussion purposes benzene was chosen as a representative compound (Figure 4.1), and generalizations and exceptions to the other gasoline compounds are noted where applicable. Data for some selected monitored gasoline compounds and the PHC F1 and F2 fractions are presented for comparison purposes in Figure 4.2. The purpose of this investigation was to observe the oxidation of gasoline compounds and to quantify oxidation kinetics under the various persulfate activation conditions explored. An investigation into oxidation mechanisms or pathways was beyond the scope of this study. It was also assumed that the loss of organic concentrations implied complete destruction of non-polar compounds whereas the examination of the polar compounds as intermediate by-products was not conducted. Oxidation rate coefficients for bulk fractions were not estimated but their general behavior has been discussed qualitatively.

4.3.1. Unactivated Persulfate Treatment

Control reactors containing only the gasoline solution indicate that the concentration of all the monitored compounds (Figures 4.1(a) and 4.2) were stable over the 28-day treatment period. Unactivated persulfate at the low concentration (Unactivated–1) was unable to significantly degrade the monitored compounds. The direct oxidation of benzene by persulfate is given by

$$C_6H_6 + 15S_2O_8^{2-} + 12H_2O \rightarrow 6CO_2 + 30SO_4^{2-} + 30H^+ \quad (4.5)$$

Assuming benzene (model organic compound) represents the entire TPH mass used in this trial, then according to Eq. 4.5 at least 1.14 g-$Na_2S_2O_8$/L is required to completely oxidize 25 mg/L of benzene. Therefore, there was insufficient persulfate available for complete oxidation of the gasoline compounds. The persulfate concentration declined by >50% (Figure 4.3) by the end of the reaction period indicating that persulfate was still present, but the concentration was not high enough to cause noticeable oxidation of the monitored compounds. In contrast, at a 20 g/L concentration (Unactivated–20) almost complete oxidation of BTEX (>99%), TMBs (>95%), and significant oxidation of naphthalene (~70%) was observed. The rate of oxidation for all the monitored compounds increased after Day 12 (Figures 4.1(a) and 4.2) due to the decrease in solution pH <3 (Figure 4.4) upon acid production (Eq. 4.5) which will enhance oxidation through acid-catalyzation of persulfate (House 1962; Block et al., 2004) and the formation of peroxymonosulfate following

$$S_2O_8^{2-} + H_2O \xrightarrow{H^+} H_2SO_5 + SO_4^{2-} \quad (4.6)$$

The overall mass action law for oxidation of a PHC compound by persulfate can be written as

$$\frac{d[C_xH_y]}{dt} = -k_{org}[S_2O_8^{2-}]^{n_{ox}}[C_xH_y]^{n_{org}} \quad (4.7)$$

where k_{org} is the reaction rate coefficient with respect to the organic compound, and n_{ox} and n_{org} is the reaction order for persulfate and the organic compound respectively. When the persulfate concentration does not change significantly over the experimental period, Eq. (4.7) can be simplified to

$$\frac{d[C_xH_y]}{dt} = -k_{obs}[C_xH_y]^{n_{org}} \quad (4.8)$$

where $k_{obs} = -k_{org}[S_2O_8^{2-}]^{n_{ox}}$ is the observed oxidation rate coefficient. Assuming that the persulfate concentration was constant during over the reaction period, the experimental data were fit to Eq. (4.8) with n_{org} of unity. Only data for the first 12 days was used to avoid the complexity from the enhanced oxidation behavior resulting from acid-catalyzed oxidation of the monitored gasoline organics (Block et al., 2004; Liang et al. 2008). This first-order rate law was able to represent the observed data extremely well for all compounds ($r^2 > 0.93$) except for 1,3,5-TMB ($r^2 = 0.82$) and naphthalene ($r^2 = 0.59$) (Table 4.2). The k_{obs} for ethylbenzene and toluene were the largest (~56×10^{-3} day^{-1}) followed by benzene > xylenes > TMBs > naphthalene. This trend is not surprising since the presence of an electron donating group (e.g., CH_3- and C_2H_5-) generally increase the oxidation rates, but the presence of these groups on multiple carbon sites (e.g., xylenes and TMBs) do not readily favor oxidation by persulfate and may destabilize reaction intermediates during oxidation (Forsey, 2004).

Huang et al. (2005) observed significant oxidation (≤ 50%) of BTEX, TMBs and naphthalene using 1 g/L persulfate at 20°C without activation. The initial concentrations of these organic compounds were generally < 100 µg/L, suggesting that unactivated persulfate at sufficiently high persulfate to gasoline compound molar ratio (e.g., >4000 mol $S_2O_8^{2-}$/mol benzene) is capable of degrading gasoline compounds. Oxidation rate coefficients for BTEX compounds in this study (Table 4.2) were ~2 to 6 times lower than those observed for 100 mM (~24 g/L) persulfate by Liang et al. (2008). This difference was likely due a slightly higher persulfate concentration and the fact that compounds were treated individually by Liang et al. (2008) as opposed to a mixture of dissolved gasoline compounds exposed to 20 g/L persulfate used in this investigation.

4.3.2. Peroxide Activated Persulfate Treatment

Peroxide controls at both concentrations (Peroxide Control–0.1 and –1.0) did not result in any significant change in concentration of the monitored compounds (Figures 4.1(a) and 4.2) indicating that peroxide by itself at the given concentrations did not oxidize these compounds. Peroxide–0.1 resulted in near complete destruction of BTEX and TMBs (> 99%) and significant destruction of naphthalene (~80%) within the 28-day reaction period. While benzene, toluene and ethylbenzene results exhibited almost complete oxidation, destruction of xylenes, TMBs and naphthalene was slightly lower (80 to 90%). Similar to the unactivated persulfate treatment trials the rate of oxidation of all the monitored compounds could also be captured by the pseudo first-order reaction rate law Eq. (4.8) (Table 4.2). Due to the complicated nature of peroxide interaction with persulfate, the k_{obs} was assumed to represent the overall oxidation rate as contributed by all the oxidizing species (e.g., $S_2O_8^{2-}$,

$SO_4^{-\bullet}$ and $OH^{\bullet}$). The k_{obs} estimated from Peroxide-0.1 trial were 5 to 300% higher than those from the Peroxide-1.0 trial. This difference for the heavier molecular weight gasoline compounds in the TPH F1 fraction (xylenes, TMBs) was more pronounced as compared to benzene, toluene or ethylbenzene (5 to 50%). Persulfate activation at both peroxide molar ratios yielded significantly higher k_{obs} (100 to 1000%) than unactivated persulfate for all the monitored compounds. The overall trend in k_{obs} between the various gasoline compounds was generally similar to the unactivated persulfate trials. The k_{obs} for these trials decreased in the following order of ethylbenzene or benzene > toluene > xylenes or TMBs > naphthalene.

Persulfate activation by peroxide or the reaction chemistry of persulfate-peroxide dual-oxidant system has not been well documented. It is speculated that this activation method may involve the formation of multiple free radicals (e.g., $SO_4^{-\bullet}$, $OH^{\bullet}$) and other active peroxygens and superoxide (Block et al., 2004). The sulfate and hydroxyl radicals have a high oxidation potential (Eqs. (4.3) and (4.4)) to react with target organic compounds leading to their partial or complete mineralization. The effectiveness of a peroxide activation system for oxidizing organic compounds with persulfate is likely governed by various factors (e.g., persulfate strength, H_2O_2: $S_2O_8^{2-}$ molar ratio, rate of formation and persistence of the radical or active species) which may depend upon the experimental conditions (e.g., $[S_2O_8^{2-}]$, $[H_2O_2]$, pH, temperature). Perhaps due to these factors and the multi-radical attack on gasoline compounds, the activation and oxidation chemistry may lead to higher k_{obs} with a lower $H_2O_2:S_2O_8^{2-}$ molar ratio. Crimi and Taylor (2007) also observed higher overall oxidation of BTEX compounds by lowering the $H_2O_2:S_2O_8^{2-}$ molar ratio from 0.035 to 0.0035. In this effort we employed only two $H_2O_2/S_2O_8^{2-}$ molar ratios and acknowledge that

further study is required for a better understanding of the multi-radical oxidation phenomenon in order to design an efficient dual-oxidant treatment system.

4.3.3. Chelated-Fe(II) Activated Persulfate Treatment

Similar to the unactivated and peroxide-activated trials, data from the chelated-Fe(II) activation trials were also able to be represented by a first-order kinetic expression (Table 4.2). Persulfate activation by chelated-Fe(II) at the two Fe(II) concentrations resulted in 3 to 15 times faster oxidation than the unactivated persulfate trials for all the monitored gasoline compounds (Figures 4.1(b) and 4.2). The Fe-600 trial yielded 1 to 3 times higher k_{obs} as compared to Fe-150 for all monitored compounds with a decreasing order of ethylbenzene and TMBs > toluene > xylenes or benzene > naphthalene. Availability of more Fe(II) appears to lead to greater activation of persulfate to generate the sulfate radical through the reaction

$$S_2O_8^{2-} + Fe^{2+} \rightarrow SO_4^{-\bullet} + SO_4^{2-} + Fe^{3+} \qquad (4.9)$$

which results in a higher rate of formation of $SO_4^{-\bullet}$. A higher concentration of Fe(II) provides for increased activation of persulfate which results in faster degradation of persulfate as shown in Figure 4.3 where the persulfate concentration decreased by ~25% for the Fe-600 trial as compared to ~18% for the Fe-150 trail. Although a higher Fe(II) concentration appears to improve the oxidation rate of the monitored gasoline compounds, it will compromise the persistence of persulfate. Activation of persulfate by chelated-iron may be a useful strategy but the upper bound of Fe(II) usage should be identified to prevent unproductive scavenging of sulfate radicals by Fe(II) ions. Although pH monitoring was not undertaken for these trials it is speculated that potentially acidic conditions caused by the

chelating agent (citric acid) and the oxidation of organics (Eq. 4.5) may have led to acid-catalyzation of persulfate and therefore influenced oxidation reactions. The presence of citric acid increased the organic load in the system and may have interfered with the oxidizing species ($S_2O_8^{2-}$, $SO_4^{-\bullet}$ or $OH^{\bullet}$). Since citric acid was not analyzed, the impact of the chelating agent on the overall oxidation efficiency and persulfate persistence was not determined.

Fe(II)-activated persulfate oxidation of some PHC compounds has been reported previously. Forsey (2004) observed significant oxidation of m-xylene and naphthalene. Liang et al. (2008) used much higher Fe(II) concentrations and hence demonstrated much faster oxidation rates of BTEX compounds than those observed during this study. Similarly, Crimi and Taylor (2007) observed almost complete (>99%) destruction of BTEX compounds under chelated-Fe(II) activation conditions. Although a direct comparison of k_{obs} from these other published studies cannot be made due to variable experimental conditions, it has been consistently observed that Fe(II)-activation is an effective strategy for the persulfate treatment of most gasoline compounds.

4.3.4. High pH Activated Persulfate Treatment

Results from pH Control–11 and pH Control–13 showed no alkaline hydrolysis of the monitored gasoline compounds (Figures 4.1(b) and 4.2). The solution pH in the pH–11 trial decreased to ~3 within 9 days whereas there was negligible change (~0.5 units) in the solution pH in the pH–13 trial (Figure 4.4). Oxidation of organics by persulfate results in the formation of H^+ (Eq. 4.5) and limited availability of OH^- will eventually result in continual drop in pH as observed in the pH–11 trial. The rate of oxidation of the monitored gasoline compounds in the pH–11 trial increased beyond Day 9 due to decrease in pH which led to an acid-catalyzed persulfate situation Eq. (4.5). Considering this condition, it is not surprising

that the alkaline activation of persulfate at pH 11 resulted in significantly higher oxidation of the monitored gasoline compounds as compared to activation at pH 13.

Therefore, to avoid complexity arising from acid-catalyzation of persulfate, data from ≤ 9 days for the pH–11 trial was used to extract first-order kinetic information while the entire data set for pH–13 was considered. For the pH–11 trial, k_{obs} were ~2 times higher than the unactivated results. Activation by pH 13 was much less effective resulting in <65% oxidation of gasoline compounds during entire the reaction period. Oxidation rates were 5 to 100% higher than the unactivated results only for the heavier molecular weight monitored compounds (e.g., xylenes, TMBs and naphthalene) while the rates were ~50% lower than unactivated trial for the remaining monitored compounds. The k_{obs} for pH–13 were up to 4 times lower than those for pH–11 trials. Overall, pH 11 activation increased k_{obs} relative to the unactivated trial but these values were 20 to 90% lower than observed in either the peroxide or chelated-Fe(II) activation trials. It is acknowledged that, similar to the unactivated experiments, the pH–11 trials may have been impacted by reduced pH conditions. Near-neutral conditions may be more efficient for oxidation of some compounds than slightly alkaline conditions (Forsey 2004; Liang et al., 2007). Sulfate radicals may promote the formation of hydroxyl radicals at high pH which may be scavenged by sulfate and carbonate species (Peyton, 1993; Liang et al., 2007) resulting in lower efficiency of oxidation of gasoline compounds at higher pH conditions (pH 13, and pH 11 at early time). Hydroxyl radicals may be formed at elevated pH which can also be scavenged by carbonate (Buxton, 1988). Oxidation may be more effective at a lower pH where less reactive carbonic species (H_2CO_3) are dominant (Forsey, 2004). Persulfate decreased by ~30% for pH–11 trial while the loss was much less significant (~10%) for the pH-13 trail (Figure 4.3). This

indicates that at an extremely high pH (~13) the overall persulfate activation and oxidation is a slower process.

4.3.5. Natural Activated Persulfate Treatment

The Natural Control–Borden and Natural Control–LC34-LSU represent loss of gasoline compounds from the aqueous phase due to sorption which was observed to be significant (up to 25%) for both aquifer materials (Figures 4.1(c) and 4.2). When persulfate is present, the data represents the total mass loss of gasoline compounds from the aqueous phase due to both sorption and chemical oxidation. Therefore, destruction of organics due to oxidation alone was estimated from the difference between control and the activation trial time series (Figure 4.1(c)).

Oxidation of organic compounds was once again captured by the first-order rate law (Table 4.2); however, data for 1,2,4-TMB, 1,3,5-TMB and naphthalene during the Borden trial were inconsistent and therefore not used. Comparison of k_{obs} from natural activation and unactivated trials support the hypothesis that acid-catalyzation (pH <3) of persulfate beyond Day 12 during the unactivated persulfate trial was responsible for enhanced oxidation of gasoline compounds.

Unlike the unactivated trial, the buffering capacity of the aquifer materials (Sra et al., 2010) prevented a significant pH drop (Figure 4.4) and hence the k_{obs} could be estimated from data collected from the entire experimental period. Unactivated persulfate may represent the minimum oxidation rate of a gasoline compound which was enhanced by the presence of aquifer materials. In general, the k_{obs} were up to 80% larger than the values from the unactivated trial; however, the data is not sufficient to identify aquifer material is better to

naturally activate persulfate. Enhanced oxidation in soil slurry experiments was also reported by Liang et al. (2008). The k_{obs} from natural activation experiments are more representative of oxidation of gasoline compounds under subsurface conditions compared with the unactivated persulfate trials. Although k_{obs} from these natural activation trials were not as high as k_{obs} from activation strategies employing external reagents (e.g., peroxide and CA-Fe), the results elucidate that reactivity of gasoline compounds due to persulfate is quite high in the presence of aquifer materials.

During these natural activation trials, persulfate concentration decreased by ~15% for the Borden aquifer material trial and by ~25% for the LC34-LSU aquifer material trial (Figure 4.3). This loss of persulfate mass was ~10% higher than reported by Sra et al. (2010) for the interaction of persulfate with these aquifer materials without organic compounds present.

4.3.6. Impact on TPH and PHC Fractions (F1 and F2)

The control reactors showed no significant loss of the PHC F1 or F2 fractions over the experimental period (Figure 4.1(d-e)). No oxidation of the PHC F1 fraction and TPH concentration was observed when the low persulfate concentration (1 g/L) was used; however, a significant (~75%) decrease in the concentration of the PHC F2 fraction was observed (Figure 4.2(d-e)) during the early time (<10 days). The rapid loss of the PHC F2 fraction indicates the presence of a readily oxidizable portion whereas the remaining portion of the F2 fraction seems to be resistant to persulfate treatment consistent with the findings by Forsey (2004) who observed only a partial decrease in pyrene ($C_{16}H_{10}$) concentration in a Fe(II)-activated persulfate system. The PHC F1 fraction accounts for 85 to 90% of the TPH mass, and is predominantly (90%) composed of BTEX compounds and therefore, by

extension, both the F1 fraction and the TPH concentration followed trends similar to those of the BTEX compounds.

Use of 20 g/L persulfate concentration under activated or unactivated conditions resulted in significant (50 to 97%) destruction of PHC F1 fraction and TPH concentrations consistent with the trends observed for BTEX compounds. The PHC F2 fraction did not undergo enhanced oxidation as a result of activated persulfate treatment. Almost all trials demonstrated an initially (<10 days) fast destruction of the PHC F2 fraction followed by relatively slower oxidation rate or complete stalling. The overall oxidation of the PHC F2 faction was observed to be significant (60 to 85%) across most of the trials. Moderate oxidation (40 to 60%) of PHC F2 fraction was observed during natural activation but both chelated-Fe(II) and pH–13 trials resulted in relatively poor treatment (20 to 40%). The presence of a readily oxidizable portion in the PHC F2 fraction was also observed in the peroxide controls where a 50 to 70% loss of the PHC F2 fraction occurred.

4.3.7. Treatment Efficiency

Residual persulfate decreased by approximately 55% and 20% in the 1 g/L and 20 g/L unactivated persulfate trials, respectively (Figure 4.3). For the peroxide activation trials, residual oxidant concentration was expressed as the total oxidant strength which decreased by ~30% at both peroxide molar ratios (Figure 4.3). For the remaining activation trials, the degradation of persulfate was <40%. Interaction with activating agents including aquifer materials, direct oxidation of the PHCs, and acid-catalyzed decomposition (Eq. 4.6) were responsible for this loss of persulfate mass. This high residual persulfate concentration after

28 days indicates excellent persistence in a gasoline solution and suggests that time-dependant persulfate transport processes may occur at gasoline contaminated sites.

The overall bulk gasoline stoichiometry for these experimental trials was quantified as the ratio of persulfate mass ($S_2O_8^{2-}$) consumed to gasoline mass destroyed as represented by TPH (Table 4.2). This estimate varied from 120 to 340 g-$S_2O_8^{2-}$/g of TPH for the different trials and, as expected, is substantially higher than the value of 37 g-$S_2O_8^{2-}$/g determined for benzene from Eq. (4.5). Persulfate consumption was higher in the presence of activating agents which led to higher stoichiometric ratios. The treatment efficiency was defined as the inverse of the bulk stoichiometric measure. Based on this, the 20 g/L unactivated persulfate trial resulted in the best treatment efficiency followed closely by the Fe-150 trial.

4.4. SUMMARY

All the monitored gasoline compounds were found to be amenable to persulfate oxidation at a concentration of 20 g/L with or without activation and their degradation was captured by first-order kinetics. Relative to unactivated persulfate, oxidation rates were significantly improved using either peroxide (2 to 12 times) or chelated-Fe(II) (3 to 18 times) activation and were moderately improved for pH–11 (1.7 to 2.3 times) or natural activation (1 to 1.8 times). Alkaline activation at a pH of 13 adversely impacted oxidation rates for low molecular weight monitored compounds. The highest oxidation rates were delivered by either a low peroxide molar ratio of 0.1 mol H_2O_2/mol $S_2O_8^{2-}$ or a high chelated-Fe(II) concentration of 600 mg/L. Oxidation rates increased in the unactivated persulfate or the pH–11 activation trial when the solution pH <3, creating an acidic condition that triggered acid-catalyzed activation of persulfate. Near similar oxidation results were observed for the

natural activation and unactivated trials indicating that either the potential activation by minerals was not significant or that this activation is offset by radical scavenging by aquifer material constituents. The PHC F1 fraction was susceptible to significant oxidation but the PHC F2 fraction exhibited only partial destruction by unactivated or activated persulfate.

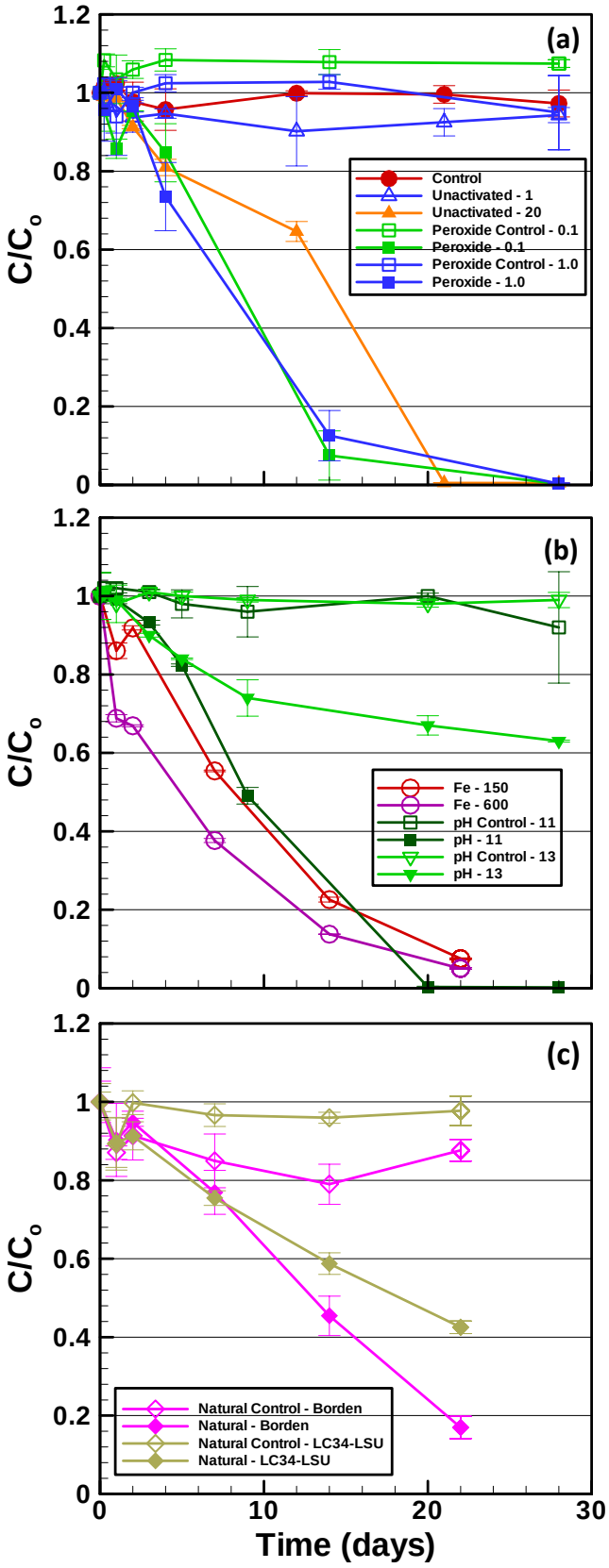

Figure 4.1. Benzene concentration profiles during persulfate oxidation (a) unactivated persulfate or peroxide activation conditions, (b) chelated-Fe(II) or alkaline activation conditions, and (c) natural activation conditions.

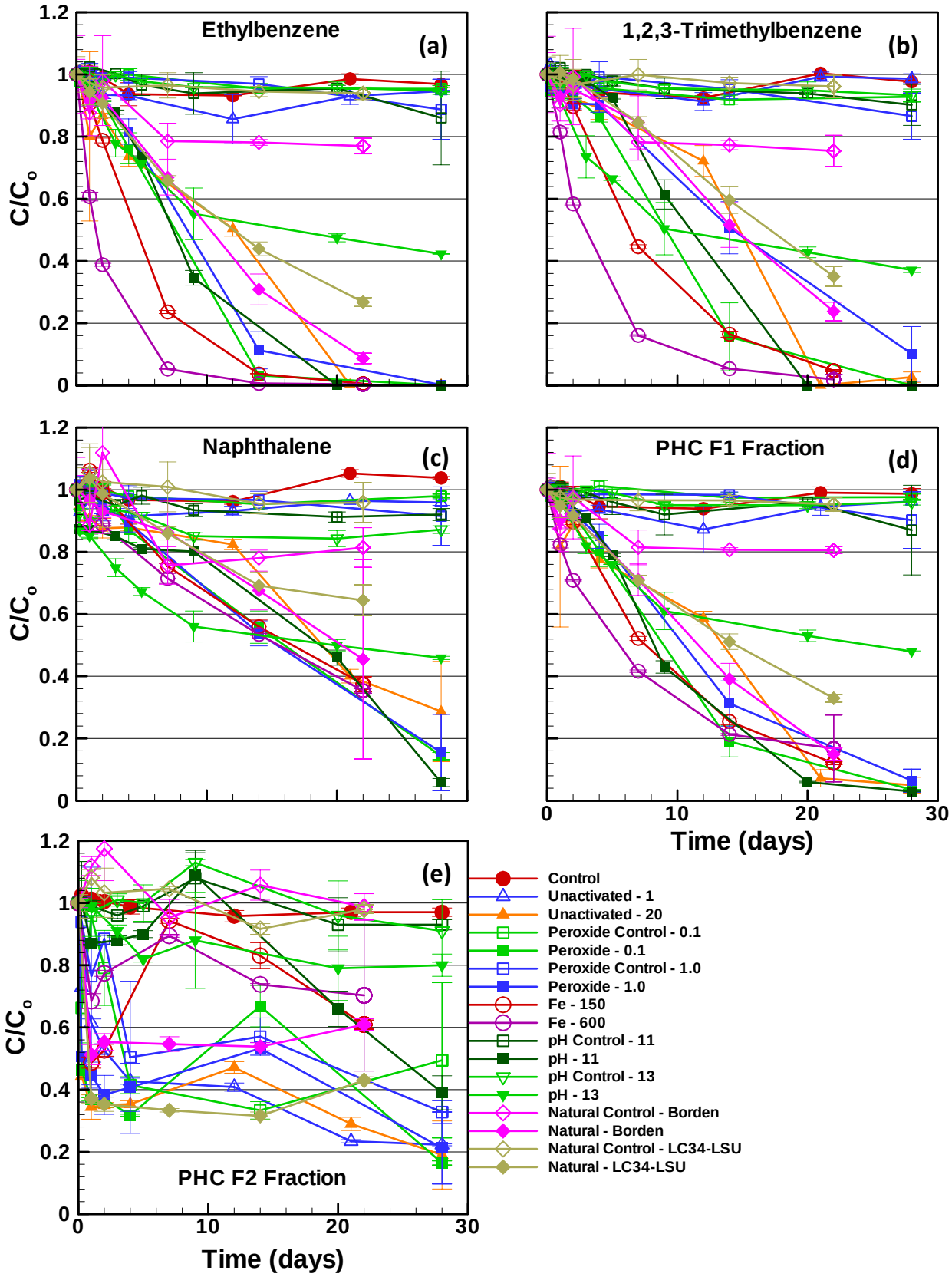

Figure 4.2. Concentration profiles of selected gasoline compounds and PHC fractions during oxidation by unactivated and activated persulfate: (a) ethylbenzene, (b) 1,2,3-trimethylbenzene, (c) naphthalene, (d) PHC F1 fraction, and (e) PHC F2 fraction.

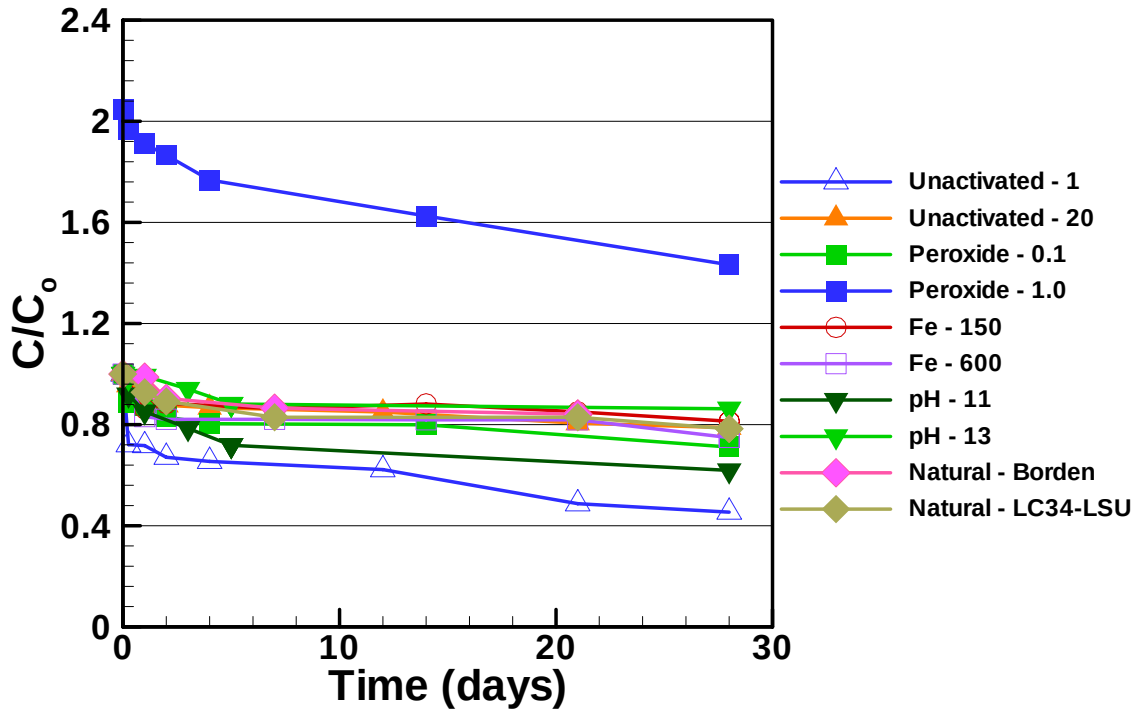

Figure 4.3. Residual persulfate or total oxidation strength profiles during oxidation of gasoline compounds by unactivated and activated persulfate.

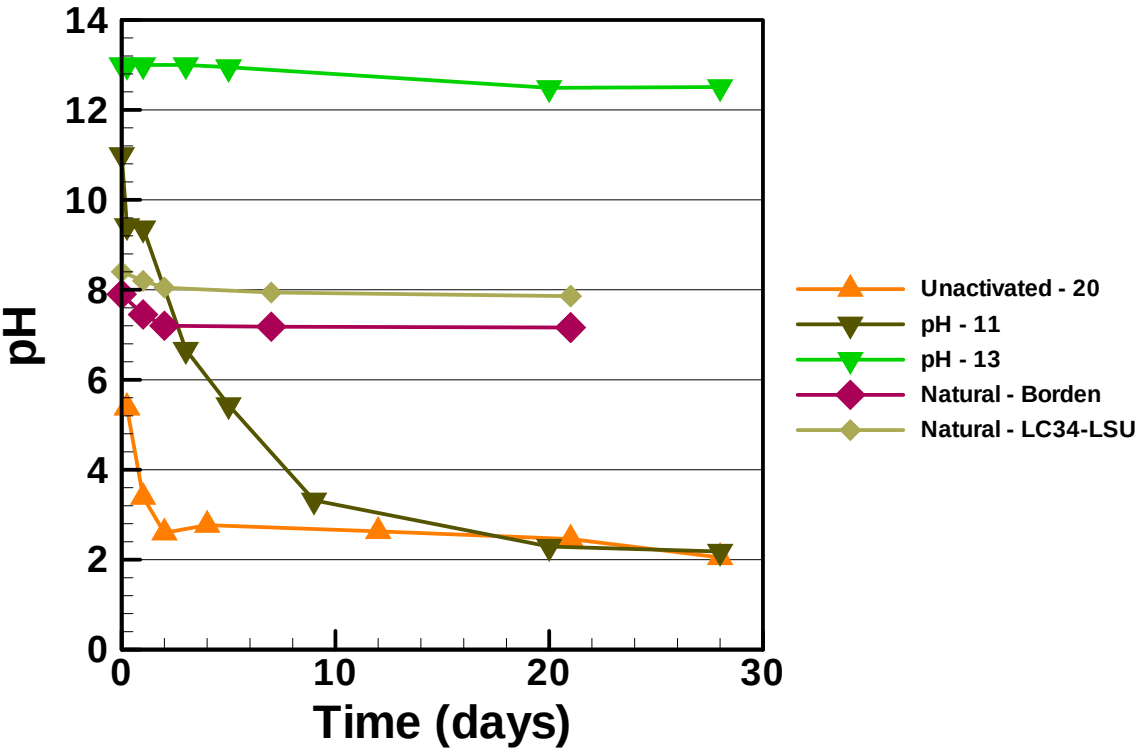

Figure 4.4. pH profiles during oxidation of gasoline compounds by unactivated and activated persulfate.

Table 4.1. Summary of experimental conditions for persulfate oxidation of gasoline compounds

Trial Label (Activator)		Initial Reactor Conditions	
		Persulfate Concentration (g/L)	Activator Concentration
Control	(-)	-	-
Unactivated–1	(-)	1	-
Unactivated–20	(-)	20	-
Peroxide Control–0.1	(H_2O_2)	-	[a]0.1 mol H_2O_2 /mol $S_2O_8^{2-}$
Peroxide Control–1.0	(H_2O_2)	-	[a]1.0 mol H_2O_2 /mol $S_2O_8^{2-}$
Peroxide–0.1	(H_2O_2)	20	0.1 mol H_2O_2 /mol $S_2O_8^{2-}$
Peroxide–1.0	(H_2O_2)	20	1.0 mol H_2O_2 /mol $S_2O_8^{2-}$
Fe–150	($FeSO_4.7H_2O$)	20	[b]150 mg/L Fe(II)
Fe–600	($FeSO_4.7H_2O$)	20	[b]600 mg/L Fe(II)
pH Control–11	(NaOH)	-	pH 11
pH Control–13	(NaOH)	-	pH 13
pH–11	(NaOH)	20	pH 11
pH–13	(NaOH)	20	pH 13
Natural Control–Borden	(Solids)	-	[c]1
Natural Control–LC34-LSU	(Solids)	-	[c]1
Natural–Borden (Solids)		20	[c]1
Natural–LC34-LSU (Solids)		20	[c]1

[a] Concentration of peroxide with respect to 20 g/L persulfate. Persulfate was not actually added to the peroxide control reactors.

[b] Fe(II) chelated with Citric acid (CA) at CA:Fe(II) molar ratio of 1:1

[c] Concentration of activator in g of solids/mL aqueous volume

Table 4.2. First-order oxidation rate coefficients and bulk stoichiometry

Compounds	MDL (µg/L)	k_{obs} [10^{-3} day^{-1}], (r^2)								
		Unactivated	Peroxide		Chelated-Fe(II)		Alkaline		Natural	
		Unactivated-20	Peroxide-0.1	Peroxide-1.0	Fe-150	Fe-600	pH-11	pH-13	Borden	LC34-LSU
Benzene	1.3	36.8 ± 1.8 (0.97)	225 ± 7 (0.98)	215 ± 11 (0.96)	117 ± 3 (0.99)	131 ± 2 (0.99)	76.0 ± 7 (0.89)	17.0 ±1.1 (0.92)	51.5 ±4.8 (0.87)	36.3 ±1.3 (0.98)
Toluene	1.1	56.3 ± 1.8 (0.98)	249 ± 10(0.97)	161 ± 8 (0.95)	162 ± 4 (0.99)	161 ± 2 (0.99)	114 ± 10 (0.90)	28.9 ± 1.6 (0.94)	60.8 ±3.7 (0.94)	58.1 ±1.3 (0.99)
Ethylbenzene	1.5	56.9 ± 2.1 (0.98)	269 ± 1 (0.96)	209 ± 9 (0.96)	240 ± 3 (0.99)	271 ± 17 (0.94)	112 ± 9 (0.91)	30.8 ± 1.9 (0.93)	48.1 ±3.1 (0.94)	52.0 ±1.3 (0.99)
p,m-Xylene	2.6	30.8 ± 1.6 (0.96)	205 ± 1 (0.95)	56.9 ± 3 (0.97)	112 ± 3 (0.99)	128 ± 1 (0.99)	68.4 ± 6.7 (0.86)	32.5 ± 2.0 (0.93)	37.1 ±3.7 (0.86)	46.4 ±1.9 (0.97)
o-Xylene	1.8	28.3 ± 1.1 (0.98)	186 ± 8 (0.97)	55.5 ± 2.9 (0.95)	102 ± 3 (0.99)	135 ± 1 (0.99)	63.6 ± 7.5 (0.82)	21.4 ± 1.9 (0.93)	41.2 ±4.3 (0.85)	49.2 ±2.2 (0.97)
1,3,5-TMB	1.2	24.8 ± 1.8 (0.93)	71.4 ± 7.9 (0.83)	47.5 ± 2.7 (0.94)	115 ± 10 (0.91)	360 ± 3 (0.93)	56.0 ± 6.1 (0.84)	38.4 ± 4.3 (0.82)	[a]-	44.2 ±6.7 (0.73)
1,2,4-TMB	1.0	15.4 ± 1.9 (0.82)	179 ± 11(0.93)	56.7 ± 2.2 (0.97)	160 ± 2 (0.99)	273 ± 3 (0.99)	26.9 ± 2.6 (0.87)	31.6 ± 2.2 (0.91)	[a]-	18.1 ±1.5 (0.90)
1,2,3-TMB	1.0	26.6 ± 1.8 (0.94)	166 ± 7 (0.84)	63.9 ± 3.0 (0.96)	141 ± 2 (0.99)	181 ± 9 (0.96)	50.8 ± 6.2 (0.80)	34.9 ± 2.3 (0.92)	29.4 ±3.8 (0.79)	44.0 ±2.3 (0.96)
Naphthalene	2.2	12.1 ± 2.8 (0.59)	68.2 ± 3.0 (0.96)	52.6 ± 1.4 (0.99)	47.0 ± 1.3 (0.99)	47.2 ± 0.9 (0.99)	[a]-	25.1 ± 2.0 (0.88)	[a]-	17.5 ±2.1 (0.91)
$S_2O_8^{2-}$ /TPH (g/g)		120	160	340	130	180	260	180	150	190

[a]Insufficient data quality (r^2<0.5)

Chapter 5

In Situ Gasoline Source Zone Treatment Using Persulfate

Overview

A 2000 L solution of unactivated sodium persulfate ($Na_2S_2O_8$) at 20 g/L concentration was injected into a gasoline source zone. Concentrations of inorganic species ($S_2O_8^{2-}$, SO_4^{2-}, Na^+, $CO_{2(aq)}$), high impact gasoline compounds (benzene, toluene, ethylbenzene, xylenes, trimethylbenzenes and naphthalene) and petroleum hydrocarbon (PHC) fractions (F1 and F2) were monitored across a fence-line equipped with 90 multilevel sampling points for over 4 months post-injection. Mass loading for the plume ($\dot{M}$) was used to measure performance and was estimated using the concentration time series data. Breakthrough of the inorganic species was observed when the injection slug crossed the monitoring fence-line. Increase in $\dot{M}_{SO_4^{2-}}$ indicated consumption of persulfate during oxidation of gasoline compounds or due to degradation in the presence of aquifer materials. $\dot{M}_{CO_2}$ increased by >100% suggesting complete mineralization of gasoline compounds during persulfate oxidation. Transport of Na^+ appeared to be retarded due to ion exchange processes with the aquifer materials. Mass loading for all the monitored gasoline compounds (MGCs) and PHC fractions reduced by 45 to 86% as the inorganic slug crossed the monitoring fence-line. The cumulative mass crossing this fence-line was 20 to 50% lower than that expected without persulfate treatment. The inorganic concentrations approached the pre-treatment conditions and a partial rebound of MGC concentrations was observed after the inorganic injection slug was flushed from the source.

5.1. INTRODUCTION

Gasoline is among the most extensively used petroleum hydrocarbons (PHCs) worldwide and its accidental release, spill or leakage from underground storage tanks (USTs) often causes soil and groundwater contamination (Park et al., 2009). Gasoline consists of the low molecular weight carbon fraction composed primarily of C_6 to C_{16} compounds including acutely toxic and highly persistent aromatics such as benzene, toluene, ethylbenzenes and xylenes (BTEX) in addition to trimethylbenzenes and naphthalene (Prince et al., 2007). Benzene and ethylbenzene are established human carcinogens and health impacts of BTEX compounds, in general, include neurological impairment and hematological effects (ATSDR, 2004). Gasoline and other PHC source zones are persistent and hence act as long term sources of groundwater contamination until the source zone is removed, quarantined, attenuated by natural processes or treated in place (Lundegaard and Johnson, 2007). In this investigation, the *in situ* persulfate oxidation of gasoline range PHCs was examined as a remediation option for the treatment of a well characterized gasoline source zone.

Contemporary efforts to remediate gasoline-contaminated soil and groundwater have included the use of various technologies (e.g., biodegradation, air-sparging, pump-and-treat, phyto-remediation), but the physical and geochemical subsurface heterogeneities and contaminant characteristics can significantly limit the benefits of these technologies (Nadim et al., 2000; ITRC, 2004; Zhou et al., 2005; Dadkhah and Akgerman, 2007; Kunucku 2007). *In situ* chemical oxidation (ISCO) offers an alternative and aggressive remediation option either alone or as an important step within a "treatment train" (Tsitonaki et al., 2006; Tsai and Kao, 2009). During the past 5 years, persulfate has emerged as a potentially useful oxidant for the destruction of a wide range of organic contaminants including PHCs. Its

effectiveness in the treatment of these organic compounds has been reported in a number of bench-scale investigations (Liang et al., 2004; Huang et al., 2005; Crimi and Taylor, 2007; Liang et al. 2008; Sra et al., 2010). Sra et al. (2010) specifically demonstrated the ability of unactivated or activated persulfate to destroy a mixture of gasoline compounds. However, the peer-reviewed literature reporting its usefulness and application at pilot- or full-scale gasoline-contaminated sites is scarce.

In order to establish remediation goals, it is important to understand the response of a source zone to persulfate-based ISCO remediation in a controlled manner. While reduction in the aqueous phase concentration or mass flux emanating from a treatment area may be a useful performance metric, overlooking system rebound (Thomson et al., 2008; Suthersan et al., 2010) or dilution caused by the injected solution (Payne et al., 2008) may lead to erroneous estimation of treatment efficiency and effectiveness. This is particularly important immediately following treatment. Rebound of organic concentration or mass flux occurs when the oxidant is removed from or consumed within the treatment area, and dissolution or mass transfer of contaminants from untreated contaminant mass takes place (Mundle et al., 2008; Suthersan et al., 2010). Similarly, mixing of the uncontaminated solution with contaminated ambient groundwater during oxidant injection can potentially dilute the organic concentrations and over-estimate oxidation efficiency. Frequent and timely monitoring for target organics, potential inorganic by-products and other geochemical indicators is one approach to avoid error in assessment of remediation goals and treatment performance.

In this investigation, we undertook the treatment of a gasoline-contaminated source zone by unactivated persulfate and frequently examined the evolution and breakthrough of organic

compounds, residual persulfate, and oxidation by-products (e.g., SO_4^{2-}, Na^+, $CO_{2(aq)}$) over a 4 month period following treatment. Oxidation performance efficiency was measured by estimating organic and inorganic concentrations and/or mass loading across a monitoring fence-line down-gradient of the gasoline treatment area. Systematic evaluation of the observations was made to differentiate loss of organic mass loading due to persulfate oxidation from the effects of dilution. Prolonged and frequent sampling was conducted to enable rebound assessment.

5.1.1. Site Description

A 48 kg modern gasoline fuel source with 5% methyl *tert*-butyl ether (MTBE) and 5% *tert*-butyl alcohol (TBA) (collectively known as GMT) was emplaced below the water table within a sheet pile-walled gate area at the University of Waterloo research facility at Canadian Forces Base (CFB), Borden, Canada in 2004. This emplacement was conducted as a part of another study (Mocanu, 2006) evaluating the distribution and flux of dissolved PHCs through an extensive network of monitoring fences perpendicular to the groundwater flow. The monitoring network consisted of 4 fences identified as Row 1 to Row 4 installed 6 m apart in the direction of groundwater flow. Each row contained 6 multilevel monitoring wells (MW1 to MW6) separated by 1.2 m (Figure 5.1(a)) and equipped with 14 multilevel (ML) sampling points (ML1 to ML14) vertically spaced by 18 cm with the shallowest multilevel (ML1) starting at ~1.5 m bgs (Figure 5.1(b)). A PVC center stalk was screened from 4.84 to 5.34 m bgs and represented ML15. The gasoline fuel source was emplaced between Row 1 and Row 2 using 15 PVC injection wells (internal diameter 5 cm) screened

from 2.25 to 4.5 m. The injection wells were arranged in 2 rows spaced ~30 cm apart located ~3.5 m up-gradient of Row 2 (Figure 5.1(a)).

Significant total petroleum hydrocarbon (TPH) concentrations up to 35 mg/L have historically (over 2 years) existed in the Row 2 monitoring network suggesting significant residual mass in the source zone. Based on historical monitoring episodes, it was estimated that at the time of treatment ~40 kg of gasoline remained in the source zone that occupied a volume (V_{source}) of 1.7×3.5×1.2 m^3 (≡7.1 m^3) (Mocanu, 2006). No MTBE or TBA was detected after the first year of monitoring following emplacement suggesting that these mobile and highly soluble GMT constituents have been depleted from the source zone. Additional information on emplacement and source zone characteristics are provided by Mocanu (2006). Soil cores were withdrawn from the source zone and analyzed in 2007 to construct a vertical profile for TPH concentration (mg/kg) which showed that the majority of the gasoline mass was limited between 3.0 to 4.2 m bgs (Freitas et al., 2008; Yang, 2009).

The aquifer material at CFB Borden is generally homogenous and is composed of well-sorted fine to medium grain sand (hydraulic conductivity 2.00×10^{-4} to 6.00×10^{-6} m/s) with some microscale heterogeneity in the form of silty sand and coarse sand lenses (Mackay et al., 1986; Sudicky, 1986). The water table is usually located at ~1 m bgs but may vary seasonally. The underlying aquitard is located at ~11 m bgs and is ~8 m thick (Morrison, 1998). A historical leachate plume is known to exist >5 m bgs and is responsible for an elevated pre-treatment SO_4^{2-} concentration in the deeper horizons starting at ~5 m bgs (MacFarlane et al., 1983).

5.2. METHODS

5.2.1. Oxidant Injection

Unactivated persulfate at a 20 g/L concentration was demonstrated to be effective for significant to near-complete destruction of the monitored gasoline compounds (MGCs) (benzene, toluene, ethylbenzene, p,m-xylene and o-xylene (>99%), 1,2,3-trimethylbenzene, 1,2,4-trimethylbenzene and 1,3,5-trimethylbenzene (>95%), and naphthalene (>70%)) over a 28 day reaction period. Significant oxidation (~80%) of PHC fractions F1 (C_6 to C_{10}) and F2 (C_{10} to C_{16}), and TPH was also reported (Sra et al., 2010). Natural activation conditions using Borden aquifer material exhibited 1 to 1.8 times higher oxidation rate coefficients for MGCs as compared to the unactivated persulfate. Therefore, anticipating some natural activation, unactivated persulfate was injected into the gasoline source zone at a concentration of 20 g/L.

In order to achieve the required spatial coverage during persulfate injection, 3 of the 15 injection wells used by Mocanu (2006) as identified on Figure 5.1(a) were used to inject ~2000 L of persulfate. This volume was sufficient for complete coverage of the assumed source zone (PV = 0.3×7.1 ≈2100 L). The injection water was collected in a 2200 L polyethylene (PE) tank from a nearby uncontaminated well at the research facility (Table 5.1). Following addition of persulfate mass (~40 kg Klozur, FMC), the solution was mechanically stirred using an electrically-operated drill mixer. Concurrently, to enhance dissolution of the solid persulfate and to obtain a homogenous concentration throughout the tank, solution was withdrawn from an outlet at the bottom of the tank and re-cycled back into the top of the tank at a flow rate of 30 L/min. The pump was equipped with a ball-valve flow

controller and connected to the tank via PE plastic pipes (internal diameter 2.54 cm). After mixing and recycling for ~1 hr, the pump and mixer were switched off, and the pump outlet was then connected to an injection manifold (Figure 5.2). The manifold distributed the injection solution to three outlet PE pipes using a combination of 90^{o} and T-shape galvanized steel barb-fittings. A cumulative flow meter was placed between the pump and the 3 injection outlets. Each of these outlets was equipped with a flow control gate valve, a vent valve and a pressure gauge (0-100 kPa) to enable flow control during injection. PE pipes were used to connect manifold outlets to the riser pipes of the three injection wells which were remodeled to accommodate 2.54 cm barb-fittings. Persulfate solution was injected into the 3 wells under a pressure of 14 to 21 kPa at an average flow rate of 13 L/min/well for ~1 hr. Samples from the injection line were collected every 20 min to quantify the injection persulfate concentration.

5.2.2. Performance Monitoring

Breakthrough of inorganic (persulfate, SO_4^{2-}, Na^+, $CO_{2(aq)}$) and MGC concentrations were anticipated to be useful in the overall assessment of oxidation performance (Table 5.1). Na^+ and SO_4^{2-} are released upon dissociation and degradation of sodium persulfate and can identify transport and evolution of the injected solution. While Borden aquifer material has a low cation exchange capacity (CEC ~0.5 meq/100 g), Na^+ may be potentially retarded (retardation factor of 1 to 2) due to sorption or ion exchange processes (Dance and Reardon, 1983; Christensen and Kjeldsen, 1984). Assuming non-sulfate reducing conditions at shallow depths (MacFarlane et al., 1983), the persulfate-SO_4^{2-} system can be employed to capture the transport of injected solution through the aquifer. SO_4^{2-} is a by-product of

persulfate degradation and in conjunction with Na^+ can be used as a potential measure for the overall persulfate degradation as a result of oxidation of organics and/or interaction with aquifer materials. From a stoichiometric viewpoint, 1 mol of sodium persulfate will yield 2 mol of Na^+ and 2 mol of SO_4^{2-} upon complete degradation. In other words, when persulfate is completely degraded, the injection slug should contain ~4.2 g SO_4^{2-} per 1 g of Na^+ assuming that both these species are conservative. Therefore, the relative strength of the two species may be indicative of the overall extent of persulfate degradation. Complete mineralization of target organics leads to CO_2 production and therefore, oxidation of MGCs, if proceeding to completion, will elevate $CO_{2(aq)}$ concentration. It should be noted that in a calcite-rich subsurface geochemical environment such as the Borden aquifer carbonate equilibrium may influence the dissolved CO_2 concentration.

In addition to the breakthrough concentration (BTC) profiles at individual monitoring points, mass loading of the inorganic species, MGCs and PHC fractions across the Row 2 fence-line was determined. The temporal variation in mass loading for all these species and compounds was used to provide a comprehensive evaluation of the source zone treatment. The mass loading ($\dot{M}$) defined as "the mass of a compound or species crossing the Row 2 fence-line per unit time" was calculated as the integration of the mass flux (Borden et al., 1997; Mackay and Einarson, 2001). Each sampling monitor with a given compound or species concentration (C_i) was assigned a representative area (A_i). Specific discharge (q) was assumed to be constant and was estimated from the average travel time of the centre of mass (t_{CoM}) of the injected solution.

To capture changes in the mass loading to the plume as a result of the source zone treatment, only the Row 2 monitoring wells were used. Samples collected 16 months prior to treatment from MW1 and MW6 in the Row 2 fence-line indicated that the concentration of all the MGCs was below the method detection limits (MDLs) and hence these wells were excluded from the monitoring program. Monitoring of MW2 to MW5 was conducted 2 weeks prior to persulfate injection to establish pre-treatment conditions. Monitoring was continued for >4 months post-injection (weekly for the first 2 months and then biweekly for the next 2 months) and samples were analyzed for organic and inorganic compounds. At least triplicate samples were collected from each multilevel sampler using a sampling glass vial (40 mL) placed between the multilevel and a peristaltic pump. For sample collection, the glass vial was fitted to an in line, stainless steel screw cap sample head. Several (2-3) groundwater volumes of the vial were passed through before the vial was detached from the sample head. Two samples were used for organic and/or CO_2 analysis and the third sample was used for analysis of inorganics (e.g., persulfate, SO_4^{2-} and Na^+). Samples for organic analysis were preserved with sodium azide (0.4 mL of 10% solution) and sealed with Teflon lined screw caps. All samples were stored at 4°C and held for <14 days prior to analysis at the University of Waterloo.

5.2.3. Analytical Methods

Organic analysis consisted of benzene, toluene, ethylbenzene, p,m-xylene, o-xylene, 1,2,3-trimethylbenzene, 1,2,4-trimethylbenzene, 1,3,5-trimethylbenzene and naphthalene. This comprehensive suite of analytes (MGCs) was assumed to sufficiently capture the total contaminant load and provide evidence of source zone treatment. All samples and standards

were equilibrated to room temperature. Methylene chloride, containing internal standards m-fluorotoluene and fluorobiphenyl (25 mg/L), was used as the solvent to extract organics from the aqueous phase. Five mL of sample was discarded with a glass/stainless syringe prior to the addition of the solvent (2.0 mL). The vial was quickly resealed and agitated on its side at 350 rpm on a platform shaker for 20 min. After shaking, the vial was inverted and the phases were allowed to separate for 30 min. The solvent phase (~1 mL) was removed through the Teflon septum from the inverted vial with a gas tight glass syringe. The extracted solvent was placed in a 2 mL Teflon-sealed auto-sampler vial and injected into HP 5890 capillary gas chromatograph equipped with a flame ionization detector. Extracted methylene chloride (3 μL) was injected in splitless mode (purge on 0.5 min, purge off 10.0 min) into a 0.25 mm × 30 m length, DB5 capillary column with a stationary phase film thickness of 0.25 μm. Helium column flow rate was 2 mL/min with a make-up gas flow rate of 30 mL/min. Injection temperature was 275^{o}C, detector temperature was 325^{o}C and initial column oven temperature was 35 ^{o}C held for 0.5 min, then ramped at 15 ^{o}C/min to a final temperature of 300 ^{o}C held for 2 min. Chromatographic run time was 10 min. Data integration was completed with SRI model 302 Peak Simple chromatography data system. Concentrations of PHC fractions F1 (MDL 5 μg/L) and F2 (MDL 5 μg/L), and TPH were also determined and used to explore changes in bulk organic mass load. Results for F1 and F2 fractions and TPH were obtained from chromatographs generated during hydrocarbon (BTEX, TMBs and naphthalene) analysis. The PHC F1 fraction included integration of all area counts beginning just after the hexane (nC_6) peak to the apex of the decane (nC_{10}) peak, while the PHC F2 fraction included integration from the apex of the decane peak to the apex of the hexadecane (nC_{16}) peak. TPH was estimated as the sum of F1 and F2 fractions.

Inorganic analysis consisted of persulfate, SO_4^{2-}, Na^+ and $CO_{2(aq)}$ concentrations. Persulfate was measured following the approach used by Huang et al. (2002). Persulfate analytical reagents were prepared using ACS grade ferrous ammonium sulfate (FAS) ($Fe(NH_4)_2(SO_4)_2 .6H_2O$) (EMD, Gibbstown, NJ), ammonium thiocyanate (NH_4SCN) (J.T. Baker, Phillipsbourg, NJ) and sulfuric acid (H_2SO_4) (EMD, Gibbstown, NJ) in Milli-Q water. Analyses for SO_4^{2-} and Na^+ were conducted using Ion Chromatograph (Dionex, DX-3000) (MDL for Na^+ of 0.1 mg/L, and for SO_4^{2-} of 0.3 mg/L).

For dissolved CO_2 analysis a 20 ml aliquot was withdrawn from the bottom of the sample vial into a 30 mL glass syringe containing 10-20 mL of pre-purified helium. The syringe was shaken and allowed to equilibrate for several hours at room temperature. Then a 6 mL aliquot of the gas phase from the syringe was injected into a 2 mL gas sample loop where a valve switch introduced the sample into the carrier gas stream of a GOW-MAC (Series 350GP) gas chromatograph equipped with a thermal conductivity detector. Peak areas are measured by a HP3380A integrator. MDL for $CO_{2(aq)}$ was 0.98 mg/L.

5.3. RESULTS AND DISCUSSION

The average MGC concentrations along the Row 2 fence-line determined 2 weeks before persulfate injection were within ±15% of the average concentrations for 6 out of 9 MGCs observed >16 months previously. The general similarity between MGC concentrations over this period indicates that, in the absence of any treatment, the concentrations and, by implication, mass loadings across the Row 2 fence-line would have remained consistent with the pre-treatment levels for the duration of this pilot-scale trial monitoring period.

The pre-treatment concentration profile along MW3 and MW4 shows a distinct and consistent trend with lower MGC concentrations (e.g., <200 μg/L ethylbenzene) to a depth of 2.8 m bgs and higher MGC concentrations (e.g., 1200 to 3500 μg/L ethylbenzene) between 2.8 and 4.0 m bgs (Figure 5.3(a)). This is consistent with the profile of bulk soil concentrations from soil core extracted from the source zone which indicates the presence of a higher residual gasoline mass between 3 to 4.2 m bgs (Figure 5.3(b)) (Freitas et al., 2008; Yang, 2009). Note that the pre-treatment MGC concentrations in groundwater at ML15 were insignificant (<2.4 μg/L).

The pre-treatment SO_4^{2-} and Na^+ concentrations along MW3 and MW4 were low (1 to 40 mg/L for SO_4^{2-}, and 1 to 13 mg/L for Na^+) but as expected (MacFarlane et al., 1983), the deepest monitors (ML15) were impacted (~220 mg/L SO_4^{2-}, ~37 mg/L Na^+) by the underlying leachate plume (Figure 5.3(c,d)). To avoid complexity arising from the leachate plume interference, these monitors (ML15) were neglected during inorganic data analysis.

5.3.1. Persulfate, SO_4^{2-} and Na^+ Concentration

The first post-injection sampling episode was conducted 8 days after persulfate injection. Concentration time series data for persulfate, SO_4^{2-} and Na^+ (Figure 5.4) was used to estimate the average travel time of the center of mass (t_{CoM}) for the three inorganic species.

The average t_{CoM} was estimated to be 64 days for persulfate and SO_4^{2-}, and 75 days for Na^+. Estimated t_{CoM} for persulfate may be deemed representative of the inorganic plug flow and groundwater flow conditions. Sulfate evolves from persulfate and hence the t_{CoM} for SO_4^{2-} could have been biased by initially higher concentrations when all persulfate was

converted to SO_4^{2-}. The estimate for Na^+ may be impacted by its attenuation due to sorption by the aquifer material (Christensen and Kjeldsen, 1984) and hence an average delay of 11 days was observed as compared to persulfate or SO_4^{2-}. Assuming an ideal distribution of the injected solution around the 3 injection wells, the inorganic slug length would be ~1.1 m. Further, assuming persulfate is unretarded with respect to groundwater, the travel time for this idealized plug to cross Row 2 would be 54 to 74 days. Using this information, the retardation factor for Na^+ was estimated to be ~1.2 which is within the range observed by Christensen and Kjeldsen (1984) for different soils.

The first persulfate breakthrough was observed on Day 21 but was limited to only two monitors at MW3 (ML1 and ML11). Persulfate was more consistently encountered in the subsequent sampling episodes across an increasing number of monitors until Day 103 after which no persulfate breakthrough was observed. Within 8 days of persulfate injection, Na^+ and SO_4^{2-} concentrations were up to 10 times higher than the pre-treatment concentrations at some of the monitors (e.g., ML1 to ML4, ML11 and ML 12 in both MW3 and MW4). Significant increase in Na^+ and SO_4^{2-} concentrations was observed in all monitors leading to an average concentration of >100 mg/L for SO_4^{2-} and >15 mg/L for Na^+ until Day 103. Hydrodynamic dispersion and the presence of high conductivity layers caused an earlier breakthrough of persulfate, Na^+ and SO_4^{2-} (Figure 5.4) than that anticipated from ideal plug flow. Earlier arrival of SO_4^{2-} than persulfate indicates either oxidation of gasoline compounds or persulfate degradation in the presence of Borden aquifer material. Persulfate concentration in individual monitors was generally <500 mg/L indicating significant mixing between ambient and injected water and/or persulfate degradation in the presence of aquifer

materials and MGCs. SO_4^{2-} and Na^+ concentrations were <1000 mg/L and <300 mg/L, respectively, and the maximum concentrations were 10 to 20 times lower than those anticipated from the injection concentrations. SO_4^{2-} concentration decreased after Day 71 whereas Na^+ concentrations generally began to decrease after Day 103. These concentrations appeared to approach the pre-treatment conditions after Day 121 suggesting that the majority of the injection slug had crossed the Row 2 monitoring fence-line and the sampling was terminated after Day 135.

5.3.2. Mass loading: SO_4^{2-}, Na^+ and $CO_{2(aq)}$

As expected from the observations made from the time series data, the $\dot{M}_{SO_4^{2-}}$ and $\dot{M}_{Na+}$ were initially observed to increase over time, reach a maximum value and then decrease as the monitored inorganic species were flushed from the treatment zone (Figure 5.6(a)). Consistent with the time series data, the initial increase in $\dot{M}_{SO_4^{2-}}$ was faster than for $\dot{M}_{Na+}$ suggesting that Na^+ may be slightly retarded by ion exchange or sorption (Dance and Reardon, 1983; Christensen and Kjeldsen, 1984). The increase in Na^+ mass load after Day 71 also indicated a typical desorption response as background ambient groundwater flushed through Na^+-sorbed soil (Christensen and Kjeldsen, 1984) and the SO_4^{2-} to Na^+ mass ratio was generally >4.2 up to Day 71. The maximum $\dot{M}_{SO_4^{2-}}$ and $\dot{M}_{Na+}$ were observed at Day 44, and the SO_4^{2-} to Na^+ mass ratio was observed to be <4.2 at this time. The decrease in the SO_4^{2-} to Na^+ mass ratio corresponded with significant persulfate breakthrough as high as 130 mg/L in almost all monitors implying that not all persulfate was consumed or decomposed to generate SO_4^{2-} and hence a SO_4^{2-} to Na^+ mass ratio of <4.2 was not unexpected. As these

inorganic species were flushed from the treatment zone the mass load across Row 2 was observed to decrease. Na^+ mass load increased due to desorption and consequently the SO_4^{2-} to Na^+ mass ratio was <4.2 The estimated average concentration of SO_4^{2-} and Na^+ in the inorganic slug indicated that the overall SO_4^{2-} (112.9 mg/L) to Na^+ (26.5 mg/L) mass ratio was ~4.3 which was very similar to that expected based on stoichiometry.

Complete oxidation of gasoline compounds would potentially result in their mineralization to CO_2 and hence the mass load of $CO_{2(aq)}$ would increase as the slug of injected solution moved across the Row 2 fence-line. This behavior was indeed observed as the dissolved CO_2 mass load increased in tandem with SO_4^{2-} or Na^+ increase. The maximum $\dot{M}_{CO_2}$ at Day 44 corresponded with the maximum mass load for SO_4^{2-} and Na^+. Beyond Day 44 the $\dot{M}_{CO_2}$ gradually reduced indicating a decrease in oxidation of gasoline compounds.

5.3.3. Concentration of MGCs

To simplify data analyses and to illustrate changes in the concentration of MGCs upon persulfate oxidation, ethylbenzene and naphthalene were selected since they generally captured the range of first-order oxidation rate coefficients as reported by Sra et al. (2010). This discussion can be qualitatively extrapolated to the other MGCs since the relative response of concentration and mass loading of all MGCs was consistent in behavior. The pre-treatment concentration of MGCs appeared to primarily occur between 3.0 and 4.0 m bgs (Figure 5.3(a)) and MW3 exhibited higher concentrations than MW4. Consistent with the breakthrough of inorganic species, depletion of MGC concentrations occurred as the inorganic slug moved across the Row 2 fence-line (Figure 5.5). The largest decrease in

MGC concentrations was observed between Day 65 and 79 corresponding with the exit of the idealized inorganic slug. Ethylbenzene concentration was reduced significantly by Day 79 with very low concentrations (<200 μg/L) in MW4, and relatively much lower concentrations (<1400 μg/L) in MW3 as compared to the pre-treatment concentration (~3200 μg/L) for all depths (Figure 5.5(a)). Similarly, naphthalene concentration was <90 μg/L in MW4 and <380 μg/L in MW3 (Figure 5.5(b)). The decrease in MGC concentrations was more evident on one end of the Row 2 fence-line (MW4) than the other (MW3) particularly during early time which corresponded with the occurrence of higher SO_4^{2-} and Na^+ concentrations in MW4. Dilution of the ambient organic concentrations by the injected, uncontaminated water may have also contributed to the decreased MGC concentrations. In accordance with the high mass loading observed for SO_4^{2-} and CO_2, this decrease in MGC concentrations was likely due to oxidation rather than dilution. Moreover, since Na^+ or SO_4^{2-} breakthrough was much lower (<10%) than the injected concentration, the mixing between ambient and injected solutions caused only a minor dilution of MGC concentrations (Payne et al., 2008). After inorganic slug was flushed across the Row 2 fence-line, re-equilibration of background groundwater with the gasoline source resulted in rebound. Therefore, ethylbenzene and naphthalene concentrations approached pre-treatment levels when sampling was terminated at Day 135.

5.3.4. Mass loading: MGCs

Mass loading across the Row 2 fence-line for all MGCs and PHC fractions were normalized to the pre-treatment mass loading ($\dot{M}_o$) (Figure 5.6(b)). These normalized data clearly demonstrate that by Day 28 a significant reduction in $\dot{M}/\dot{M}_o$ crossing Row 2 fence-line was

observed for all MGCs. The mass loading appears to increase temporarily but then further decreased to a minimum $\dot{M}/\dot{M}_o$ of 14 to 55% between Day 65 and 79 days (Table 5.2). The minimum mass loading for toluene was observed ~14 days earlier than the other compounds presumably because it exhibited the highest oxidation rate coefficient among all MGCs (Sra et al., 2010). The initial decrease of $\dot{M}/\dot{M}_o$ at Day 44 corresponds with the maximum Na^+, SO_4^{2-} and CO_2 mass loading implying significant oxidation of gasoline compounds during this time. Dilution of MGCs due to mixing of ambient groundwater and injection solution may have also contributed to this initial decrease. Further reduction in $\dot{M}/\dot{M}_o$ after Day 44 was due to continual persulfate oxidation of the MGCs. Theoretically, the persulfate injection solution was spread around its center of mass arriving at Row 2 at Day 64. The tail of this inorganic slug resulted in further decrease of MGC concentration. The $\dot{M}_{CO_2}$ remained elevated and was also suggestive of this continual oxidation. After Day 79, the concentration of the inorganic species, particularly persulfate, along the Row 2 fence-line dropped significantly indicating passage of the inorganic slug. In the absence of persulfate, $\dot{M}$ gradually increased to within 40 to 80% of $\dot{M}_o$ when monitoring was terminated at Day 135.

Similar to the observations for the MGCs, a significant decrease in $\dot{M}_{F1}$, $\dot{M}_{F2}$ and $\dot{M}_{TPH}$ was also observed (Figure 5.6(b)). The maximum reduction of $\dot{M}_{F1}$ (74%) and $\dot{M}_{TPH}$ (68%) occurred between Day 71 and 79, whereas for $\dot{M}_{F2}$ the maximum decrease was 54% at Day 51. As expected from bench-scale studies (Sra et al., 2010), the decrease in $\dot{M}_{F2}$ was lower than that for $\dot{M}_{F1}$ or $\dot{M}_{TPH}$ but the maximum decrease in $\dot{M}_{F2}$ occurred earlier than for MGCs or F1 fraction mass loadings. During the gasoline treatability study by Sra et al. (2010), up to a 60% decrease in PHC F2 fraction concentration was observed to have

occurred quickly (<10 days) followed by very low rate of destruction, unlike the MGCs or PHC F1 fraction. This suggested that the PHC F2 fraction consists of an oxidizable sub-fraction which can be quickly oxidized. Therefore, the fast destruction of this oxidizable portion in the PHC F2 fraction resulted in the minimum $\dot{M}_{F2}$ occurring earlier than the MGCs and the other bulk measures. Similar to the MGCs mass loadings, $\dot{M}_{F1}$, $\dot{M}_{F2}$ and $\dot{M}_{TPH}$ increased after Day 79 and were 45 to 50% lower than the pre-treatment mass loadings when monitoring was terminated at 135 days.

In general, the decrease in mass loadings for MGCs and PHC fractions was caused by persulfate oxidation of gasoline compounds resulting in the reduction of the source mass strength and due to dilution of organic compounds after injection of persulfate solution. In order to distinguish between the reduction in organic mass load due to physical dilution by 2000 L of injection solution and due to oxidation by persulfate, observed cumulative mass curve (CMC) and two theoretical CMCs for each MGC crossing the Row 2 fence-line were constructed. The observed CMC was calculated by assuming that mass loading between two sampling episodes was representative of the average of mass loading over each time interval. One theoretical CMC represents the cumulative mass expected based on the pre-treatment conditions and was assumed to be constant over 135 days given that these concentrations along the Row 2 fence-line were similar for ~16 months prior to treatment (Figure 5.7). The second theoretical CMC was constructed using the pre-treatment conditions but incorporating the potential dilution by the addition of 2000 L of uncontaminated injection solution. To represent the scenario for complete dilution, it was assumed that the 2000 L did not contain any dissolved gasoline compounds as it crossed the Row 2 fence-line. This assumption led to a CMC that coincided with the theoretical pre-treatment CMC until Day 54 when the front

end of the idealized injection slug reached the Row 2 fence-line. The total volume crossing the Row 2 fence-line from Day 54 to 74 consisted of a portion of injection slug with no gasoline compounds while the remaining portion carried MGC concentrations consistent with the pre-treatment conditions. Therefore, the increase in mass was near minimal from Day 54 to Day 74 after which the increase in cumulative mass was again consistent with the pre-treatment loading conditions.

The CMC for MGCs demonstrated that the observed cumulative mass was significantly lower than that from dilution-embedded CMC (Figure 5.8). By Day 135, the observed cumulative mass was 24 to 53% lower than that expected after incorporating dilution (Table 5.2), which clearly indicates that persulfate oxidation led to a significant decrease in mass load across the Row 2 fence-line. A larger decrease was observed for ethylbenzene, xylenes and toluene (≥42%) than for TMBs, benzene and naphthalene (20 to 33%) which was expected from the treatability study results (Sra et al., 2010). Overall, the relative decrease in observed cumulative mass for MGCs was also synonymous with earlier observations related to the inorganic data in which dilution was shown to play only a minor role. The slope of the CMC at Day 135 can be assumed to provide a quantitative estimate of the source zone strength since it represents the overall MGC dissolution rate. Slopes of the observed CMCs were 22 to 62% lower than those for dilution-embedded CMCs at Day 135 (Table 5.2) indicating that the source zone strength was depleted after persulfate treatment. Dissolution rates for ethylbenzene and naphthalene decreased from 99.5 mg/day and 12.3 mg/day, respectively, for dilution-embedded CMCs to 37.5 mg/day and 7.9 mg/day, respectively, for observed CMCs.

Analyses of the organic and inorganic data, particularly the mass loading trends for oxidation by-products and MGCs, and CMCs for the organic compounds illustrate a distinguishable impact of oxidation by persulfate in treatment of gasoline source zone. For lack of accurate and consistent source zone representation because of hydrogeological heterogeneity and variability in contaminant distribution, soil cores were not examined for visualization or quantification of persulfate oxidation impact on source zone mass. Decrease in contaminant mass in the source zone can be interpreted from the concentration and mass flux data across Row 2 indicating that a partial destruction of source zone mass was accomplished during this pilot-scale effort.

5.4. CONCLUSIONS

Persulfate oxidation of this gasoline source zone led to a significant reduction in organic mass load across the monitoring fence line. Mass loadings of selected gasoline compounds and PHC fractions were decreased by 45 to 86% compared with the pre-treatment conditions. Mass loading for SO_4^{2-}, Na^+ and CO_2 increased as the injection slug crossed the monitoring fence-line. However, Na^+ transport was relatively retarded due to ion exchange or sorption with the aquifer material. SO_4^{2-} breakthrough signified consumption of persulfate during oxidation of gasoline compounds or degradation in the presence of aquifer materials. Increase in CO_2 mass loading was due to mineralization of gasoline compounds as a result of persulfate oxidation. The oxidation of gasoline compounds was also captured by the decrease in mass loading for MGCs and PHC fractions. The overall maximum decrease in mass loadings was in accordance with oxidation rates of the MGCs reported during bench-scale investigations (Sra et al., 2010). Decrease in the cumulative mass of the MGCs crossing the

monitoring fence-line was primarily (60 to 80%) due to persulfate oxidation. After the inorganic slug was flushed from the source, inorganic concentrations and mass loadings dropped to near pre-treatment conditions whereas a partial rebound was observed for the MGCs.

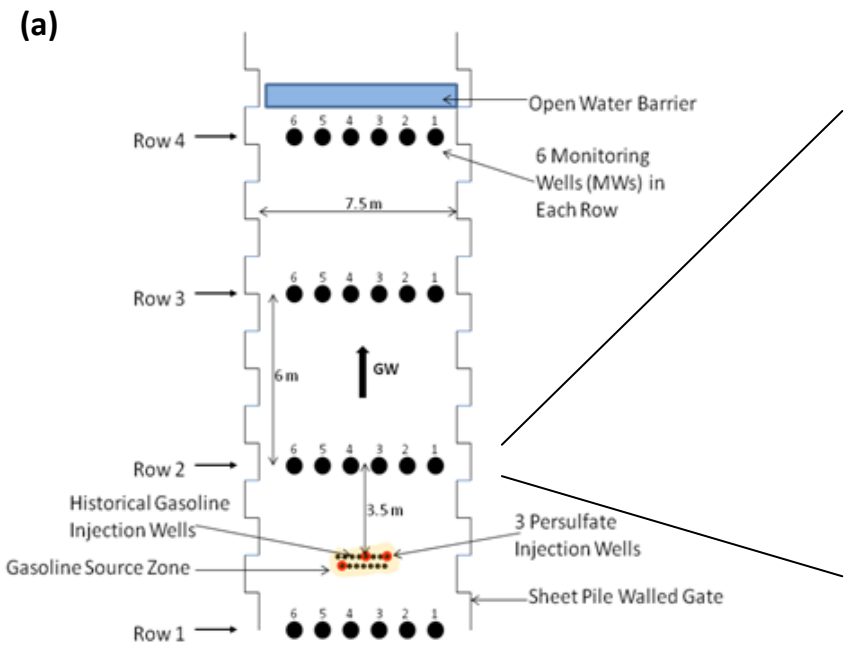

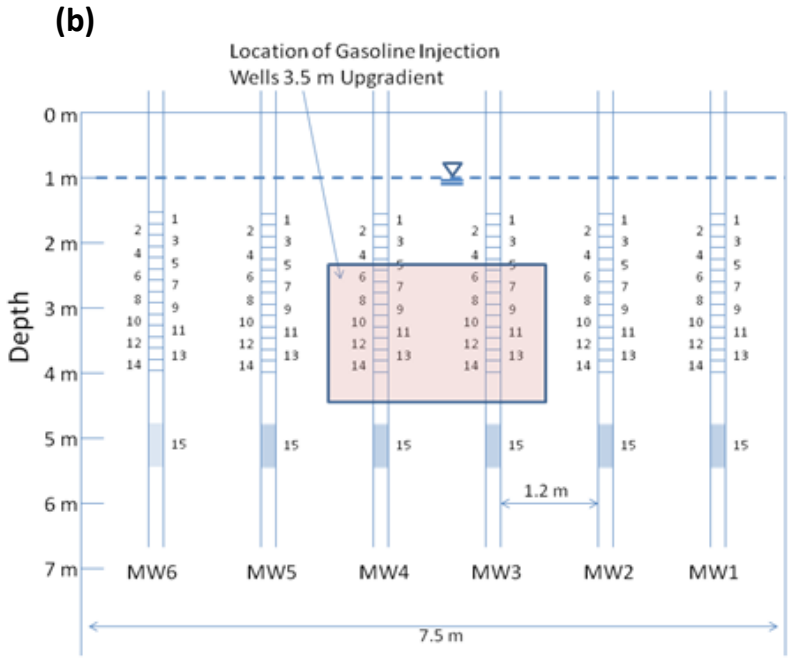

Figure 5.1(a): Plan view of the sheet-pile walled gate within the Borden groundwater research facility and the location of gasoline source zone used for this pilot-scale study.

Figure 5.1(b): Cross-sectional view of the Row 2 monitoring fence-line with 6 monitoring wells each equipped with 15 monitoring points.

Figure 5.2. Image of the persulfate injection manifold equipped with flow control gate valves and pressure gauges connected to the 3 injection wells.

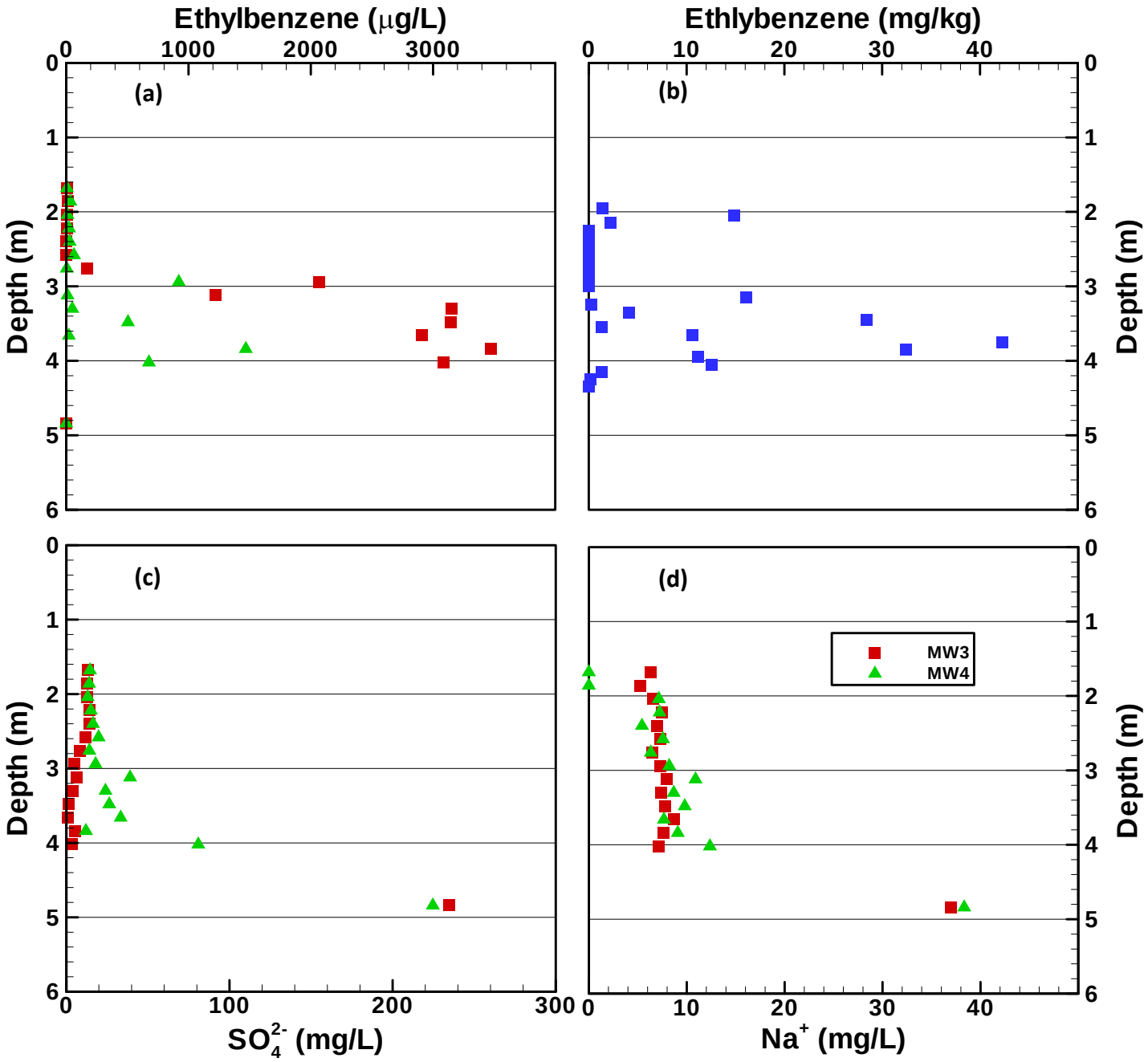

Figure 5.3. Pre-treatment concentration for (a) ethylbenzene in groundwater along MW3 and MW4, (b) ethylbenzene from a soil core extracted from the source zone, and (c) SO_4^{2-} and (d) Na^+ in groundwater along MW3 and MW4.

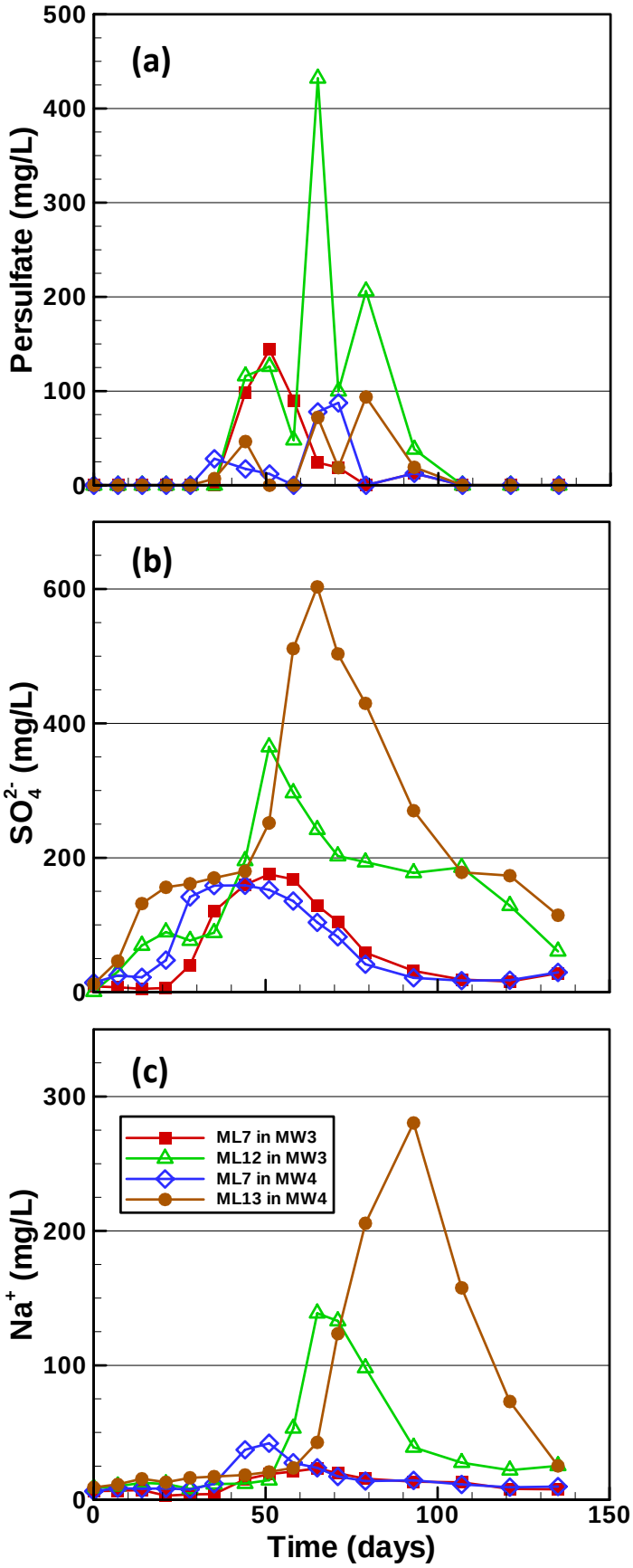

Figure 5.4. Concentration time series data for (a) persulfate, (b) SO_4^{2-} and, (c) Na^+ along selected monitors in MW3 and MW4.

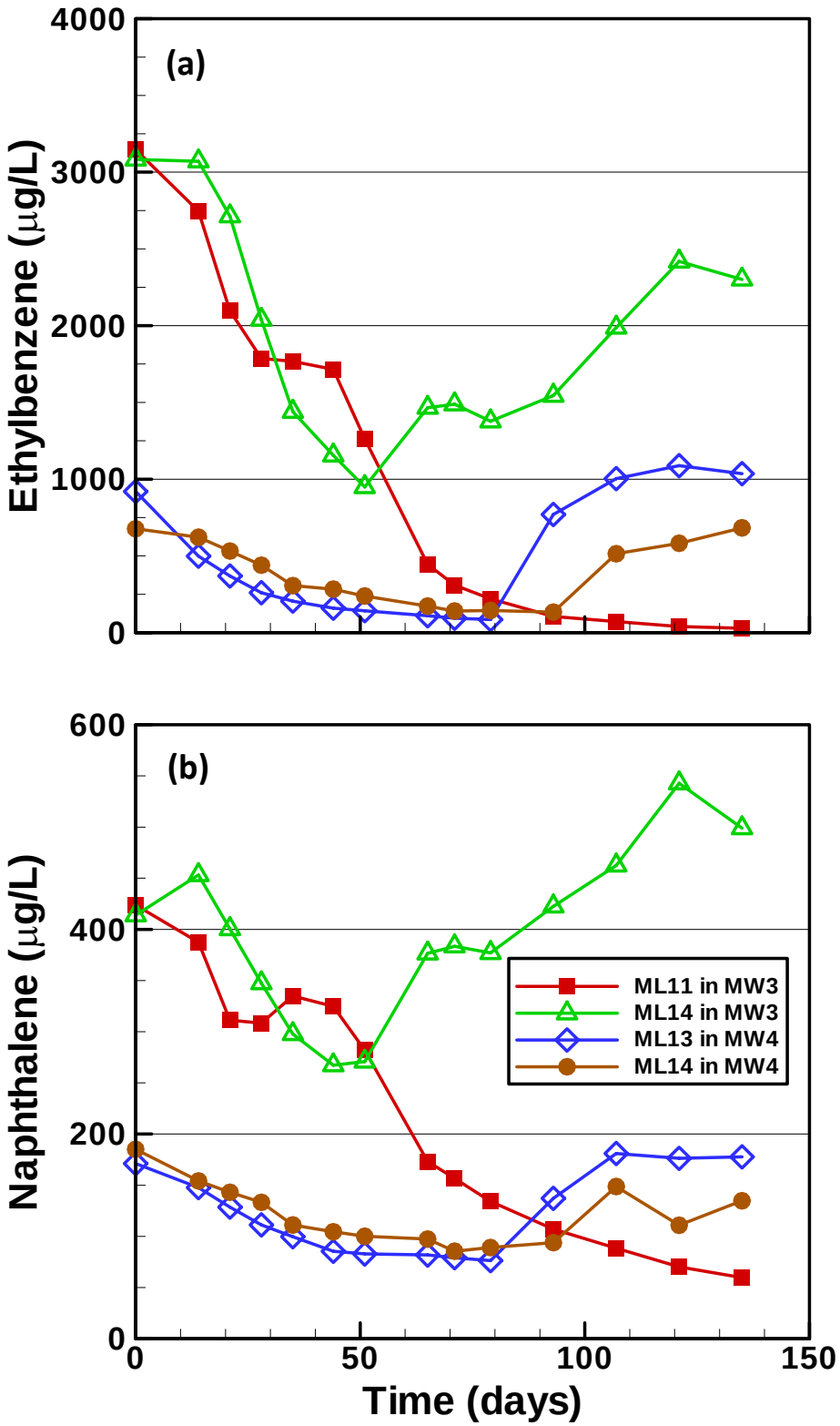

Figure 5.5. Concentration time series data for (a) ethylbenzene, and (b) naphthalene along selected monitors in MW3 and MW4.

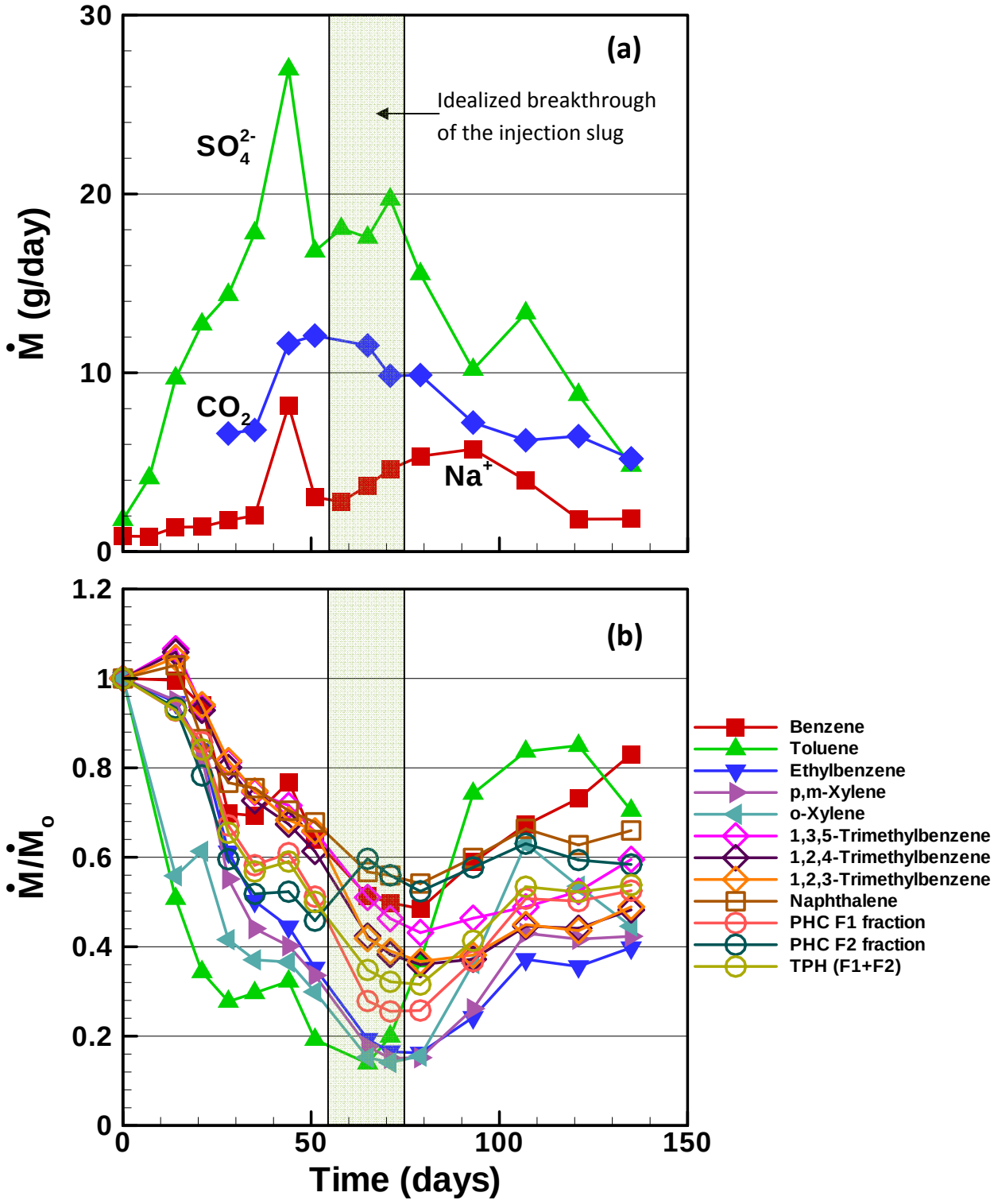

Figure 5.6. Temporal variation in (a) the mass loading for Na^+, SO_4^{2-}, $CO_{2(aq)}$ and (b) the normalized mass loading for all the monitored gasoline compounds and PHC fractions.

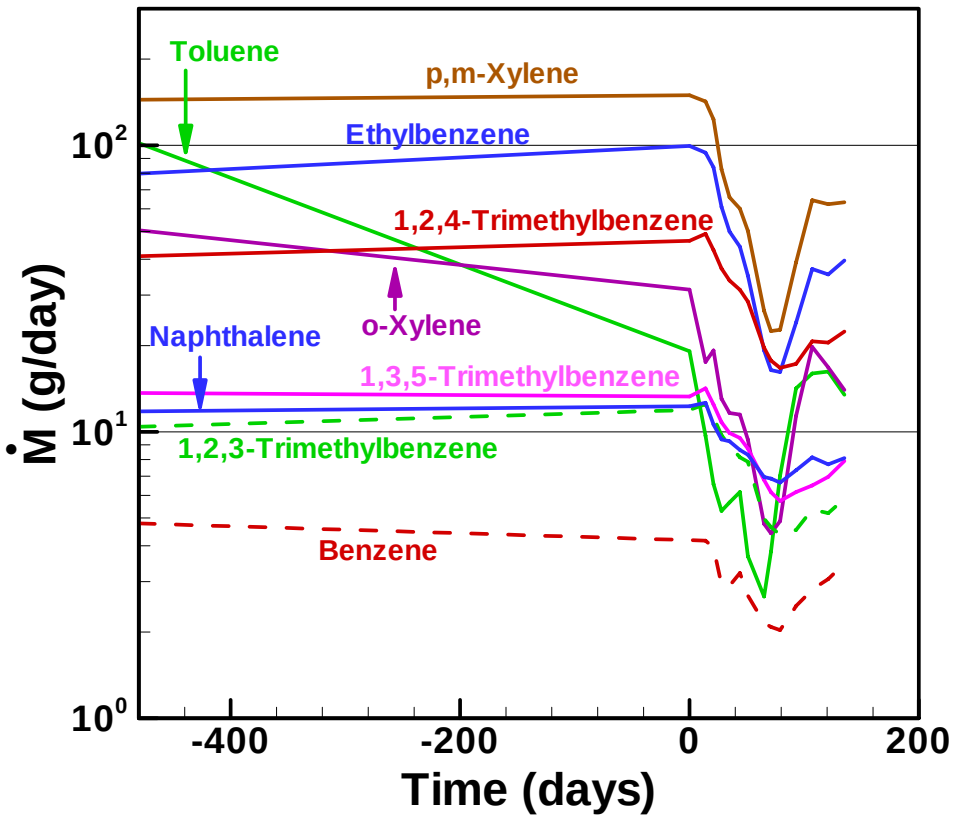

Figure 5.7. Mass loading (log-scale) for the monitored gasoline compounds.

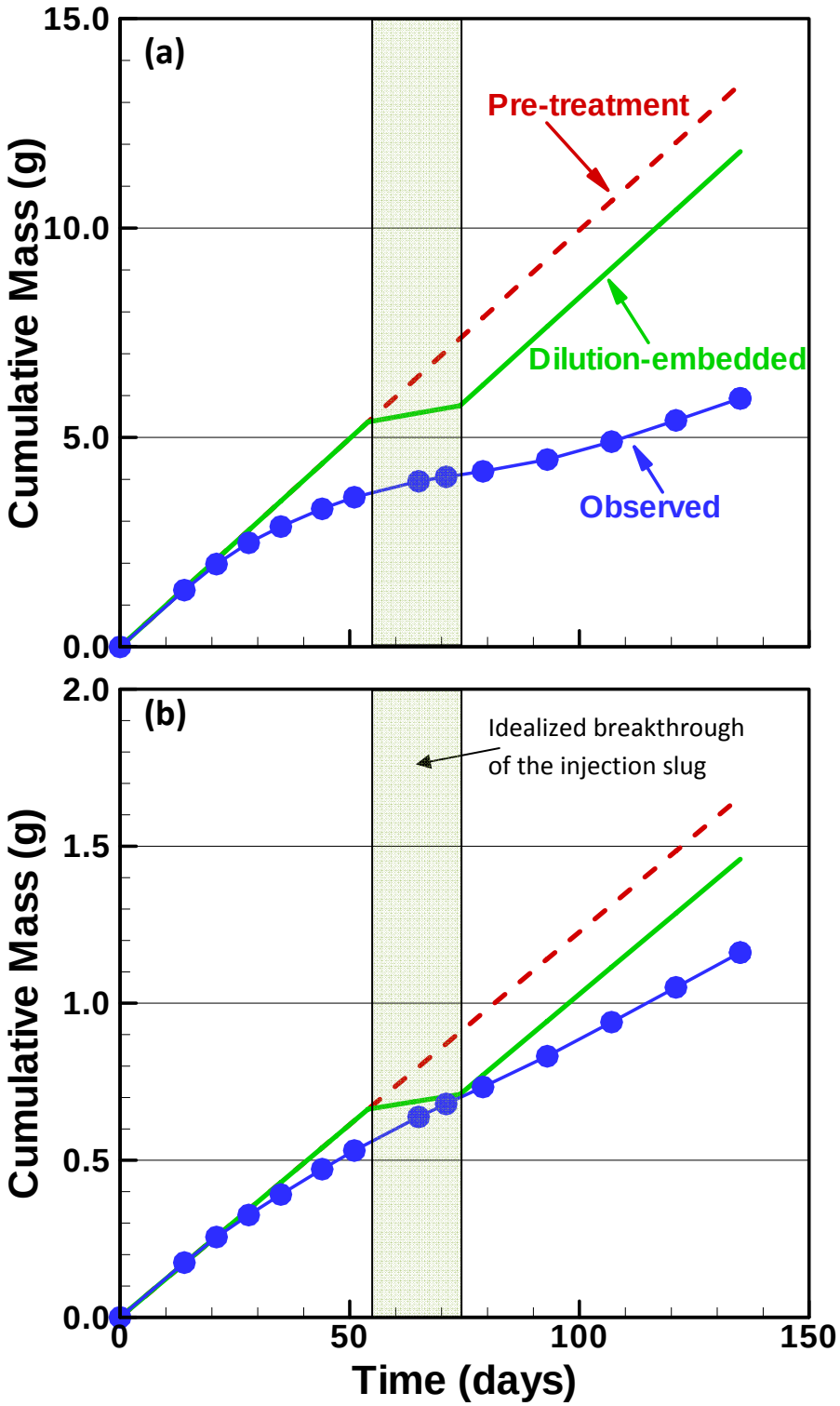

Figure 5.8. Observed and theoretical cumulative mass curves for (a) ethylbenzene, and (b) naphthalene.

Table 5.1 Summary of contaminated source zone and treatability investigation

Item	Detail
Source zone	Gasoline
Source zone emplacement year	2004
Emplaced mass	48 kg
Treatment year	2009
Treatment/remedial agent	Sodium persulfate
Injection volume	2000 L
Injection concentration	20 g/L
Inorganic analytes	$S_2O_8^{2-}$, SO_4^{2-} , Na^+, $CO_{2(aq)}$
Organic analytes	Benzene, Toluene, Ethylbenzene, o and p,m-Xylene, 123-, 124- and 135-Trimethylbenzene, Naphthalene, PHC F1 and F2 fractions, Total Petroleum Hydrocarbons
Sampling frequency	Weekly to biweekly
Monitoring period	4.5 months

Table 5.2 Summary of oxidation performance during gasoline source zone treatment

Gasoline Constituents (MDL in µg/L)		Maximum mass loading decrease (%)	Cumulative mass reduction at Day 135 (%)	Mass load rate at Day 135 (mg/day)	
				Theoretical pre-treatment (dilution-embedded)	Observed
Benzene	(1.3)	[a]51.5	20.1	4.2	3.3
Toluene	(1.1)	[b]86.0	41.6	19.1	14.8
Ethylbenzene	(1.5)	[a]83.7	49.8	99.5	37.5
p,m-Xylene	(2.6)	[c]85.0	49.6	149.5	62.8
o-Xylene	(1.8)	[c]86.0	51.3	31.4	15.4
1,3,5-Trimethylbenzene	(1.2)	[a]56.8	26.8	13.3	7.4
1,2,4-Trimethylbenzene	(1.0)	[a]64.0	32.9	46.4	21.4
1,2,3-Trimethylbenzene	(1.0)	[a]63.3	32.0	11.9	5.5
Naphthalene	(2.2)	[a]45.8	20.4	12.3	7.9
PHC F1 fraction	(5.0)	[c]74.5	38.8	501.4	257.6
PHC F2 fraction	(5.0)	[a]54.2	28.8	139.4	82.2
TPH	(-)	[a]68.5	36.6	640.9	340.0

[a]Observed on Day 79
[b]Observed on Day 65
[c]Observed on Day 71

Chapter 6

Closure

6.1. CONCLUSIONS AND CONTRIBUTIONS

The goals of this research were to understand the persistence of persulfate under activated and unactivated conditions in the presence of aquifer materials and to evaluate the oxidation of high impact gasoline compounds and the treatability of a gasoline source zone. Persulfate degradation was quantified in terms of degradation rate coefficients and their dependence upon system parameters was identified. Oxidation rate coefficients were estimated for the selected gasoline compounds under various activated persulfate conditions. The results obtained from these investigations were employed for selection of a persulfate remediation system for gasoline source zone treatment.

The major conclusions emerging from this research and significant contributions to the field of persulfate-based ISCO are listed below.

- Persistence of unactivated persulfate in the presence of aquifer materials described in Chapter 2 is the first comprehensive evaluation and quantification of persulfate degradation kinetics. It showed that persulfate followed first-order degradation for all materials and the estimated first-order reaction rate coefficient depended upon ionic strength, Fe_{Am} and TOC content of aquifer materials, and the solids mass to pore volume ratio. These were identified as the controlling factors for non-target persulfate mass loading requirements for *in situ* applications.

- Based on these observations, a persulfate degradation kinetic model was developed which predicted the scaled-up *in situ* degradation behavior captured during the push-pull tests. This also demonstrated that the kinetic model can be used in developing a predictive tool and that the bench tests can be used as robust experimental approaches for estimation of *in situ* persulfate degradation rate.
- In accordance with the literature, persulfate degradation was found to reduce solution pH. However, materials with a strong buffering capacity were capable of stabilizing the pH during persulfate degradation whereas the poorly buffered systems resulted in continual pH decrease. The drop in pH <3 resulted in enhanced persulfate degradation due to acid-catalyzation. This observation showed that enhanced persulfate loss due to the pH drop should be considered before designing and implementing a field-scale remediation system for a realistic estimation of persulfate persistence over the long-term. Similarly for hydroxide activation, a systematic assessment of hydroxide loading requirement should include consideration of buffering capacity and evolution of pH upon persulfate degradation in order to create sustainable hydroxide-activated conditions.
- Persulfate degradation kinetics implied that aquifer materials did not exhibit a finite NOD demand for persulfate. Change in reductive capacity of these materials captured through chemical oxidant demand (COD) was found to be affected by persulfate strength and exposure time. Since this investigation was conducted on different aquifer materials with a wide range of physical and chemical properties, this observation is more illustrative than any other study on the subject.
- Chapter 3 on persistence of activated persulfate employing different contemporary activator conditions is also the first systematic effort to understand the activated

persulfate kinetic behavior. It highlighted critical issues and governing factors that can act as guidelines for field-scale applications. Persulfate activation generally decreased persulfate stability as compared to the unactivated case. The additional loss of persulfate was a function of activator type and concentration, and aquifer material properties.

- Overall, a lower persistence was observed upon increase in peroxide or chelated-ferrous concentration. Peroxide degradation rate coefficients, which depend upon Fe_{Am} content of aquifer materials, and peroxide concentration, influenced the overall stability of the persulfate-activator system. In the presence of high Fe_{Am} materials, quick loss of peroxide was followed by slow persulfate degradation at a rate similar to that of unactivated persulfate. On the other hand, for low Fe_{Am} materials, peroxide degradation was relatively slower allowing for persulfate-peroxide interaction that resulted in lower persulfate stability. For field-scale applications, peroxide in Fe_{Am}-rich materials will degrade without causing significant impact on persulfate persistence but will be unavailable for persulfate activation over a long-term. Therefore, peroxide kinetics should be considered before designing peroxide-activated persulfate remediation system.
- Citric acid chelation of Fe(II) was found to be insufficient for controlling persulfate-Fe(II) interaction. Therefore, rapid initial persulfate loss was observed which was equivalent to the Fe(II) concentration employed indicating that Fe(II) was oxidized to Fe(III). After this initial loss, persulfate generally followed unactivated persulfate degradation kinetics. The degradation rate coefficients were impacted by the presence of citric acid and Fe(III). Stability of citric acid chelated-Fe(II) is doubtful for sustaining persulfate activation over a long-term.

- Persistence of persulfate was least impacted by alkaline activation. The degradation rate coefficients were generally similar to the unactivated persulfate persistence results. The pH was observed to decrease over time, and rate of this decrease was found to depend upon aquifer material buffering and initial pH conditions employed. The evolution of pH should be considered for design of alkaline-activated persulfate remediation system to ensure maintenance of required pH conditions.
- This study on persistence of activated persulfate represented general expectations of degradation response when applying these activating agents at the range of activator strengths utilized. Particular persulfate-activating agent combinations should be investigated for contaminant treatability evaluation and should be considered along with results from the current study for overall performance estimate.
- Bench-scale treatability of gasoline compounds in Chapter 4 enabled estimation of oxidation rates of the high impact organic compounds and decrease in strength of bulk PHC fractions under a wide range of persulfate activation and oxidation conditions. To date, this is the most comprehensive study evaluating oxidation of gasoline compounds and PHC fractions as they occur in dissolved phase. The most significant finding from this investigation was that unactivated persulfate at a high concentration was capable of completely destroying the majority of the gasoline compounds. Significant depletion in PHC fractions, particularly F1 and TPH, was also observed. Activation by peroxide and chelated-Fe(II) provided the highest oxidation rates for all the compounds explored and were 2 to 18 times higher than those observed during oxidation by unactivated persulfate. Alkaline activation reduced oxidation rates in general. Oxidation rate coefficients in the presence of aquifer materials were similar to that during oxidation by unactivated

persulfate implying that substantial oxidation of gasoline compounds should be expected to occur in the subsurface.

- This research identified first-order oxidation rate coefficients of gasoline compounds for all unactivated and activated persulfate trials. The quantification of oxidation rates contributes to the scientific knowledge required for the selection of an appropriate activation system for treating gasoline or specific gasoline compounds. These investigations are expected to serve as important benchmarks in assessing the field-scale use of persulfate-based oxidation of the target contaminants.
- The overall bench-scale treatability and persulfate persistence studies highlighted the significance of employing activated versus unactivated persulfate systems. Activation of persulfate by peroxide or chelated-Fe(II) drove higher oxidation rates of target compounds, but failed to maintain persistent persulfate or activator conditions, whereas unactivated and alkaline activated persulfate yielded relatively lower oxidation rates but exhibited higher persistence than activated systems.
- Lab-scale experiments are illustrative but often overlook the nuances of operating under real-field systems and prematurely judge upon the capability and performance of a remediation technology. Real source zone treatment attempted to bridge this gap and the lab-scale results were tested in the treatment of gasoline source zone. Concentration and mass loading of the target contaminants was observed to decrease which was primarily the result of chemical oxidation by persulfate.
- As anticipated, the field-scale remediation performance was limited by subsurface complexities associated with the aquifer and the contaminant mass. This investigation highlighted the need for and introduced some performance estimation tools. Mass loading

and cumulative mass flow of target contaminants and residual inorganics across monitoring fences was utilized in the estimation of performance efficiency during gasoline source zone treatment. This study also documents some of the challenges encountered during (near) field-scale operation thereby assisting in furthering the understanding of the natural systems. The source zone treatability experiment also identified the need for sufficient oxidant loading, multiple injection episodes and contact/residence time for oxidation of the organic mass, in order to achieve source zone clean-up goals.

6.2. FUTURE RECOMMENDATIONS

This research attempted to address specific issues related to persulfate-based ISCO of gasoline compounds. While several important conclusions and contributions have been cited in the previous section, some questions remained unanswered and some interesting questions have arisen during the course of this research and require further understanding. These avenues for future research are recommended as follows.

- Rate of persulfate degradation in the presence of aquifer materials was quantified at the bench- and pilot-scale and a kinetic model was developed. However, a systematic experimental study of persulfate fate and transport following its injection into a well and numerical modeling of this behavior was beyond the scope of this research. This is likely to further improve our understanding of persulfate degradation kinetics and distribution in field-systems.
- Push-pull tests were limited to the unactivated persistence experiments with exception of experiment with peroxide activation. These tests are more representative of *in situ*

conditions than bench-scale studies and are, therefore, expected to provide further insights into degradation of activated persulfate. Similar to the above recommendation, a subsequent fate and transport study of activated persulfate will be very helpful in providing a more comprehensive understanding for *in situ* applications.

- Treatability of gasoline compounds was studied for several activation conditions. However, more exploratory studies can be carried out to better understand the underlying oxidation mechanisms. Also, more research should be focused on determination of optimum activator dosing conditions for maximizing persulfate oxidation performance. Another avenue of research can be identification of suitable chelating agents for stabilizing Fe(II) and controlling its oxidation in the presence of persulfate.
- Oxidation performance assessment, particularly in field-applications, is prone to uncertainty because of various factors and processes (e.g., pre-oxidation dilution, and post-oxidation rebound). While concentration data and mass load estimates for organics and inorganics provide important performance metrics, isotope fractionation analysis can provide a more confident measure and identify contribution of chemical oxidation to reduction in contaminant concentration.
- Upon oxidation, strength of a source zone or the organic mass within the source zone will decrease. Evolution of dissolved organics concentrations emanating from this source zone are a good indicator of change in contaminant mass loading. However, a direct measure of contaminant mass before and after oxidation will be a very useful assessment tool. The challenges to this approach include complexity of contaminant distribution within the source zone, hydrogeological heterogeneity, natural organic matter etc. and necessitate further research. Adequate sampling and analytical techniques, and spatial

sampling frequency for different types of soils and contaminants also need to be developed for assistance in source mass estimation.

- Treatability studies almost always rely upon the destruction of target compounds without emphasizing on the existence, stability and toxicity of the intermediate compounds. In situations where the potential oxidation pathways contain intermediate compounds that are even more toxic than the parent compounds, the chemical oxidation strategy may not be a viable option. Therefore, apart from establishing the removal of target compounds, quantitative and/or qualitative assessment of the intermediate products needs to be made to avoid counter-productive situations. As a specific suggestion, total organic carbon (TOC) and carbon dioxide analysis may be employed for carbon mass balance on the system and estimation of complete mineralization of organic compounds.

References

CHAPTER 1

Appelo, C.A.J., Postma, D., 1996. Geochemistry, groundwater and pollution. A.A.Balkema, Rotterdam Brookfield.

Block, P.A., Brown, R.A., Robinson, D., 2004. Novel activation technologies for sodium persulfate in situ chemical oxidation, In *Proceedings of the Fourth International Conference of Remediation of Chlorinated and Recalcitrant Compounds* 2004, Gavaskar, A.R., Chen, A.S.C., Eds., Battelle Press, Columbus, Ohio.

Brown, R.A., Robinson, D. 2004. Response to naturally occurring organic material: permanganate versus persulfate. In *Proceedings of the Fourth International Conference Remediation of Chlorinated and Recalcitrant Compounds*, Monterey, USA, May 24-27, 2004, Gavaskar, A.R., Chen, A.S.C., Eds., Battelle: Columbus, OH.

Christensen, T.H., Bjerg, P.L., Banwart, S.A., Jakobsen, R., Heron, G., Albrechtsen, H.J., 2000. Characterization of Redox Conditions in Groundwater Contaminant Plumes. *J. Contam. Hydrol.*, 45, 165-241.

Cleasby, J.L., Baumann, E.R., Black, C.D., 1964. Effectiveness of Potassium Permanganate for Disinfection. *J. AWWA*. 56, 466-474.

Crimi, M.L., Taylor, J., 2007. Experimental Evaluation of Catalyzed Hydrogen Peroxide and Sodium Persulfate for Destruction of BTEX Contaminants. *Soil Sediment Contam.*, 16, 29–45.

Dahmani, M.A., Huang, K., Hoag, G.E. Sodium persulfate oxidation for the remediation of chlorinated solvents (USEPA Superfund Innovative Technology Evaluation Program). *Water Air Soil Pollut.*: Focus, 2006, 6, 127–141.

Ferrarese, E., Andreotolla, G., Oprea, I.A, 2008. Remediation of PAH-contaminated sediments by chemical oxidation. *J. Hazard. Mats.*, 152, 128–139.

Gates-Anderson, D.D., Siegrist, R.L., Cline, S.R., 2001. Comparison of Potassium Permanganate and Hydrogen Peroxide for Organically Contaminated Soils. *J. Environ. Eng.*, 337 – 347.

Haselow, J.S., Siegrist, R.L., Crimi, M., Jarosch, T. Estimating the total oxidant demand for in situ chemical oxidation design. *Remediation*, 2003, 5–16.

Houston, A.C., 1913. Studies in Water Supply, MacMillan and Co., London.

Huang, K., Couttenye, R.A., Hoag, G.E., 2002. Kinetics of heat-assisted persulfate oxidation of methyl tertbutyl ether (MTBE). *Chemosphere*, 49, 413–420.

Huang, K., Zhao, Z., Hoag, G.E., Dahmani, A., Block, P.A., 2005. Degradation of volatile organic compounds with thermally activated persulfate oxidation. *Chemosphere*, 61, 551–560

Huling, S.G., Pivetz, B.E., 2006. In-Situ Chemical Oxidation. USEPA, Engineering Issue. National Risk Management Research Laboratory, R.S.Kerr Environmental Research Center, Ada, Oklahoma, EPA/600/R-06/072. http://www.epa.gov/ada/topics/oxidation_issue.html.

ITRC, 2001. Technical and Regulatory Guidance for In Situ Chemical Oxidation of Contaminated Soil and Groundwater. Ed. 1. Interstate Technology and Regulatory Cooperation Work Group, In Situ Chemical Oxidation Work Team. June 2001. http://www.itrcweb.org/gd_ISCO.asp

ITRC, 2005a. Technical and Regulatory Guidance for In Situ Chemical Oxidation of Contaminated Soil and Groundwater. Ed. 2. Interstate Technology and Regulatory Cooperation Work Group, In Situ Chemical Oxidation Work Team. January 2005. http://www.itrcweb.org/gd_ISCO.asp

ITRC, 2005b. Overview of Groundwater Remediation Technologies for MTBE and TBA. The Interstate Technology and Regulatory Council (ITRC), MTBE and Fuel Oxygenates Team. February 2005.http://www.itrcweb.org/Documents/MTBE-1.pdf

Kronholm, J. and Reikkola, M.-L.,1999. Potassium Persulfate as Oxidant in Pressurized Hot Water. *Environ. Sci. Technol.*, 33, 2095 – 2099.

Langmuir, D., 1997. Aqueous Environmental Geochemistry; Prentice Hall: New Jersey.

Liang, C., Bruell, C.J., Marley, M.C., Sperry, K.L., 2004. Persulfate oxidation for in situ remediation of TCE. I. Activated by ferrous ion with and without a persulfate-thiosulfate redox couple. *Chemosphere*, 55, 1213–1223.

Liang, C., Su, H.-W., 2009. Identification of sulfate and hydroxyl radicals in thermally activated persulfate. *Ind. Eng. Chem. Res.*, 48, 5558–5562.

Liang, C.J., Bruell, C.J., Marley, M.C., Sperry, K.L., 2003. Thermally Activated Persulfate Oxidation of trichloroethylene (TCE) and 1,1,1-trichloroethane (TCA) in Aqueous Systems and Soil Slurries. *Soil Sediment Contam.*, 12,(2), 207 – 228.

Lundegard, P.D., Johnson, P.C., 2007. Source zone natural attenuation at petroleum hydrocarbon spill sites—II: Application to a former oil field. *Ground Water Monit. Rem.*, 26 (4), 93–106.

Mumford, K.G., Lamarche, C.S., Thomson, N.R., 2004, Natural oxidant demand of aquifer materials using the push-pull technique. *J. Environ. Eng.*, 1139-1146.

NFESC, 2004. In Situ Chemical Oxidation (ISCO) Tool. Naval Facilities Engineering Service Center. Environmental Restoration Technology Transfer (ERT2). http://www.ert2.org/isco/tool.aspx

Pankow, J.F., Cherry, J.A., 1996. Dense Chlorinated Solvents & Other DNAPLs in Groundwater: History, Behavior, and Remediation. Portland, Oregon, Waterloo Press.

Schnarr, M., Truax, C., Farquhar, G., Hood, E., Gonullu, T., Stickney, B.,1998. Laboratory and Controlled Field Experiments Using Potassium Permanganate to Remediate trichloroethylene and perchloroethylene DNAPLs in Porous Media. *J. Contam. Hydrol.*, 29, 205 – 224.

Shih, T., Rong, Y., Harmon, T., Suffet, M., 2004, Evaluation of the impact of fuel hydrocarbons and oxygenates on groundwater resources. *Environ. Sci. Technol.*, 38, 42–48.

Siegrist, R. L., Urynowicz, M.A, West, O.R., Crimi, M.L., Lowe, K.S., 2001. Principles and Practices of In Situ Chemical Oxidation Using Permanganate. Battelle Press, Columbus, OH, USA.

Smith, B., Crawford, S.C., Osgerby, I.T., Acone, S.E., Boeckeler, A.J., Getchell, S.A., 2005. Field Scale Comparison of Activated Persulfate and Modified Fenton's Reagent for Treatment of Chlorinated Benzene Compounds. In *Abstracts of The Annual International Conference on Soil*, Sediments and Water, University of Massachusetts, Amherst (2005).

Sra, K.S. Thomson, N.R., Barker, J.F., 2010. Persistence of persulfate in uncontaminated aquifer materials. *Environ. Sci. Technol.*, 44 (8), 3098–3104.

Taki, M., Hashimoto, R., 1977, Sterilization of biologically treated water. I. Sterlizing effects of chlorine and hydrogen peroxide. *Mizu Shori Gijutsu* (Jap.), 18 (2), 149-156.

Tiburtius, E.R.L., Peralta-Zamora, P., Emmel, A., 2005. Treatment of gasoline-contaminated waters by advanced oxidation processes. *J. Hazard. Mats.*, B126, 86–90.

USEPA, 1999. Use of Monitored Natural Attenuation at Superfund, RCRA Corrective Action, and Underground Storage Tank Sites, Office of Solid Waste and Emergency Response, Directive 9200.4-17P. http://www.epa.gov/OUST/directiv/d9200417.pdf

USEPA, 2006. MTBE in Drinking Water.
http://www.epa.gov/safewater/contaminants/unregulated/mtbe.html

Watts, R.J., Teel, A.L., 2006. Treatment of contaminated soils and groundwater using ISCO. *Pract. Period. Hazard. Toxic Radioact. Waste Manage.*, 2–9.

Watts, R.J., Udell, M.D., Rauch, P.A., Leung, S.W., 1990. Treatment of pentachlorophenol-contaminated soils using Fenton's reagent. *Haz. Waste Haz. Mat.*, 7 (4), 335–345.

Xu, X., Thomson, N.R., 2009. A long-term bench-scale investigation of permanganate consumption by aquifer materials. *J. Contam. Hydrol.*, 110, 73-86.

Xu, X., Thomson, N.R. 2010. Hydrogen peroxide persistence in the presence of aquifer materials. In press: *Soil Sed. Contam.*, 19 (5).

Xu, X., Thomson, N.R., 2008. Estimation of the maximum consumption of permanganate by aquifer solids using a modified chemical oxygen demand test. *J. Environ. Eng.*, 134 (5), 353–361.

CHAPTER 2

Balazs, G.B., Cooper, J.F., Lewis, P.R., Adamson, M.G., 2000. Transition metal catalysts for the ambient temperature destruction of organic wastes using peroxydisulfate. *Emerg. Technol. Hazard. Waste Manage.*, *8*, 229–239.

Barcelona, M.J., Holm, T.R., 1986. Oxidation-reduction capacities of aquifer solids. *Environ. Sci. Technol.*, *25* (9), 1565–1572.

Berlin, A.A., 1986. Kinetics of radical-chain decomposition of persulfate in aqueous solutions of organic compounds. *Kinet. Catal.*, *27* (1), 34–39.

Block, P.A., Brown, R.A., Robinson, D., 2004. Novel activation technologies for sodium persulfate in situ chemical oxidation, In: *Proceedings of the Fourth International Conference of Remediation of Chlorinated and Recalcitrant Compounds* (Monterey, CA, May 24-27, 2004), (Gavaskar, A.R., & Chen, A.S.C., Eds.), Battelle Press, Columbus, Ohio.

Brown, R.A., Robinson, D., 2004 Response to naturally occurring organic material: permanganate versus persulfate. In *Remediation of Chlorinated and Recalcitrant Compounds*, Proceedings of the Fourth International Conference, Monterey, USA, May 24-27, 2004, Gavaskar, A.R., Chen, A.S.C., Eds., Battelle: Columbus, OH.

Clifton, C.L., Huie, R.E., 1989. Rate constants for hydrogen abstraction reactions of the sulfate radical, $SO_4^{\cdot-}$ Alcohols. *Int. J. Chem. Kinet.*, 21, 677 – 687.

Crimi, M.L., Siegrist, R.L., 2005. Factors affecting effectiveness and efficiency of DNAPL destruction using potassium permanganate and catalyzed hydrogen peroxide. *J. Environ. Eng.*, *131* (12), 1724–1732.

Cuypers, C., Grotenhuis, T., Nierop, K.G.J., Franco, E.M., de Jager, A., Rulkens, W., 2002. Amorphous and condensed organic matter domains: the effect of persulfate oxidation on the composition of soil/sediment organic matter. *Chemosphere*, *48*, 919–931.

Dahmani, M.A., Huang, K., Hoag, G.E., 2006. Sodium persulfate oxidation for the remediation of chlorinated solvents (USEPA Superfund Innovative Technology Evaluation Program). *Water Air Soil Pollut.: Focus*, *6*, 127–141.

Devlin, J.F., McMaster, M., Barker, J.F., 2002. Hydrogeologic assessment of in situ natural attenuation in a controlled field experiment. *Water Resour. Res.*, *38* (1), 1–11.

Eberson, L., 1987. *Electron Transfer Reactions in Organic Chemistry*, Spring-Verlag: Berlin.

Eusterhues, K., Rumpel, C., Kleber, M., Kögel-Knabner, 2003. I. Stabilization of soil organic matter by interactions with minerals as revealed by mineral dissolution and oxidative degradation. *Org. Geochem.*, *34*, 1591–1600.

Gates-Anderson, D.D., Siegrist, R.L., Cline, S.R., 2001. Comparison of potassium permanganate and hydrogen peroxide as chemical oxidants for organically contaminated soils. *J Environ. Eng.*, *127* (4), 337–347.

Goulden, P.D., Anthony, D.H.J., 1978 Kinetics of uncatalyzed peroxidisulfate oxidation of organic material in fresh water. *Anal. Chem.*, *50* (7), 953–958.

Haggerty, R., Schroth, M.H., Istok, J.D., 1998. Simplified method of "push-pull" test data analysis for determining in situ reaction rate coefficients. *Ground Water*, *36* (2), 314–324.

Haselow, J.S., Siegrist, R.L., Crimi, M., Jarosch, T., 2003. Estimating the total oxidant demand for i*n situ* chemical oxidation design. *Remediation*, 5–16.

Henderson, J.F., Winkler, C.A., 1959. The reaction of potassium persulphate with thioglycolic acid in aqueous solution. *Can. J. Chem.*, *37*, 1082–1093.

Henton, D.E., Powell, C., Reim, R.E., 1997. The decomposition of sodium persulfate in the presence of acrylic acid. *J. Appl. Polym. Sci.*, *64* (3), 591–600.

House, D.A., 1962. Kinetics and mechanisms of oxidations by peroxydisulfate. *Chem. Rev.*, *62* (3), 185–203.

Huang, K., Couttenye, R.A., Hoag, G.E., 2002. Kinetics of heat-assisted persulfate oxidation of methyl tert-butyl ether (MTBE). *Chemosphere*, **2002**, *49*, 413–420.

Johnson, R.L., Tratnyek, P.G., Johnson, R.O., 2008. Persulfate persistence under thermal activated conditions. *Environ. Sci. Technol.*, *42* (24), 9350–9356.

Kiem, R., Kögel-Knabner, I., 2002. Refractory organic carbon in particle-size fractions of arable soil II: Organic carbon in relation to mineral surface area and iron oxide fractions < 6 μm. *Org. Geochem.*, *33*, 1699–1713

Kim, S., Chon, K., Kim, S.J., Lee, S., Lee, E., Cho, J., 2009. Uncertainty in organic matter analysis for seawater reverse osmosis (SWRO) desalination. *Desalination*, *238*, 30–36.

Kislenko, V.N., Berlin, A.A., Litovchenko, N.V., 1995. Kinetics of glucose oxidation with persulfate ions, catalyzed by iron salts. *Russ. J. Gen. Chem.*, *65* (7-2), 1092–1096.

Kislenko, V.N., Berlin, A.A., Litovchenko, N.V., 1996. Kinetics of the oxidation of organic sunstances by persulfate in the presence of variable-valence metal ions. *Kinet. Catal.*, *37* (6), 767–774.

Kolthoff, I.M., Medalia, A.I., Raaen, H.P., 1951. The Reaction between ferrous iron and peroxides. IV. Reaction with potassium persulfate. *J. Am. Chem. Soc.*, *73*, 1733–1739.

Kolthoff, I.M., Miller, I.K., 1951. The chemistry of persulfate. I. The kinetics and mechanism of the decomposition of the persulfate ion in aqueous medium. *J. Am. Chem. Soc.*, *73*, 3055–3059.

Langmuir, D., 1997. *Aqueous Environmental Geochemistry*, Prentice Hall: New Jersey.

Liang, C., Wang, Z.-S., Bruell, C.J., 2007. Influence of pH on persulfate oxidation of TCE at ambient temperatures. *Chemosphere*, *66*, 106–113.

Menegatti, A.P., Fruh-Green, G.L., Stille, P., 1999. Removal of organic matter by disodium peroxodisulphate: effects on mineral structure, chemical composition and physicochemical properties of some clay minerals. *Clay Miner.*, 34, 247–257.

Mikutta, R., Kleber, M., Kaiser, K., Jahn, R., 2005. Review: Organic matter removal from soils using hydrogen peroxide, sodium hypochlorite, and disodium peroxodisulfate. *Soil Sci. Soc. Am. J.*, 69, 120 – 135.

Mumford, K.G., Thomson, N.R., Allen-King, R.M., 2005. Bench-scale investigation of permanganate natural oxidant demand kinetics. *Environ. Sci. Technol.*, *39* (8), 2835–2840.

Peyton, G.R., 1993. The free-radical chemistry of persulfate-based total organic carbon analyzers. *Mar. Chem.*, *41*, 91–103.

Sharp, J.H., 1973. Total organic carbon in seawater – comparison of measurements using persulfate oxidation and high temperature combustion. *Mar. Chem.*, *1*, 211–229.

Tsitonaki, A., Smets, B.F., Bjerg, P.J., 2008. The effects of heat-activated persulfate oxidation on soil microorganisms. *Water Res.*. *42*, 1013–1022.

Watts, R.J., Teel, A.L., 2006. Treatment of contaminated soils and groundwater using ISCO. *Practice Periodical of Hazardous, Toxic and Radioactive Waste Management*, *10* (1), 2–9.

Xu, X., Thomson, N.R., 2008. Estimation of the maximum consumption of permanganate by aquifer solids using a modified chemical oxygen demand test. *J. Environ. Eng.*, *134* (5), 353–361.

Xu, X., Thomson, N.R., 2009. A long-term bench-scale investigation of permanganate consumption by aquifer materials. *J. Contam. Hydrol.*, *110*, 73–86.

Xu, X., Thomson, N.R., 2010. Hydrogen peroxide persistence in the presence of aquifer materials. In press: *Soil Sed. Contam.*, *19* (5).

CHAPTER 3

Anipsitakis, G.P., Dionysiou, D.D., 2004. Radical generation by the interaction of transition metals with common oxidants, *Environ. Sci. Technol.*, 38, 3705-3712.

Block, P.A., 2008. Personal communication.

Block, P.A., Brown, R.A., Robinson, D., 2004. Novel activation technologies for sodium persulfate in situ chemical oxidation, In *Proceedings of the Fourth International Conference of Remediation of Chlorinated and Recalcitrant Compounds* 2004 (Monterey, CA, May 24-27, 2004), (Gavaskar, A.R., & Chen, A.S.C., Eds.), Battelle Press, Columbus, Ohio.

Crimi, M.L., Siegrist, R.L., 2005. Factors affecting effectiveness and efficiency of DNAPL destruction using potassium permanganate and catalyzed hydrogen peroxide, *J. Environ. Eng.*, 131 (12), 1724-1732.

Cronk, G., Cartwright, R., 2006. Optimization of a chemical oxidation treatment train process for groundwater remediation, In *Proceedings of the Fifth International Conference of Remediation of Chlorinated and Recalcitrant Compounds* 2006 (Monterey, CA, May 22-25, 2004), (Sass, B.M., Ed.), Battelle Press, Columbus, Ohio.

Dahmani, M.A., Huang, K., Hoag, G.E., 2006. Sodium persulfate oxidation for the remediation of chlorinated solvents (USEPA Superfund Innovative Technology Evaluation Program), *Water Air Soil Pollut.*: Focus, 6, 127-141.

De Laat, J., Gallard, H., 1999. Catalytic decomposition of hydrogen peroxide by Fe(III) in homogeneous aqueous solution: mechanism and kinetic modeling, *Environ. Sci. Technol.*, 33 (16), 2726-2732.

Hastings, A.B., Van Slyke, D.D., 1922. The determination of the three dissociation constants of citric acid, *J. of Biological Chemistry*, 269-276.

Hayon, E., Treinin, A., J. Wilf, 1972. Electronic spectra, photochemistry, and autoxidation mechanism of the sulfite-bisulfite-pyrosulfite systems. The SO_2^-, SO_3^-, SO_4^- and SO_5^- radicals. *J. Am. Chem. Soc.*, 94 (1), 47–57.

House, D.A., 1962. Kinetic and mechanisms of oxidations by peroxydisulfate. *Chem. Rev.*, 62 (3), 185 – 203.

Huang, K., Couttenye, R.A., Hoag, G.E., 2002. Kinetics of heat-assisted persulfate oxidation of methyl tert-butyl ether (MTBE), *Chemosphere*, 49, 413-420.

Huang, K., Zhao, Z., Hoag, G.E., Dahmani, A., Block, P.A., 2005. Degradation of volatile organic compounds with thermally activated persulfate oxidation. *Chemosphere*, 61, 551–560.

Kolthoff, I.M., Medalia, A.I., Raaen, H.P., 1951. The Reaction between ferrous iron and peroxides. IV. Reaction with potassium persulfate. *J. Am. Chem. Soc.*, 73, 1733 – 1739.

Killian, P.F., Bruell, C.J., Liang, C. Marley, M.C., 2007. Iron (II) activated persulfate oxidation of MGP contaminated soil. *Soil Sediment Contam.*, 16 (6), 523–537.

Kwan, W.P., Voelker, B.M., 2003. Rates of hydroxyl radical generation and organic compound oxidation in mineral-catalyzed Fenton-like systems. *Environ. Sci. Technol.*, 37, 1150 – 1158.

Langmuir, D., 1997. Carbonate Chemistry: Aqueous Environmental Geochemistry.

Li,Y., Bachas, L.G., Bhattacharyya, D., 2005. Kinetics studies of trichlorophenol destruction by chelate-based fenton reaction, *Environ. Eng. Sci.*, 22, 756–771.

Liang, C.J., Bruell, C.J., Marley, M.C., Sperry, K.L, 2003. Thermally activated persulfate oxidation of trichloroethylene (TCE) and 1,1,1-trichloroethane (TCA) in aqueous systems and soil slurries. *Soil Sed. Contam.*, 12 (2), 207-228.

Liang, C., Bruell, C.J., Marley, M.C., Sperry, K.L., 2004. Persulfate oxidation for in situ remediation of TCE. I. Activated by ferrous ion with and without a persulfate-thiosulfate redox couple. *Chemosphere*, 55, 1213–1223.

Liang, C., Huang, C., Chen, Y., 2008. Potential for activated persulfate degradation of BTEX Contamination. *Water Res.*, 42, 4091–4100.

Mikutta, R., Kleber, M., Kaiser, K., Jahn, R., 2005. Review: Organic matter removal from soils using hydrogen peroxide, sodium hypochlorite, and disodium peroxodisulfate. *Soil Sci. Soc. Am. J.*, 69, 120 – 135.

Miraglio, M.A., 2009, Base-activated persulfate treatment of contaminated soils with pH drift from alkaline to circumneutral. Master thesis, Washington State University, USA.

Muller, J.G., Zheng, P., Rokita, S.E., Burrows, C.J., 1996. DNA and RNA modification promoted by $[Co(H_2O)_6]Cl_2$: guanine selectivity, temperature dependence and mechanism, *J. Am. Chem. Soc.*, 118, 2320–2325.

Mummery, C.S., 1913. Studies on oxidation. II. – The nature of the process in which hydrogen peroxide is utilized. Iron salts as catalysts. *J. Chem. Technol. Biot.*, 32 (18), 889–893.

Neta, P., Huie, R.E., Ross, A.B., 1988. Rate constants for reactions of inorganic radicals in aqueous solution, *J. Phys. Chem. Ref. Data*, 17 (3), 1027-1258.

Rastogi, A., Souhail, R.A.,Dionysiou, D.D., 2009. Sulfate radical-based ferrous-peroxymonosulfate oxidative system for PCBs degradation in aqueous and sediment systems, *Applied Catalysis B: Environmental*, 85, 171-179.

Singh, U.C., Venkatarao, K., 1976. Decomposition of peroxodisulphate in aqueous alkaline solution, *J. Inorg, Nucl. Chem.*, 38, 541-543.

Sra, K.S. Thomson, N.R., Barker, J.F., 2010a. Persulfate oxidation of gasoline. In preparation.

Sra, K.S. Thomson, N.R., Barker, J.F., 2010b. Persistence of persulfate in uncontaminated aquifer materials. *Environ. Sci. Technol.*. 44 (8), 3098-3104.

Stirling, J.D., 1934. The catalysis of peroxide oxidation by ferrous ions. Biochem. J., 28, 1048–1062.

Tsai, T.T., Kao, C.M., Yeh, T.Y., Lee, M.S., 2008. Chemical oxidation of chlorinated solvents in contaminated groundwater: review. *Practice Periodical of Hazardous, Toxic and Radioactive Waste Management*, 12 (2), 116-126.

Watts, R.J., Teel, A.L. 2005. Chemistry of modified Fenton's Reagent (catalyzed H2O2 propagations-CHP) for in situ soil and groundwater remediation. *J. Environ. Eng.*, 131, 612–622.

Watts, R.J., Teel, A.L., 2006. Treatment of contaminated soils and groundwater using ISCO. *Practice Periodical of Hazardous, Toxic and Radioactive Waste Management*, 10 (1), 2 – 9.

Xu, X., Thomson, N.R., 2010. Hydrogen peroxide persistence in the presence of aquifer materials. In Press: *Soil Sed. Contam.*, 19 (5).

Xu, X., Thomson, N.R., 2009. A long-term bench-scale investigation of permanganate consumption by aquifer materials. *J. Contam. Hydrol.*, 110 (3-4), 73-86.

CHAPTER 4

Agency for Toxic Substances and Disease Registry (ATSDR), 2004. Interaction profiles for: Benzene, Toluene, Ethylbenzene, and Xylenes (BTEX). U.S. Department of Health and Human Services, Public Health Service.
http://www.atsdr.cdc.gov/interactionprofiles/ip05.html

Block, P.A., Brown, R.A., Robinson, D., 2004. Novel activation technologies for sodium persulfate in situ chemical oxidation. In *Proceedings of the Fourth International Conference of Remediation of Chlorinated and Recalcitrant Compounds* 2004. Gavaskar, A.R., Chen, A.S.C. (Eds.), Battelle Press, Columbus, OH.

Buxton, G.V., Greenstock, C.L., Helman, W.P., Ross, A.B., 1988. Critical review of rate constants for reactions of hydrated electrons, hydrogen atoms and hydroxyl radicals ($^{\bullet}OH$, $^{\bullet}O^-$) in aqueous solution. *J. Phys. Chem. Ref. Data*, 17 (2), 513–886.

Crimi, M.L., Taylor, J., 2007. Experimental Evaluation of Catalyzed Hydrogen Peroxide and Sodium Persulfate for Destruction of BTEX Contaminants. *Soil Sediment Contam.*, 16, 29–45.

Dadkhah, A.A., Akgermanm ,A., 2006. Hot water extraction with in situ wet oxidation: Kinetics of PAHs removal from soil. *J. Hazard. Mats.*, B137, 518–526

Eberson, L., 1987. Electron Transfer Reactions in Organic Chemistry, Spring-Verlag, Berlin.

Ferguson, S.H., Woinarski, A.Z., Snape, I., Morris, C.E., Revill, A.T., 2004. A field trial of in situ chemical oxidation to remediate long-term diesel contaminated Antarctic soil. *Cold Reg. Sci. Technol.*, 40, 47–60.

Ferrarese, E., Andreotolla, G., Oprea, I.A, 2008. Remediation of PAH-contaminated sediments by chemical oxidation. *J. Hazard. Mats.*, 152, 128–139.

Forsey, S.P., 2004. In situ chemical oxidation of creosote/coal tar residuals: experimental and numerical investigation. PhD thesis, University of Waterloo, Canada.

Freitas, J.G., Barker, J.F., 2008. Sampling VOCs with porous suction samplers in the presence of ethanol: How much are we losing? *Ground Water Monit. Rem.*, 28 (3), 83–92.

Hayon, E., Treinin, A., J. Wilf, 1972. Electronic spectra, photochemistry, and autoxidation mechanism of the sulfite-bisulfite-pyrosulfite systems. The SO_2^-, SO_3^-, SO_4^- and SO_5^- radicals. *J. Am. Chem. Soc.*, 94 (1), 47–57.

House, D.A., 1962. Kinetics and mechanisms of oxidations by peroxydisulfate. *Chem. Rev.*, 62 (3), 185–203.

Huang, K., Couttenye, R.A., Hoag, G.E., 2002. Kinetics of heat-assisted persulfate oxidation of methyl tertbutyl ether (MTBE). *Chemosphere*, 49, 413–420.

Huang, K., Zhao, Z., Hoag, G.E., Dahmani, A., Block, P.A., 2005. Degradation of volatile organic compounds with thermally activated persulfate oxidation. *Chemosphere*, 61, 551–560

Huling, S.G., Pivetz, B.E., 2006. In-Situ Chemical Oxidation. USEPA, Engineering Issue. National Risk Management Research Laboratory, R.S.Kerr Environmental Research Center, Ada, Oklahoma, EPA/600/R-06/072. http://www.epa.gov/ada/topics/oxidation_issue.html.

Interstate Technology and Regulatory Cooperation (ITRC), 2001. Technical and regulatory guidelines for in situ chemical oxidation of contaminated soil and groundwater. www.itrcweb.org.

Jeffers, P.M., Ward, L.M., Woytowitch, L.M., Wolfe, N.L., 1989. Homogeneous hydrolysis rate constants for selected chlorinated methanes, ethanes, ethenese and propanes. *Environ. Sci. Technol.*, 23(1), 965–969.

Killian, P.F., Bruell, C.J., Liang, C. Marley, M.C., 2007. Iron (II) activated persulfate oxidation of MGP contaminated soil. *Soil Sediment Contam.*, 16 (6), 523–537.

Kolthoff, I.M., Miller, I.K., 1951 The chemistry of persulfate. I., The kinetics and mechanism of the decomposition of the persulfate ion in aqueous medium. *J. Am. Chem. Soc.*, 73, 3055–3059.

Kunukcu, Y.K., 2007. In situ bioremediation of groundwater contaminated with petroleum constituents using oxygen release compounds (ORCs). *J. Environ. Sci. Health, Part A Environ. Sci. Eng.*, 42, 839–845.

Latimer, W.M., 1952. Oxidation Potentials, second ed. Prentice-Hall, New York.

Liang, C., Bruell, C.J., Marley, M.C., Sperry, K.L., 2004a. Persulfate oxidation for in situ remediation of TCE. I. Activated by ferrous ion with and without a persulfate-thiosulfate redox couple. *Chemosphere*, 55, 1213–1223.

Liang, C., Bruell, C.J., Marley, M.C., Sperry, K.L., 2004b. Persulfate oxidation for in situ remediation of TCE. II. Activated by chelated ferrous ion. *Chemosphere*, 55, 1225–1233.

Liang, C., Wang, Z.-S., Bruell, C.J., 2007. Influence of pH on persulfate oxidation of TCE at ambient temperatures. *Chemosphere*, 66, 106–113.

Liang, C., Huang, C., Chen, Y., 2008. Potential for activated persulfate degradation of BTEX Contamination. *Water Res.*, 42, 4091–4100.

Liang, C., Su, H.-W., 2009. Identification of sulfate and hydroxyl radicals in thermally activated persulfate. *Ind. Eng. Chem. Res.*, 48, 5558–5562.

Lundegard, P.D., Johnson, P.C., 2007. Source zone natural attenuation at petroleum hydrocarbon spill sites—II: Application to a former oil field. *Ground Water Monit. Rem.*, 26 (4), 93–106

McCarthy, K., Walker, L., Vigoren, L., 2004. Subsurface fate of spilled petroleum hydrocarbons in continuous permafrost. *Cold Reg. Sci. Technol.*, 38, 43–54.

Miraglio, M.A., 2009, Base-activated persulfate treatment of contaminated soils with pH drift from alkaline to circumneutral. Master thesis, Washington State University, USA.

Mummery, C.S., 1913. Studies on oxidation. II. – The nature of the process in which hydrogen peroxide is utilized. Iron salts as catalysts. *J. Chem. Technol. Biot.*, 32 (18), 889–893.

Nadim, F., Hoag, G.E., Liu S., Carley, R.J Zack, P., 2000. Detection and remediation of soil and aquifer systems contaminated with petroleum products: an overview. *J. Pet. Sci. Eng.*, 26,169–178.

Peyton, G.R., 1993. The free-radical chemistry of persulfate-based total organic carbon analyzers. *Mar. Chem.*, 41, 91–103.

Prince, R.C., Parkerton, T.F., Lee C., 2007. The primary aerobic biodegradation of gasoline hydrocarbons. *Environ. Sci. Technol.*, 41, 3316–3321

Shih, T., Rong, Y., Harmon, T., Suffet, M., 2004, Evaluation of the impact of fuel hydrocarbons and oxygenates on groundwater resources. *Environ. Sci. Technol.*, 38, 42–48.

Sra, K.S. Thomson, N.R., Barker, J.F., 2010. Persistence of persulfate in uncontaminated aquifer materials. *Environ. Sci. Technol.*, 44 (8), 3098–3104.

Stirling, J.D., 1934. The catalysis of peroxide oxidation by ferrous ions. *Biochem. J.*, 28, 1048–1062.

Tiburtius, E.R.L., Peralta-Zamora, P., Emmel, A., 2005. Treatment of gasoline-contaminated waters by advanced oxidation processes. *J. Hazard. Mats.*, B126, 86–90.

Watts, R.J., Udell, M.D., Rauch, P.A., Leung, S.W., 1990. Treatment of pentachlorophenol-contaminated soils using Fenton's reagent. *Haz. Waste Haz. Mat.*, 7 (4), 335–345.

Watts, R.J., Teel, A.L., 2006. Treatment of contaminated soils and groundwater using ISCO. Pract. Period. Hazard. Toxic Radioact. *Waste Manage.*, 2–9.

Xu, X., Thomson, N.R. 2010. Hydrogen peroxide persistence in the presence of aquifer materials. In press: *Soil Sed. Contam.*, 19 (5).

Xu, X., Thomson, N.R., 2009. A long-term bench-scale investigation of permanganate consumption by aquifer materials. J. *Contam. Hydrol.*, 110, 73-86.

Zhou, Q., Suna, F., Liu, R., 2005. Joint chemical flushing of soils contaminated with petroleum hydrocarbons. *Environ. Int.*, 31, 835–839.

CHAPTER 5

Agency for Toxic Substances and Disease Registry (ATSDR), 2004. Interaction profiles for: Benzene, Toluene, Ethylbenzene, and Xylenes (BTEX). U.S. Department of Health and Human Services Public Health Service.
http://www.atsdr.cdc.gov/interactionprofiles/ip05.html

Crimi, M.L., Taylor, J., 2007. Experimental Evaluation of Catalyzed Hydrogen Peroxide and Sodium Persulfate for Destruction of BTEX Contaminants. *Soil Sediment Contam.*, 16, 29–45.

Dadkhah, A.A., Akgermanm ,A., 2006. Hot water extraction with in situ wet oxidation: Kinetics of PAHs removal from soil. *J. Hazard. Mats.*, B137, 518–526.

Dance, J.T., Reardon, E.J., 1983. Migration of contaminants at a landfill: A case study, 5. A cation migration in the dispersion test. *J.Hydrol.*, 63, 109-130.

Freitas, J., Yang, T., Barker, J., Mocanu, M., Molson, J., 2008. Attenuation of dissolved aromatic hydrocarbons from residual gasoline: source depletion and bioattenuation controls, *In Proceedings of GeoEdmonton* 2008, 1580-1585.

Huang, K., Couttenye, R.A., Hoag, G.E., 2002. Kinetics of heat-assisted persulfate oxidation of methyl tertbutyl ether (MTBE). *Chemosphere*, 49, 413–420.

Huang, K., Zhao, Z., Hoag, G.E., Dahmani, A., Block, P.A., 2005. Degradation of volatile organic compounds with thermally activated persulfate oxidation. *Chemosphere*, 61, 551–560.

Interstate Technology and Regulatory Cooperation (ITRC), 2001. Technical and regulatory guidelines for in situ chemical oxidation of contaminated soil and groundwater. www.itrcweb.org.

Kjeldsen, P., Christensen, T.H., 1984. Soil attenuation of acid phase landfill leachate. *Waste Management and Research*, 2, 247-263.

Kunukcu, Y.K., 2007. In situ bioremediation of groundwater contaminated with petroleum constituents using oxygen release compounds (ORCs). *J. Environ. Sci. Health, Part A Environ. Sci. Eng.*, 42, 839–845.

Liang, C., Bruell, C.J., Marley, M.C., Sperry, K.L., 2004. Persulfate oxidation for in situ remediation of TCE. I. Activated by ferrous ion with and without a persulfate-thiosulfate redox couple. *Chemosphere*, 55, 1213–1223.

Liang, C., Huang, C., Chen, Y., 2008. Potential for activated persulfate degradation of BTEX Contamination. *Water Res.*, 42, 4091–4100.

Lundegard, P.D., Johnson, P.C., 2007. Source zone natural attenuation at petroleum hydrocarbon spill sites—II: Application to a former oil field. *Ground Water Monit. Rem.*, 26 (4), 93–106.

MacFarlane, D.S., Cherry, J.A., Gillham, R.W., Sudicky, E.A., 1983. Migration of contaminants in groundwater at a landfill: A case study, 1. Groundwater flow and plume delineation, *J. Hydrol.*, 63, 1-29.

Mackay, D. M., D. L. Freyberg, and P. V. Roberts, 1986: A Natural Gradient Experiment on Solute Transport in a Sand Aquifer .1. Approach and Overview of Plume Movement. *Water Resources Research*, **22,** 2017-2029.

Mocanu, M., 2006. Behavior of oxygenates and aromatic hydrocarbons in groundwater from gasoline residuals, Master thesis, University of Waterloo, Canada.

Morrison, W.E., 1998. Hydrogeological controls on flow and fate of PCE DNAPL in afractured and layered clayey aquitard: a Borden experiment. Master thesis, University of Waterloo, Canada.

Mundle, K., Reynolds, D.A., West, M.R., Kueper, B.H., 2007. Concentration rebound following in situ chemical oxidation in fractured clay. *Ground Water*, 45 (6), 692-702.

Nadim, F., Hoag, G.E., Liu S., Carley, R.J Zack, P., 2000. Detection and remediation of soil and aquifer systems contaminated with petroleum products: an overview. *J. Pet. Sci. Eng.* 26,169–178.

Park, I.-B., Son, Y., Song, I.-S., Kim, J., Khim, J., 2008. Remediation of diesel-contaminated soil using supercritical carbon dioxide and ultrasound, *Japanese J. of Applied Physics*, 47 (5), 4314-4316.

Payne, F.C., Quinnan, J.A., Potter S.T., Remediation Hydraulics, CRC Press, Boca Raton, Florida.

Prince, R.C., Parkerton, T.F., Lee C., 2007. The primary aerobic biodegradation of gasoline hydrocarbons. *Environ. Sci. Technol.* 41, 3316–3321.

Sra, K.S., Thomson, N.R., Barker, J.F., 2010. Persulfate oxidation of gasoline. In preparation.

Sudicky, E.A., 1986. A natural gradient experiment on solute transport in a sand aquifer:Spatial variability of hydraulic conductivity and its role in the dispersion process. *Water Resources Research* 22(13): 2069-2082.

Suthersan, S., Divine, C., Quinnan, J., Nichols, E., 2010. Flux-informed remediation decision making, *Ground Water Monit. Remediation*, 30 (1), 34-43.

Thomson, N.R., Fraser,M.J., Lamarche, C., Barker, J.F., Forsey, S.P., 2008. Rebound of a coal tar creosote plume following partial source zone treatment with permanganate, *J. Contam. Hydrol.*, 102, 154-171.

Tsai, T.T., Kao, C.M., 2009. Treatment of petroleum-hydrocarbon contaminated soils using hydrogen peroxide oxidation catalyzed by waste basic furnace slag. *J. Hazard. Mat.*, 170, 466-472.

Tsitonaki, A., Mosbaek, H., Bjerg, P.L., 2006. Activated persulfate as a first step in a treatment train. Paper D-77, In *Proceedings of the Fifth International Conference on Remediation of Chlorinated and Recalcitrant Compound*, Monterey, CA, May 2006, Battelle Press, Columbus, OH, ISBN 1-57477-157-4.

Yang, T., 2009. Investigation of residual gasoline in the GMT and E10 source in Borden aquifer, Master thesis, University of Waterloo, Canada.

Zhou, Q., Suna, F., Liu, R., 2005. Joint chemical flushing of soils contaminated with petroleum hydrocarbons. *Environ. Int.*, 31, 835–839.